OREGON HEALTH & SCIENCE UNIVERSITY
SCHOOL OF MEDICINE – GRADUATE STUDIES

Ph.D. Dissertation

LESION OF THE PERFORANT PATH TRIGGERS A BIPHASIC NEUROGENIC RESPONSE IN THE ADULT DENTATE GYRUS

by

Julia V. Perederiy

Presented to the Neuroscience Graduate Program and
the Oregon Health & Science University School of Medicine
in partial fulfillment of the requirements for the degree of
Doctor of Philosophy

December, 2012

OREGON HEALTH & SCIENCE UNIVERSITY
SCHOOL OF MEDICINE – GRADUATE STUDIES
Approval for Completion of Ph.D. Degree

School of Medicine

Oregon Health & Science University

CERTIFICATE OF APPROVAL

This is to certify that the PhD dissertation of Julia V. Perederiy has been approved

_____
Gary L. Westbrook – Mentor/ Advisor

_____
Craig Jahr – Member

_____
Phillip Copenhaver – Member

_____
Tianyi Mao – Member

_____
Lawrence Sherman – Member

Mary Logan – Member

TABLE OF CONTENTS

ACKNOWLEDGEMENTS iii

ABSTRACT iv

INTRODUCTION

STRUCTURAL PLASTICITY IN THE DENTATE GYRUS- REVISING A CLASSIC INJURY MODEL

Plasticity in the adult brain, implications for injury-induced circuit reorganization 1

- Synaptic and dendritic plasticity in the adult brain
- Sprouting and the axonal response to injury
- Glial and extracellular response to injury

Perforant path lesion as a model of post-injury plasticity in the adult brain 6

- Advantages of model
- Post-lesion circuit reorganization – axons
- Post-lesion circuit reorganization – dendrites/ spines
- Post-lesion glial and extracellular matrix response

Figures 11

CHAPTER 1

NEURAL INJURY TRIGGERS A BIPHASIC RESPONSE IN ADULT-GENERATED NEURONS IN THE DENTATE GYRUS

Introduction 15

Methods 17

Results 24

- Proliferation and Migration of newborn neurons following perforant path lesion
- Dendritic outgrowth and synapse formation post-lesion

- *de novo* dendritic spines in the denervated zone

Discussion ……..…... 31

- An initial neurogenic response to perforant path lesion
- Circuit reorganization following denervation
- Is a spine a marker of a functional excitatory synapse post-lesion?
- Limits to growth

Figures ……... 36

CHAPTER 1 – ADDENDUM
MECHANISMS OF LESION-INDUCED PROLIFERATION AND DISPERSION OF NEWBORN GRANULE CELLS IN THE DENTATE GYRUS

Possible mechanisms of injury-induced proliferation and dispersion of newborn granule cells in the dentate gyrus ……... 46

- Circuit activity
- Growth factors
- Reelin
- Radial glia

Figures …….. 52

CHAPTER 2
ROLE OF EXTRACELLULAR ENVIRONMENT IN POST-LESION CIRCUIT REORGANIZATION

Laminar borders and axonal sprouting following lesion ……. 56

- Laminar specificity of excitatory afferents
- Pre- and postsynaptic components of lesion-induced circuit reorganization

Extracellular matrix in development and following lesion …….. 58

- Role of the extracellular matrix in generation and maintenance of laminar borders
- Manipulation of the post-lesion extracellular environment
- Dendritic outgrowth and spine density following digestion of CSPG

Figures ……. 66

GENERAL DISCUSSION …… 71
LIMITS OF PLASTICITY

SUMMARY AND CONCLUSIONS 73

REFERENCES 75

ACKNOWLEDGMENTS

This work would not have been possible without the multitude of people around me that, despite their own dynamic lives, had moments for deeply meaningful philosophical conversations and shared laughs. These people are family, friends, mentors, and even strangers, that all inspired me in many ways. The examples they set forth will be forever integrated into my path forward and I will continue to be thankful for their guidance.

This work was also supported by NIH grant MH46613 and by Oregon Partnership for Alzheimer's Research Tax Check-Off grant. We thank Oswald Steward for training in the perforant path lesion procedure. We thank Stephanie Kaech-Petrie with the Jungers Center Microscopy Core for assistance with imaging parameters and Sue Aicher, Melissa Williams, Lisa Dirling, and Robert Kayton with the Electron Microscopy Core for tissue preparation and assistance with imaging equipment (supported by NIH, P30 NS06180).

ABSTRACT

The adult brain is in a continuous state of remodeling. This is nowhere more true than in the dentate gyrus, where competing forces such as neurodegeneration and neurogenesis dynamically modify neuronal connectivity, and can occur simultaneously. This plasticity of the adult nervous system is particularly important in the context of traumatic brain injury or deafferentation because it illustrates the potential for regeneration in the central nervous system. Here, we summarize a classic injury model, lesioning of the perforant path, which removes the main extrahippocampal input to the dentate gyrus. Early studies revealed that in response to deafferentation, axons of remaining fiber systems and dendrites of mature granule cells undergo lamina-specific changes, providing one of the first examples of structural plasticity in the adult brain. Given the increasing role of adult neurogenesis in the function of the dentate gyrus, we also compare the response of newborn and mature granule cells following lesioning of the perforant path. We find that the lesion triggered a marked proliferation and increased outward migration of newborn neurons in the deafferented dentate gyrus. The dendrites of these cells show reduced complexity within the denervated zone, but dendritic spines with intact post-synaptic densities still form, despite the absence of glutamatergic nerve terminals. Following entorhinal lesion, newborn neurons, but not mature granule cells, have a higher density of dendritic spines in the non-denervated inner molecular layer, accompanied by an increase in miniature EPSC amplitudes and rise times. Laminar borders are maintained post-lesion and show lamina-specific reactive gliosis and changes in the extracellular matrix. Our results demonstrate that injury causes an increase in newborn neurons and lamina-specific synaptic reorganization, indicative of enhanced plasticity. The presence of *de novo* dendritic spines in the denervated zone suggests that the post-lesion environment provides the necessary signals for spine formation even if excitatory innervation is absent. These studies provide insights not only to plasticity in the dentate gyrus, but also to the response of neural circuits to brain injury.

INTRODUCTION

STRUCTURAL PLASTICITY IN THE DENTATE GYRUS-REVISING A CLASSIC INJURY MODEL

(The following will be published as a review in Frontiers in Neural Circuits in 2013)

Plasticity in the adult brain

The ability of the mammalian brain to change with experience is perhaps its most important feature. At the organismal level, the positive (adaptive) benefits of experience-dependent changes underlie our abilities to learn, speak multiple languages, ride a bicycle and so on. However, equally important are enduring negative (maladaptive) effects that are associated with experience-dependent changes, including benign habits as well as more disruptive conditions such as anxiety, post-traumatic stress, and drug addiction. In both cases, these changes are manifested at the level of circuits and individual neurons as a reordering of gene expression profiles, synaptic strength, and circuit connectivity. Reorganization reflects the adaptation of the network to a changing environment, either encoding new information or compensating for injury-induced degeneration. Reorganization following a brain injury inevitably perturbs the dynamic equilibrium, which can affect many aspects of neuronal structure and function, including intrinsic neuronal properties, synaptic interactions, and connectivity within and between networks. The cellular and molecular landscape can impose limits on plasticity and regenerative capacity of the adult brain.

A variety of injury models have been used to examine the response of the brain, such as crush injuries to peripheral nerves, cortical stab wounds, and spinal cord injury (SCI) models. For example, SCI models have been extensively examined for factors that

limit the growth of axons following damage or transection (Tuszynski and Steward, 2012; Akbik et al., 2012). Here we focus on the perforant path lesion, a brain injury model that interrupts the main excitatory input to the dentate gyrus of the hippocampus. This model has the experimental advantages of a highly laminated structure and allows analysis of not only the axonal response to injury, but also changes in dendrite morphology and synaptic reorganization. This classic lesion provided some of the first evidence for structural plasticity following injury in the CNS, and also provides an opportunity to examine the injury response of some of the most highly plastic neurons in the brain, adult-generated newborn granule cells. We first highlight features of neuronal and non-neuronal plasticity that drive adaptive and maladaptive changes in brain circuits. Subsequently, we discuss the perforant path lesion model as an example of injury-induced plasticity in the adult brain.

Synaptic and dendritic plasticity in the injured brain

It is well known that synaptic and dendritic plasticity occur in sensory systems following deprivation, and in motor systems following disuse (Hickmott and Steen, 2005; Hofer et al., 2006). However, spines and dendrites also undergo dynamic functional and structural changes following acute injury or neurodegeneration. These changes fall into several categories, including retraction of dendritic arbors following loss of inputs; compensatory increases in dendritic arbors in domains of afferent inputs unaffected by the injury; transient changes in spine densities; and alterations in the types or shapes of dendritic spines. For example, dendritic reorganization occurs after ischemia (Hosp and Luft, 2011), but the degree of remodeling depends on the proximity of dendrites to the site of infarction. Brown et al. (2010) reported dendritic retraction following ischemic injury in

cortex adjacent to the infarct, but compensatory dendritic outgrowth away from the site of injury. On the other hand, Mostany and Portera-Cailliau (2011) saw only dendritic pruning at cells in peri-infarct cortex. Dendritic spine density is also sensitive to ischemia (Brown et al., 2008) and spinal cord injury (Kim et al., 2006), both of which lead to a reduction in spine density and elongation of the remaining spines, albeit at different time scales. Because spine elongation is associated with synaptogenesis, the underlying mechanisms for these changes are in many cases thought to be sensitive to injury-induced alterations in network activity. For example, the intense neuronal activity associated with kainate-induced seizures triggers beading of dendrites and subsequent loss of spines (Drakew et al., 1996; Zeng et al., 2007). However, brief seizure activity can also trigger more 'physiological' responses, such as the induction LTP in CA3 pyramidal neurons (Ben-Ari and Gho, 1988). This dichotomy suggests that network responses to injury are likely to be context-specific, and may reflect exaggerations of the normal adaptive responses to stimuli (Figure 1).

Sprouting and the axonal response to injury

Axons can also recover and/ or reorganize following injury, although the extent of regeneration varies. In the peripheral nervous system, regenerating axons can grow long distances and re-innervate their targets, thus leading to functional recovery. However, regenerating axons in the central nervous system are often unable to penetrate the lesion, thus limiting long-range axonal outgrowth. Perhaps most extensively studied examples are experimental models of spinal cord injury, in which cut or damaged axons of the corticospinal tract form retraction bulbs and eventually move away from the lesion site unable to penetrate the gliotic scar (Hill et al., 2001; Fitsch and Silver, 2008). However, if

the transection is incomplete, sprouting of uninjured axons, as well as cortical reorganization can lead to partial functional recovery following injury (Raineteau and Schwab 2001; Maier and Schwab 2006). The difference in the capacity for axonal regeneration in the peripheral and central nervous systems reflects differences in intrinsic neuronal properties (Liu et al., 2011) and in post-injury changes in the extracellular environment (Giger et al., 2010). Whereas degenerating material in the peripheral nervous system is effectively cleared following injury (Chen et al., 2007; Bosse, 2012), these processes are much slower in the central nervous system (Vargas and Barres 2007; Giger et al., 2010), and may thus interfere with reinnervation of deafferented target areas. Axonal structural plasticity may also be maladaptive following injury, as can occur in the brain of patients with temporal lobe epilepsy. Following seizures, mossy fiber axons sprout recurrent collaterals that synapse onto granule cell dendrites in the inner molecular layer, thereby increasing excitatory connectivity within the dentate gyrus (Sutula and Dudek, 2007). Such structural reorganization can lead to an imbalance between excitation and inhibition in the circuit, which may underlie recurrent seizures.

Glial and extracellular response to brain injury

Glial cells are intimately involved in function and plasticity of the healthy adult brain; however, their contribution to recovery following injury is even more striking. Brain and spinal cord trauma, neurodegeneration, ischemia, and infection all stimulate morphological and molecular changes in surrounding astrocytes, often referred to as reactive gliosis. Depending on the triggering mechanism and its duration, the glial response can promote or inhibit recovery (Figure 2; Sofroniew, 2009). For example, during mild insults to the CNS, such as the immune reaction that follows a viral infection or as

occurs in areas distant to a lesion site, astrocytes hypertrophy but remain tiled (Figure 2B; Wilhelmsson et al., 2006). In such cases, tissue reorganization is minimal, and reactive astrogliosis resolves within a few weeks. However, following more severe CNS insults such as major trauma, stroke, or neurodegeneration, astrocytes acquire expansive reactive morphology, and their processes extend beyond their original borders (Sofroniew and Vinters, 2010). The resulting dense network of newly proliferated astrocytes can recruit other cell types, including fibromeningeal cells and microglia, resulting in the formation of a permanent and impenetrable glial scar (Figure 2C). Reactive astrogliosis has traditionally been viewed as maladaptive because gliosis can contribute to glutamate toxicity (Takano et al., 2005), generation of seizures (Tian et al., 2005; Jansen et al., 2005), inflammation (Brambilla et al., 2005), and chronic pain (Milligan and Watkins, 2009). Furthermore, the glial scar can inhibit axonal regrowth (Silver and Miller, 2004). Interestingly, astrocytes have also been implicated in lymphatic drainage in the central nervous system, a process that is likely disrupted during reactive astrogliosis (Hamby and Sofroniew, 2010; Iliff et al., 2012). Although experimental interference with glial scar formation can increase axonal regeneration, it can also increase lesion size and diminish functional recovery (Sofroniew, 2009). The latter suggests that the presence of reactive astrocytes, depending on the context, can have positive effects on neuronal reorganization by stabilizing the extracellular ion balance, reducing seizure likelihood, and dampening excitotoxicity (Rothstein et al., 1996; Swanson et al., 2004; Koistinaho et al., 2004).

An important product of glial cells, the extracellular matrix (ECM), surrounds the synapse (Dityatev et al., 2006; Dityatev et al., 2010b) and is instrumental in synaptic plasticity both in the healthy and injured brain (Dityatev, et al., 2010a; Dityatev and Fellin,

2008; Frischknecht and Gundelfinger, 2012). For example, astrocyte-derived ECM components, such as thrombospondins, initiate synaptic development (Christopherson et al. 2005; Xu et al., 2010) as well as regulate synaptic plasticity (Eroglu, 2009). In addition, inactive perisynaptic matrix metalloproteases are transiently activated following induction of LTP in the hippocampus (Bozdagi et al., 2007; Nagy et al., 2006). Because extracellular matrix components at least partially originate from glia, activation of astrocytes following injury can affect expression of ECM molecules and thus post-injury neuroplasticity. Like the astroglial response, these molecules can have a dual role in recovery. For example, expression of chondroitin sulfate proteoglycans is beneficial in containing the size of a lesion, but a few days later can inhibit axonal growth (Zuo et al., 1998; Galtrey and Fawcett, 2007; Rolls et al., 2008). Likewise, matrix metalloproteinases have a positive effect on reactive synaptogenesis when transiently upregulated (Falo et al., 2006), but persistent and widespread MMP expression leads to regression of dendritic spines, degeneration of synapses, and neuronal apoptosis (Falo et al., 2006; Huntley, 2012). The complexity of the glial and ECM response underscores both the potential for, and the limitations of, repair and regeneration following brain injury.

Perforant path lesion as a model of post-injury plasticity in the adult brain

Advantages of model

Lesioning of the perforant path was one of the first models to document injury-induced plasticity in the adult brain. This lesion of the major excitatory input into the dentate gyrus affects the trisynaptic hippocampal circuit, disrupting the distinctly unidirectional progression of excitatory activity arriving from other brain regions (Knowles, 1992). Because the entorhinal lesion site is distant from the dentate gyrus, local

degenerative/ inflammatory effects at the lesion site can be easily separated from the regenerative effects of post-lesion circuit reorganization. The simple cyto- and fiber architecture and lamination pattern of the dentate gyrus also provides an experimental advantage because the lesion affects only one of many afferent fiber systems. Each afferent input terminates in a specific lamina of the molecular layer (Hjorth-Simonsen and Jeune, 1972) and each is functionally and molecularly distinct (Leranth and Hajszan, 2007). This diversity allows a comparison of heterotypic and homotypic sprouting post-lesion (Ramirez, 2001), as the balance of these inputs may have a role in functional recovery.

Post-lesion circuit reorganization – axons

Afferents to the dentate gyrus have diverse origins and neurotransmitter phenotypes that converge on the hippocampus (Figure 3, left panel). Glutamatergic inputs to the outer 2/ 3^{rds} of the dentate molecular layer include the entorhinodentate perforant path (Hjorth-Simonsen and Jeune, 1972; van Groen et al., 2003) and a weak species-specific commissural projection from the contralateral entorhinal cortex (van Groen and Kadish, 2002). Glutamatergic input to the inner molecular layer consists of the mossy cell axons from the commissural/ associational (C/ A) collaterals (Gottlieb and Cowan, 1973; Soriano and Frotscher, 1994). These excitatory synaptic inputs are complemented by cholinergic, GABAergic, noradrenergic, dopaminergic, and serotonergic projections that terminate throughout the molecular layer (Leranth and Hajszan, 2007). Because the entorhinodentate projection is the largest glutamatergic afferent fiber system, a perforant path lesion severs the majority of excitatory innervation in the dentate gyrus, thus effectively denervating the outer 2/ 3^{rds} of the molecular layer and vacating 80-90% of all synapses in that region (Matthews et al., 1976a**;** Steward and Vinsant, 1983). Subsequent degeneration of

excitatory synapses triggers compensatory axonal sprouting that can be either homo- or heterotypic, depending on the neurotransmitter involved. Homotypic sprouting, i.e. glutamatergic axons, includes the weak entorhinodentate projection from the contralateral, non-lesioned entorhinal cortex that normally terminates in the deafferented region (Steward et al., 1973; Steward, 1976a; Cotman et al., 1977; Deller et al., 1996a), and the glutamatergic component of the commissural/ associational fiber system that normally terminates in the inner molecular layer (Gall and Lynch, 1981; Deller et al., 1996b). Although homotypic reactive sprouting can partially replace lost synapses in the denervated zone (Marrone et al., 2004b), the degree of excitatory reinnervation is species-specific (del Turco et al., 2003; Deller et al., 2007). Homotypic sprouting can also partially restore postsynaptic function, as well as ameliorate some behavioral deficits (Ramirez, 2001).

Lesion of the perforant path also triggers reactive heterotypic sprouting of non-glutamatergic afferents, such as the cholinergic septodentate projection. Sprouting of this fiber system was initially detected as an increase in acetylcholinesterase (AChE) staining in the denervated zone (Figure 4, left panel; Lynch et al., 1972; Nadler et al., 1977a,b). The width of the AChE band was subsequently correlated with the extent of the lesion and the time course of reorganization (Zimmer et al., 1986; Steward, 1992), and therefore has been used as a marker for the extent and completeness of a perforant path lesion. Although the increase in AChE staining density in the denervated region has been corroborated (Vuksic et al., 2011), it remains uncertain whether this increase indicates actual cholinergic sprouting or is a consequence of post-lesion tissue shrinkage (Phinney et al., 2004). Perforant path lesions also cause sprouting of GABAergic C/ A axons (Deller et al., 1995),

as well as trigger receptor reorganization and new inhibitory synapse formation on mature granule cells (Simbürger et al., 2000; 2001). In combination with a decrease in glutamatergic innervation, these results suggest that lesions of the perforant path can alter the excitation/ inhibition balance in the dentate gyrus (Clusmann et al., 1994), which can potentially complicate functional recovery. However, heterotypic sprouting may also serve an adaptive purpose in post-lesion circuit reorganization by reinnervating vacated synapses and thus preventing or delaying transsynaptic cell death.

Post-lesion circuit reorganization – dendrites/spines

Interruption of the perforant path denervates one of the main inputs to the principal neurons in the adult dentate gyrus – the mature granule cells. These cells are part of the trisynaptic hippocampal circuit, with their dendrites receiving afferent input from the entorhinal cortex and other brain regions, and their axons forming the mossy fibers that synapse with pyramidal cells in CA3. The two subdivisions of the perforant path, medial and lateral, synapse with mature granule cell dendrites in the middle and outer molecular layers, respectively (Hjorth-Simonsen and Jeune, 1972; van Groen et al., 2003). Following a perforant path lesion, these axons degenerate (Matthews et al., 1976a), thus eliminating the majority of excitatory input onto dendritic segments in the outer two thirds of the molecular layer (Figure 3). The loss of excitatory input initiates a series of morphological and functional changes in the post-synaptic mature granule cells. Dendrites retract, resulting in less complex dendritic arbors in the denervated region (Caceres and Steward, 1983; Diekmann et al., 1996; Schauwecker and McNeill, 1996; Vuksic et al., 2011). Distal dendritic segments are progressively lost for periods up to 90 days post-lesion, with some recovery by 180 days post-lesion (Figure 4, right panel). However, this recovery

most likely reflects the extension of existing dendrites, rather than formation of new branches (Vuksic et al, 2011). Similarly, the density of dendritic spines – the postsynaptic target of the entorhinodentate projection – is significantly reduced following lesion, but only in the deafferented zone (Parnavelas et al., 1974; Vuksic et al., 2011). Surprisingly there is relatively little data assessing the functional state of the dentate gyrus circuit following such lesions. However, spontaneous neural activity in mature granule cells post-lesion appears to transiently decrease immediately following lesion, then gradually returns to pre-lesion levels by 8 days (Reeves and Steward, 1988). The source of this activity presumably reflects reorganization of synaptic inputs that follows excitatory reinnervation by sprouting afferents.

Post-lesion glial and extracellular matrix (ECM) response

Post-lesion structural reorganization in the adult dentate gyrus is influenced by the post-injury dynamics of the extracellular environment. Reactive gliosis following perforant path lesion is both rapid and sustained, and is considered adaptive in this context**.** Gliosis serves to clear degenerating debris, maintain laminar borders, and to aid reactive synaptogenesis in the deafferented region. For example, microglia proliferate and acquire reactive morphology within three days post-lesion and return to baseline by day ten (Hailer et al., 1999). However, activation of astrocytes in the denervated zone is delayed relative to microglia and persists for at least 30 days post-lesion (Hailer et al., 1999). Together, microglia and astrocytes participate in phagocytosis of degenerating axons (Bechmann and Nitsch, 2000) and may regulate axon sprouting and reactive synaptogenesis (Gage et al., 1988; Ullian et al., 2004). The efficiency of phagocytosis following injury, especially of degenerating myelinated axons, generally correlates with

the degree of regeneration in the CNS (Neumann et al., 2009). Because the glial response is limited to the denervated region, with relatively little reactive gliosis in the inner molecular layer, this lamina-specific reaction may underlie the lack of sprouting across laminar borders into the denervated zone. Reactive gliosis also triggers lamina-specific changes in the extracellular matrix, which may affect the maintenance of laminar borders following lesion. For example, tenascin-C (Deller et al., 1997) and chondroitin sulfate proteoglycans (Haas et al., 1999) are secreted by reactive astrocytes following perforant path lesion. Both these factors affect axonal outgrowth during development and following injury (Bovolenta and Fernaud-Espinosa, 2000; Bartus et al., 2012). Similarly, reactive astrocytes can secrete thrombospondins or matrix metalloproteases (Christopherson et al., 2005; Warren et al., 2012), which can provide a scaffold for lesion-induced synaptogenesis (Deller et al., 2001; Mayer et al., 2005).

In summary, lesion of the perforant path eliminates the main excitatory input in the outer two-thirds of the dentate molecular layer, thus partially denervating dendrites of mature granule cells. This lesion model illustrates both the potential for regeneration in the CNS, but also some of the limits. Within two weeks post-lesion, remaining afferent homo- and heterotypic systems can sprout, but reorganization of axons and synaptic terminals is limited by laminar borders, which are likely maintained by lesion-induced gliosis and changes in the extracellular matrix. Experiments described in this dissertation revisit the classic perforant path lesion model, but also include an additional component of the hippocampal circuit in the adult brain – ongoing neurogenesis in the dentate gyrus. Specifically, we delineate the maturation and functional integration of newborn granule cells following removal of their main excitatory input. The dendritic spine reorganization

and *de novo* synaptogenesis we observed following lesion bring into light several important aspects of the role of excitatory activity in dendritic outgrowth and the formation of dendritic spines. Similarly, these results provide a foundation for further exploration of signals that may serve as replacements for excitatory activity during synaptogenesis.

INTRODUCTION: FIGURES

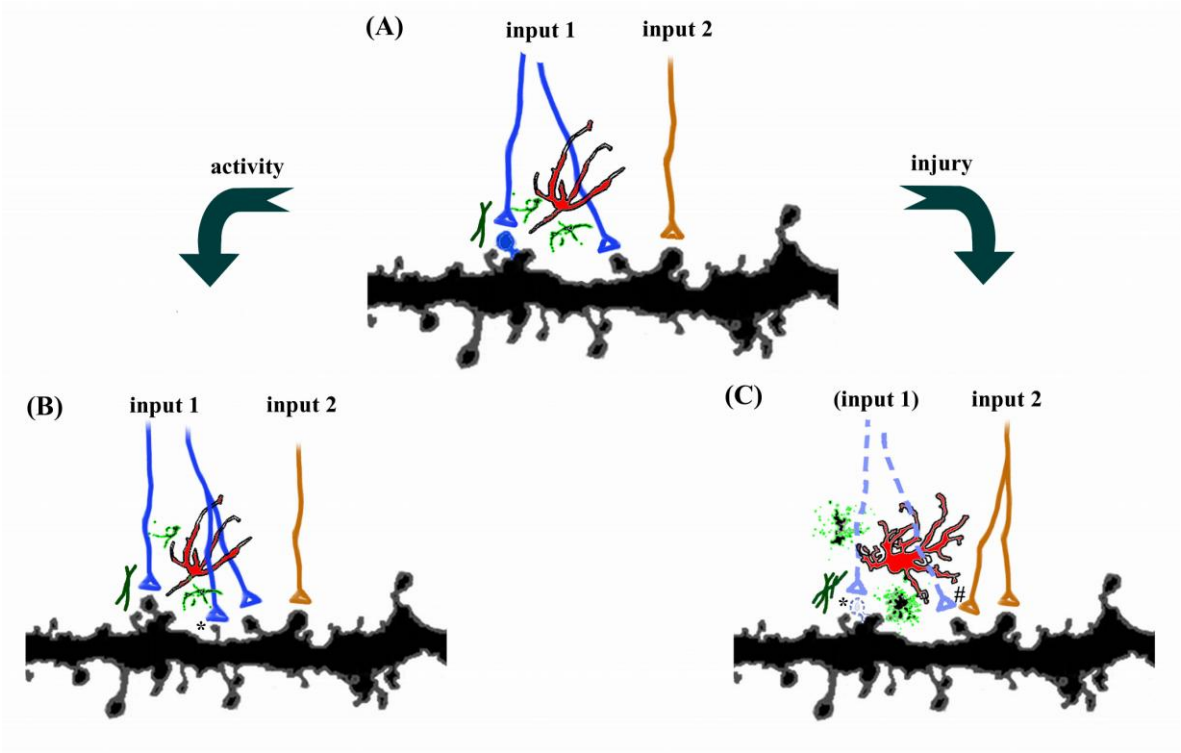

Figure 1 – Plasticity in the central nervous system.

(A) Axons from two different pathways synapse onto spines on the same dendrites. Each synapse is surrounded by astrocytes (red), microglia (green), and extracellular matrix. **(B)** Increases in activity, such as occur during learning, can strengthen connections by axonal sprouting (blue) as well as formation of new filopodia and dendritic spines (*). Adjacent afferents, surrounding glia, and extracellular matrix are relatively unaffected. **(C)** Disruption of afferents, such as following injury, leads to degeneration of damaged axons (dotted lines), activation of astrocytes, microglia, and extracellular matrix, as well as retraction of dendritic spines (*). Compensatory sprouting of undamaged afferents from

another brain region can form new synapses, including contacts with denervated spines (#).

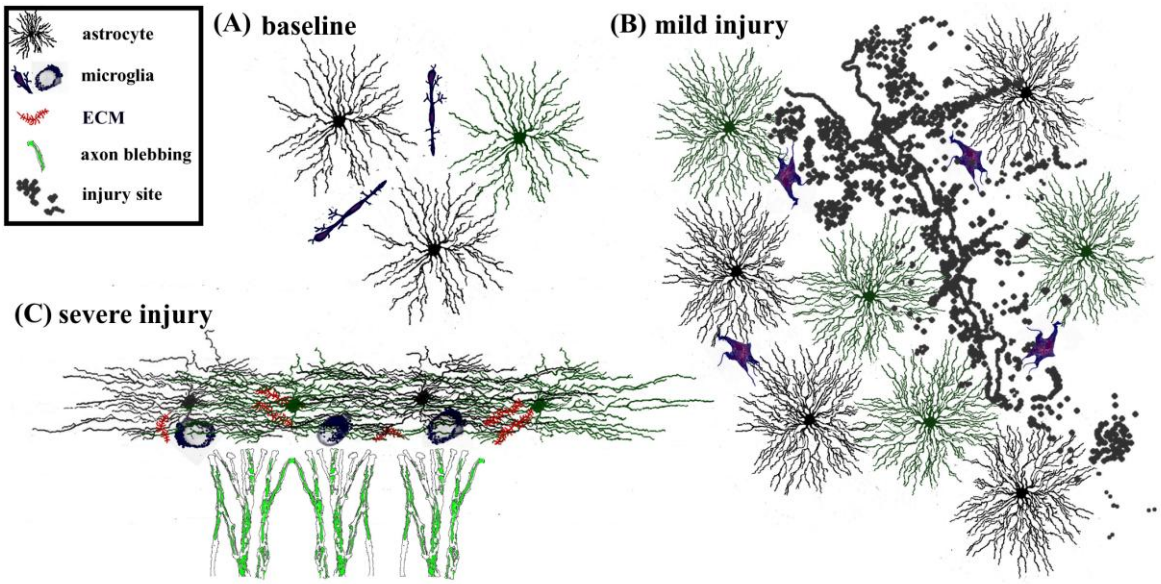

Figure 2 – Adaptive and maladaptive glial changes following injury.

The degree of astrogliosis depends on the severity of injury. **(A)** Glia and extracellular matrix at baseline. Astrocytes are tiled, i.e. their processes do not overlap with neighboring astrocytes. Microglia are interspersed throughout the region. **(B)** Mild injury triggers activation of microglia and astrocytes. Astrocytes and microglia increase in size and acquire more complex process morphology, but astrocytes maintain their tiled formation. This response is considered adaptive because it limits the spread of degeneration away from the site of injury, dampens excitotoxicity, and promotes tissue regeneration. Such glial activation typically resolves within a few weeks after a mild, transient injury. **(C)** In contrast severe injury causes reactive astrocytes to invade neighboring domains, recruit reactive microglia, and increases secretion of extracellular molecules. This results in formation of a persistent glial scar that can be impenetrable to sprouting axons.

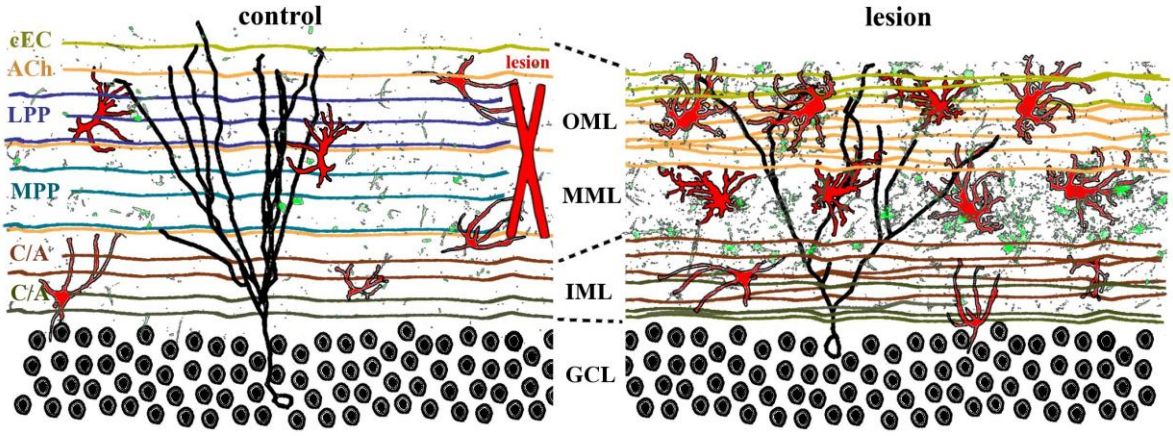

Figure 3 – Lamina-specific axon sprouting and reactive gliosis following perforant path lesion.

The molecular layer of the adult dentate gyrus is a highly laminated structure with afferent inputs segregated based on their origin and neurotransmitter phenotype. All afferent axons form either symmetrical or asymmetrical synapses with mature granule cells (black traces) in a lamina-specific manner. *Left panel:* The inner molecular layer (IML) is occupied by the glutamatergic commissural/ associational fibers (C/ A) that arise from mossy cells in the ipsi- or contralateral hilus. The middle and outer molecular layer (MML, OML) are occupied predominantly by the glutamatergic perforant path (MPP, LPP), which originates in the ipsilateral entorhinal cortex. In rats (but not in mice), there is also a crossed glutamatergic projection from the contralateral entorhinal cortex (cEC) that terminates in the outermost molecular layer (OML). Cholinergic axons (ACh) from the septal nuclei/ diagonal band of Broca are interspersed throughout the molecular layer, as are astrocytes (red) and quiescent microglia (green). *Right panel:* Lesion of the entorhinal cortex (red X, left panel) transects both medial and lateral perforant path, thus eliminating the majority of excitatory input into the dentate gyrus. Degeneration of these axons induces lamina-specific sprouting of the remaining septohippocampal (ACh), commissural/ associational (C/ A), and crossed entorhino-dentate (cEC) afferents. In the rat, the contralateral entorhino-dentate projection (cEC) partially restores excitatory innervation of the mature granule cells (black trace), however, their dendritic length and complexity are still reduced. The microglia (green) and astrocytes (red) become 'activated' following lesion, but this response is limited to the deafferented zone. Note the expansion of the inner molecular layer and shrinkage of the outer layers.

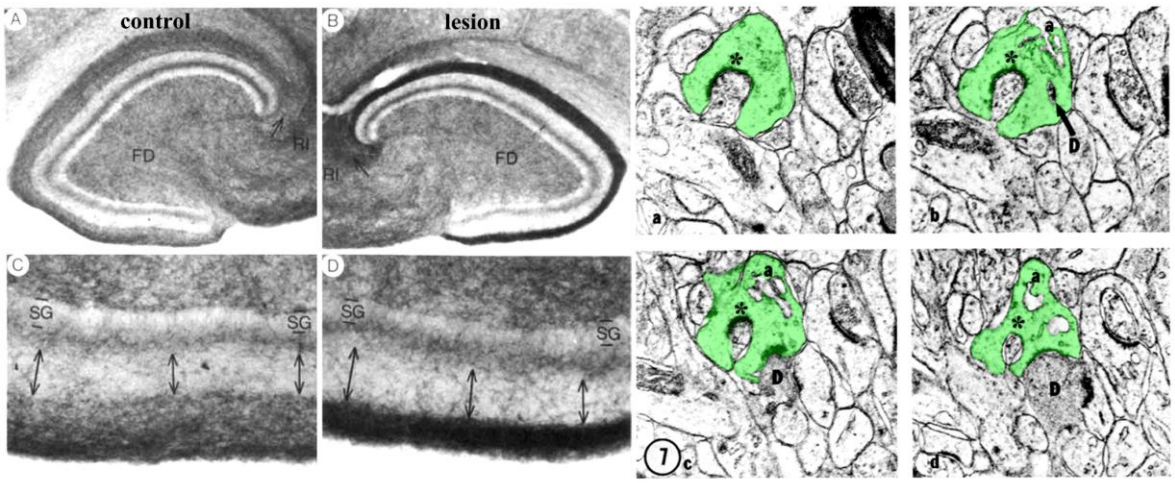

Figure 4 – Structural plasticity following perforant path lesions.

Left panels (modified from Steward, O. and J. A. Messenheimer, 1978): Mature cat hippocampus histochemically stained for acetyl cholinesterase (AChE) activity at 60 days post-lesion. The density of AChE is dramatically increased in the denervated outer molecular layer (top right, dark band), consistent with sprouting of the cholinergic septohippocampal axons following lesion. Also note that the thickness of the inner molecular layer is increased due to sprouting of the glutamatergic commissural/ associational fibers (bottom right, double arrows). *Right panels* (modified from Matthews, D. A., Cotman, C., and Lynch, G., 1976b): Ultrastructural evidence for synaptic regeneration in the denervated zone at 60 days post-lesion in the mature rat. Serial sections through a complex spine (green) show synaptic contacts with a degenerating bouton (D) as well as with a regenerating axon (*). a = spine apparatus.

CHAPTER 1

NEURAL INJURY TRIGGERS A BIPHASIC RESPONSE IN ADULT-GENERATED NEURONS IN THE DENTATE GYRUS

(These data will be published in the Journal of Neuroscience in 2013)

Introduction

Traumatic brain injury, neurodegeneration, and ischemia all involve denervation, the extent of which contributes to the severity of clinical symptoms. However, brain injury can also stimulate plasticity. An example of such plasticity in the adult brain is the synaptic reorganization following lesions in the entorhinal cortex, which irreversibly interrupt the main excitatory input into the dentate gyrus – the perforant path. The dentate gyrus provides a particularly advantageous model system for examining brain injury because its highly laminated molecular layer segregates inputs from different sources. Perforant path axons from the medial and lateral entorhinal cortex terminate in the middle and outer third of the molecular layer, respectively (Hjorth-Simonsen and Jeune, 1972; Hjorth-Simonsen, 1972, van Groen et al., 2003), where they synapse with apical dendrites of mature granule cells. When these inputs are severed, remaining intact fiber systems that also synapse onto mature granule cells reorganize by sprouting and reactive synaptogenesis (Deller and Frotscher, 1997). These changes are maximal within two weeks post-lesion but gradually stabilize by several months post-lesion (Vuksic et al., 2011).

In addition to mature cells, there is ongoing neurogenesis in the dentate gyrus, generating 5-10 thousand new granule cells per day (Cameron and McKay, 2001). A subset of these newborn neurons survive and integrate into the hippocampal circuit, show

enhanced short-term synaptic plasticity, and may contribute to normal function of the hippocampus (Dayer et al., 2003; Ge et al., 2008). Because newborn cells are exquisitely sensitive to intrinsic and extrinsic stimuli (van Praag et al., 1999; Overstreet et al., 2004; Tashiro et al., 2007; Balu and Lucki, 2009; Ming and Song, 2011), they are a potentially important source of neurons for replacement and repair following neural injury. Newborn granule cells go through a series of highly stereotyped stages, during which they extend their dendrites through the molecular layer, develop spines, and acquire excitatory synaptic inputs over a period of several weeks (van Praag et al., 2002; Overstreet-Wadiche and Westbrook, 2006). This pattern of functional maturation provides an opportunity to examine whether newborn cells integrate into a recently deafferented circuit.

Here, we focused on a population of newborn granule cells that were dividing at the time of a unilateral perforant path lesion. We hypothesized that new neurons would show enhanced structural plasticity compared to mature neurons. To identify newborn granule cells we used a POMC-EGFP transgenic mouse, in which EGFP expression is driven by transient activity of the pro-opiomelanocortin (POMC) promoter that labels these cells at approximately 14 days post-mitosis (Overstreet et al., 2004b). We also used intrahippocampal injections of a retrovirus expressing GFP to label cohorts of newborn neurons at later time points. The completeness of the lesion was confirmed morphologically and by the absence of extracellular field responses in the outer molecular layer in acute brain slices. In the ipsilateral dentate gyrus, lesions caused proliferation of newborn neurons by 2 weeks, followed by a lamina-specific rearrangement of dendritic spines and excitatory synaptic activity by 3 weeks post-lesion. Surprisingly, confocal images and immunoelectron micrographs of the denervated zone revealed that newborn

neurons formed new dendritic spines post-lesion without normal apposing presynaptic terminals.

Methods

Mice: All procedures were performed in accordance with OHSU IACUC and Biosafety committee protocols and in accord with the NIH guidelines for handling of animals. C57Bl6 mice were six to eight weeks of age at the time of the procedure. Both male and female mice were included, and were derived from multiple breedings. POMC-EGFP transgenic mice in C57Bl6 background were used for studies of newborn granule cells at 14 days post-mitosis, the peak of EGFP expression (Overstreet et al., 2004b). We also used retroviral labeling of wild-type C57Bl6 mice for visualization of newborn granule cells at 21 days post-mitosis, and lentiviral labeling for visualization of mature granule cells at 21 days post-lesion. For GFP labeling of newborn granule cells, we used a replication-deficient Moloney Murine Leukemia Virus-based retroviral vector (Lewis and Emerman, 1994) designated pRubi (Retrovirus with internal ubiquitin promoter, Luikart et al., 2011b). Isoflurane-anesthetized wild-type mice received bilateral stereotaxic injections directly into the dorsal hippocampus (2μl per hemisphere, see below). For GFP labeling of mature granule cells, we used a lentiviral vector that contains the HIV-1 Flap element, the human Ubiquitin-c promoter, GFP, and the Woodchuck hepatitis virus posttranscriptional regulatory element (FUGW, Lois et al., 2002**;** Luikart et al., 2011a). Volume for lentiviral injections was 1 μl per hemisphere. Stereotaxic coordinates were: AP -1.9, LM ±1.1, DV -2.5 and -2.3, with an injection rate of 0.25μl per minute. The needle was left in place for one minute before withdrawing from the injection site. Viral particles were prepared using established protocols with titers of 1-10 X 10^6 (Luikart et al., 2011a).

Unilateral Lesions of the Perforant Path: Mice were anesthetized in an induction chamber filled with 4% isoflurane/ oxygen and placed in a Kopf stereotaxic apparatus when

rendered unresponsive. During surgery, 2% isoflurane/ oxygen mixture was continuously administered through a nose cone. Prior to incision, the scalp was treated with 2% lidocaine, iodine mixture, and a double antibiotic. Skull was exposed and a rectangular access window was drilled using a 0.275mm diameter carbide drill (Kemmer Praezision, Placentia, CA), starting 2mm lateral to lambda, 1mm rostral to the transverse suture, and spanning the width of the hemisphere. Lesion was performed manually, using a 15° aluminum microscalpel (No. 715, Oasis Medical, San Dimas, CA), with medial to lateral path trajectory, at a depth of ~ 4.5mm. Care was taken to avoid scraping the scalpel along the bottom of the skull. Lesions alternated between left and right hemisphere with the contralateral hemisphere serving as the control. In preliminary experiments, a few animals did not survive the procedure, however refinement of the lesion site resulted in no mortality. For morphological analysis at 14 and 21 days post-lesion, animals were deeply anesthetized with 2% Avertin (2,2,2-Tribromoethanol, Sigma-Aldrich, St. Louis, MO), transcardially perfused with PBS + 4% sucrose followed by 4% paraformaldehyde (PFA) + 4% sucrose. Brains were extracted and post-fixed overnight in 4% PFA+sucrose at 4°C. After fixation, each brain was split in the coronal plane just anterior to the site of the lesion and each half was sectioned separately, using a vibratome (VT-1000S, Leica Microsystems Inc., Buffalo Grove, IL). The rostral half, containing the dorsal hippocampus, was sectioned coronally (100μm sections) and these sections were used for all morphological analysis. The caudal half, containing the lesion site, was cut horizontally into serial 300μm sections to assess the extent of lesion. Animals were excluded from analysis if the lesion injured the ventral hippocampus, which led to hippocampal atrophy, or if the lesion was incomplete (see Figure 1). A lesion was considered complete if it spanned the entire height of the entorhinal cortex and was visible even in the most ventral of the horizontal sections.

Immunohistochemistry: 100μm coronal sections were permeabilized for 30 minutes with 0.4%-TritonX in PBS (PBS-T), blocked for 30 minutes with 10% Horse Serum in PBS-T, and stained overnight with primary antibody in 1.5% Horse Serum/ PBS-T. Stains requiring secondary antibodies were washed in PBS and incubated with secondary antibody in 1.5% Horse Serum/ PBS-T for 4 hours at room temperature. Primary antibodies: rabbit anti GFP (Alexa 488-conjugated; 1:500; A21311; Invitrogen, Carlsbad, CA); rabbit anti glial fibrillary acidic protein (GFAP; 1:500, Z-0334; DAKO, Carpinteria, CA); rabbit anti vGlut1 (1:500; 135 303; Synaptic Systems, Goettingen, Germany); rabbit anti vGlut2 (1:400; 135 404; Synaptic Systems, Goettingen, Germany). Secondary antibodies (1:200 dilution): goat anti rabbit (Alexa 568; A11011; Invitrogen, Carlsbad, CA). Sections were mounted on glass slides and coverslipped using VectaShield with DAPI (H-1200; Vector Laboratories Inc., Burlingame, CA).

Imaging and Morphological Analysis: Imaging was done on an LSM 7 MP laser scanning microscope (Carl Zeiss MicroImaging; Thornwood, NY). All cell counting, dendritic arbor/ spines tracing, and Sholl analysis were done manually with ImageJ (National Institutes of Health; Bethesda, MD). At 14 day post-lesion, sections from POMC-EGFP mice were imaged with: 40x objective, 0.7x optical zoom, z-stacks of 50μm, 1μm between planes. At 21 days post-lesion, sections from retro- and lentiviral-injected mice were imaged for dendritic arborization with a 40x objective and 0.7x optical zoom. Thickness of z-stack was designed to accommodate the dendritic span of labeled granule cells, with 1μm distance between image planes. For analysis of spine density of newborn and mature granule cells at 21 days post-lesion, we used a 63x objective with 3x optical zoom. Span of

z-stack was tailored to the thickness of a single segment of dendrite with 0.5μm distance between planes. Dendritic spines were imaged and analyzed in inner and outer molecular layers of the dentate gyrus. Laser intensity and gain were adjusted to accommodate staining efficiency, but the same microscope settings were used for both control (non-lesioned) and the lesioned hemisphere.

BrdU: For proliferation measurements, two injections of BrdU (300 mg/ kg) were administered to POMC-EGFP mice at three separate intervals post-lesion: (i) 0 and 4 hours post-lesion (hpl), (ii) 16 and 20 hpl, and (iii) 40 and 44 hpl. Animals were perfused with sucrose-containing PBS followed by PFA (see above) at 8, 24, and 48 hours post-lesion (four hours after the last BrdU injection). For survival measurements, BrdU injections were at 40 and 44 hpl, and the tissue was examined at 28 days post-lesion. For BrdU immunostaining, sections were washed twice in KPBS for 10 minutes each. Antigen retrieval was performed using an acid/ base sequence: 30 minutes in 2N HCl (at 36°C) followed by 10 minutes in pH 8.5 KPBS (at room temperature). The sections were then permeabilized for 30 minutes in 0.4% KPBS-T and blocked for 30 minutes with 5% Horse Serum (HS) in KPBS-T. Primary antibody (rat anti BrdU; ab6326; AbCam, Cambridge, MA) was applied at 1:2000 in 5% HS/ KPBS-T overnight at 4°C. The sections were washed in KPBS and incubated for 4 hours with Rhodamine Red secondary antibody (goat anti rat; 112-295-003; Jackson ImmunoResearch, West Grove, PA), at 1:200 in 5% HS/ KPBS-T at room temperature. The sections were subsequently stained with Alexa 488-conjugated rabbit anti GFP (as described above). Sections were imaged on a Zeiss LSM 780 confocal microscope, using a 20x objective. Z-stacks were 60μm, with image planes 2μm apart. All BrdU-positive cells within the granule cell layer of the dorsal hippocampus were counted

for every third 100μm section and averaged for each animal. Because all sections contained both hemispheres, lesion and control hippocampi were processed in parallel.

Electrophysiology: Extracellular field potentials and whole cell recordings were performed at 14 days post-lesion, from acute slices of dorsal hippocampus, at the same antero-posterior level used for morphometric analysis. The animals were deeply anesthetized with an intraperitoneal injection of Avertin (2,2,2-Tribromoethanol, Sigma-Aldrich, St. Louis, MO) and transcardially perfused with ice-cold cutting solution, containing 110mM choline Cl, 7mM $MgCl_2$, 2.5mM KCl, 1.25mM NaH_2PO_4*$2H_2O$, 0.5mM $CaCl_2$, 1.3mM Na-ascorbate, and 25mM $NaHCO_3$, bubbled with 95% O_2-5% CO_2. For field recordings, 400 μm coronal slices were made using a Leica vibratome in artificial cerebrospinal fluid (ACSF) containing 119 mM NaCl, 2.5 mM KCl, 2.5 mM $CaCl_2$, 1.3 mM $MgSO_4$, 1 mM NaH_2PO_4, 26.2 mM $NaHCO_3$, and 11 mM glucose, bubbled with 95%O_2-5%CO_2. After 1 hour recovery, field potentials were recorded with ACSF-filled 2-3MΩglass pipettes placed in the outer molecular layer of the dentate gyrus. In pilot experiments in the deafferented dentate gyrus, we looked for field excitatory postsynaptic potentials (fEPSPs) in multiple locations and at varying depths in the supra and infrapyramidal blade, and were unable to elicit responses at the usual range of stimulus intensities. To quantify fEPSPs we constructed input/ output curves after stimulation of the infrapyramidal blade, thus reducing contamination from the adjacent CA1 region. Stimuli were delivered at 0.1Hz (duration 100 μs, AMPI Iso-Flex constant current stimulator) via a bipolar tungsten electrode (FHC, Bowdoin, ME) placed in the outer molecular layer, approximately 150 μm deep into slice and approximately 500 μm from the recording electrode. At each stimulus intensity, ten responses were averaged using IgorPro. The amplitudes of the fiber volley

and initial slope of the fEPSPs were graphed relative to the stimulation intensity. For each slice, responses were recorded in the dentate gyrus from the lesioned and non-lesioned hemispheres. For whole-cell recordings, the hemipheres were separated and sectioned at 350μm in the transverse hippocampal plane. Slices were stored and recordings performed in a solution containing 125mM NaCl, 2.5mM KCl, 2.0mM $CaCl_2$, 1.0mM $MgCl_2$, 1.25mM NaH_2PO_4, 25mM $NaHCO_3$, and 25 mM glucose, bubbled with 95%O_2-5%CO_2. For mEPSC recordings, we added 10μM SR95531 to block $GABA_A$ channels and 1μM tetrodotoxin to block action potentials. The Cs-gluconate whole-cell pipette solution contained 100mM gluconic acid, 0.2mM EGTA, 5mM HEPES, 2mM Mg-ATP, 0.3mM Li-GTP, pH=7.2, 295mOsm (pH to 7.2 using 50%CsOH for a final concentration of 100-120 Cs-gluconate). Series resistance (5–20 MΩ) was monitored, and experiments were discarded if the resistance increased by >10 MΩ. Currents were filtered at 4 kHz and sampled at 40 kHz (MultiClamp 700A Molecular Devices, Union City, CA). mEPSCs were detected using a template with rise time=1ms, decay time=6ms, baseline=10ms, length=30ms and a threshold of three (Axograph X, Sydney, AU). Captured events were manually reviewed. Rise times were defined as the time between 10% and 90% of the maximal amplitude.

Electron Microscopy: For ultrastructural analysis of mature granule cells at 21 days post-lesion, animals were transcardially perfused with PBS followed by a 0.1M Sodium cacodylate buffer containing 1.5% glutaraldehyde, 1.5% PFA, 0.05M sucrose and 0.25% $CaCl_2$ (pH 7.4). Extracted brains were post-fixed overnight in the same solution. The hemispheres were separated along the midline and each was cut sagittally into 1mm sections. The hippocampi from each 1mm section were microdissected out and further cut into 1x1x2mm blocks that included the dentate gyrus and CA1. Blocks were embedded in

coffin mold using Spurr:Epon, polymerized overnight at 60°C, trimmed, and cut along the long axis into coronal 700nm sections using a Leica EM UC6 vibratome (Leica Microsystems, Inc., Buffalo Grove, IL). Some sections were placed on glass slides and stained with 0.5% Toluidine blue in 0.5% Sodium Tetra Borate for region selection. Sections from lesioned and non-lesioned hemispheres containing the suprapyramidal blade of the dentate gyrus were embedded in resin, and further cut into 70nm sections on an ultramicrotome (Leica Microsystems, Inc., Buffalo Grove, IL). The sections were placed on 200-square mesh Copper/ Rhodium grids and counterstained with 5% uranyl acetate and Reynold's lead citrate. The inner and outer molecular layers of the suprapyramidal blade of the dentate gyrus from both lesioned and unlesioned hemispheres were imaged at 13,000x on an FEI Technai G^2 12 Biotwin at 80kV. Survey images that show reactive astrocytes were acquired at 6,800x.

For ultrastructural analysis of 21-day-old granule cells, we immunolabeled sections from retrovirus-injected animals at 21 days post-lesion. Animals were deeply anesthetized with Na-Pentabarbitol (150mg/ kg) and, when rendered unresponsive, were transcardially perfused with heparinized saline, followed by a 3.8% Acrolein in PFA and 2% PFA in PB (Hegarty et al., 2010). Tissue blocks containing both dorsal hippocampi were postfixed in 2% PFA (no acrolein) for 30 minutes; embedded in agar; and cut coronally into 40μm sections on a vibrating microtome (Leica Microsystems, Inc., Buffalo Grove, IL). Hemispheres were not separated for this experiment. Sections were stored in sucrose solution at -20°C until needed. Sections were rinsed 2x in 0.1M PB to clear the sucrose solution; placed in 1% sodium borohydride for 30 minutes; rinsed with PB until bubbles were gone; treated with a cryoprotectant solution; and freeze-thawed to permeabilize.

Once at room temperature, sections were rinsed 2X in 0.1M Tris-saline and incubated in 0.5% BSA for 30 minutes. Rabbit anti-GFP primary antibody (Millipore, AB3080, Temecula, CA) was applied at 1:1000 for 36 hours at 4°C. Following incubation, sections were rinsed 3X in 0.1M Tris-saline, 5-10 min each, followed by biotinylated goat anti-rabbit secondary antibody (Vector Labs, BA-1000, Burlingame, CA; 1:400 in 0.1% BSA, 30 minutes, room temp). Sections were incubated in ABC solution (Elite Vectastain, Vector Labs, Burlingame, CA; 30 min), rinsed with 0.1M Tris-saline, and then treated with diaminobenzidine-H_2O_2 solution (5 min). Following washes in 0.1M Tris-saline and then in 0.1M PB, sections were incubated in 2% osmium tetroxide (60 min), dehydrated, flat-embedded in EMBed-812 (RT 14120; Electron Microscopy Sciences, Hatfield, PA) between 2 sheets of ACLAR flurohalocarbon film (#50425; Electron Microscopy Sciences, Hatfield, PA), and cured at 60°C for 48 hours (Figure 8A). Regions of interest from lesioned and unlesioned hemispheres containing labeled newborn neurons in the suprapyramidal blade of the dentate gyrus were cut out and superglued onto cured resin blanks. Tissue was thin-sectioned on an ultramicrotome (Leica Microsystems, Inc., Buffalo Grove, IL) into 75nm sections and placed onto Nickel/ Copper mesh grids. Grids were counterstained and imaged as described above.

Statistical Analysis: All values are expressed as mean±SEM. A Generalized Linear Model (GLM) was used for analysis of POMC-EGFP cell counts, total dendritic length and arborization, and dendritic spine density. Kolmogorov-Smirnov (KS) test was used to analyze distributions of granule cell dispersion and of mEPSC amplitudes and rise times. Repeated Measures/ ANOVA was used for field potentials and Sholl analysis. Paired t-test was used for analysis of single mEPSCs, BrdU cell counts, and EM synaptic composition.

Chi-squared test was used to compare proportions of surviving BrdU+ cells. Significance cutoff was $p < 0.05$. p values are reported in the text.

Results

The perforant path from the entorhinal cortex is the major afferent input to hippocampus, forming excitatory synapses in the outer 2/ 3rds of the molecular layer of the dentate gyrus. To examine the impact of deafferentation on adult-generated newborn neurons in the dentate gyrus, we made unilateral surgical lesions of the perforant path in young adult mice (Figure 5A). Because surgical lesions can be variable, we verified the completeness of each lesion by serially sectioning the caudal half of the brain from dorsal to ventral in the horizontal plane (Figure 5B). In this example of a complete lesion at 14 days post-lesion (dpl), the location of the surgical cut was visible even in the ventral-most horizontal sections of the caudal half of the mouse brain (arrowheads). To account for systemic factors such as anesthesia or surgical stress, the contralateral dentate gyrus was used as an in-animal control. Animals with incomplete lesions or with damaged hippocampi were excluded from the analysis. We confirmed degeneration of perforant path fibers by extracellular field recordings in acutely prepared coronal brain slices at 14 dpl. We measured the fiber volley that represents action potential propagation in perforant path axons, and field excitatory postsynaptic potentials (fEPSPs) that reflect granule cell depolarization in response to excitatory synaptic transmission. As expected, stimulation contralateral to the lesion evoked a short latency fiber volley followed by a fEPSP as recorded with an extracellular electrode in the outer molecular layer. However, both the fiber volley and fEPSP amplitudes were greatly reduced or completely absent on the lesioned side (Figure 5C) over a wide range of stimulation intensities. For example, at

1.0 μA stimulation intensity, the fiber volley amplitude was decreased 76.1% (control: -0.30 mV; lesion: -0.07 mV, $p < 0.05$, Repeated Measures/ ANOVA; n=12 slices from 5 animals). Similarly, the fEPSP amplitude at this stimulation intensity was decreased 88.2% (control: -0.34 mV/ msec; lesion: -0.04 mV/ msec, $p < 0.0001$, Repeated Measures/ ANOVA; n=12 slices from 5 animals).

To assess the integrity of perforant path nerve terminals post-lesion, we immunolabeled the vesicular glutamate transporters, vGlut1 and vGlut2, which often show complementary distributions at excitatory synapses. vGlut1 is expressed in perforant path fibers as well as the mossy fibers of dentate granule cells, whereas vGlut2 is expressed in hilar mossy cells and extrahippocampal inputs from the supramammillary nuclei (Leranth and Hajszan, 2007). At 21dpl, vGlut1 immunolabeling was relatively homogeneous throughout the molecular layer and hilus, but was not present within the granule cell layer (Figure 5D, left panel). In the deafferented dentate gyrus, there was no detectable labeling in the outer 2/ 3rds of the molecular layer (OML staining ratio lesion/ control = 0.17, n=5 animals), although labeling was preserved in the inner molecular layer (IML). vGlut2 immunolabeling showed the expected expression in a narrow band of the supragranular layer (Boulland et al., 2009), but no detectable expression in the denervated zone (Figure 5E, right). The lack of vGlut1 (or vGlut2) staining post-lesion is consistent with complete perforant path transection.

Proliferation and migration of newborn neurons following perforant path lesion

To examine the response of newborn neurons following perforant path lesion, we used POMC-EGFP transgenic mice that transiently label newborns neurons at

approximately 10-14 days post-mitosis (Overstreet et al., 2004b, Figure 6A, left panel). There was an increase in the number of $EGFP^+$ cells in the dentate gyrus post-lesion (Figure 6A, right panel) compared to the contralateral control (Figure 6A, left panel) in the same animal (control: 74±11 X 10^3 cells/ mm^3; lesion: 107±22 X 10^3 cells/ mm^3, $p < 0.05$, GLM; n=8 animals). In addition to the increased number, $EGFP^+$ cells were no longer limited to the subgranular zone, but had migrated within the granule cell layer as shown in the close-up of the suprapyramidal blade of the dentate gyrus (Figure 6B). To quantify the migration, we measured the perpendicular distance between the center of each $EGFP^+$ cell body and the border between the subgranular zone and hilus (Figure 6C). Newborn granule cells in the deafferented dentate gyrus were nearly three times farther from the hilar border than those in the contralateral control, thus shifting the distribution of newborn neurons within the granule cell layer to the right (Figure 6D; control: 9.16±0.81μm; lesion: 25±2.47μm, $p < 0.0001$, KS-test; n=8 animals).

The increase in newborn neurons on the side of the lesion could result either from an increase in proliferation or an increase in survival. Thus we injected BrdU into lesioned mice to label dividing cells in the dentate gyrus. Two injections of BrdU, separated by 4 hours, were used in order to saturate labeling during one cell cycle (see methods). We counted the number of BrdU-labeled cells within the granule cell layer four hours after the last BrdU injection (at 8, 24, and 48 hours post-lesion) as an estimate of proliferation and at 1 month post-lesion as an estimate of survival. At 8 and 24 hours post-lesion there was only a slight increase in BrdU-labeled cells (not shown; *8 hours* – control: 6.3±1.1 X 10^3 cells/ mm^3; lesion: 7.2±1.4 X 10^3 cells/ mm^3, NS, paired t-test, n=4 animals; *24 hours* – control: 6.2± 0.8 X 10^3 cells/ mm^3; lesion: 7.3±1.4 X 10^3 cells/ mm^3, NS, paired t-test, n=5

animals). However, by 48 hours post-lesion, there was a doubling of BrdU-labeled cells (Figure 7A, control: 10.6±1.3 X 10^3 cells/ mm^3; lesion: 21.6±2.6 X 10^3 cells/ mm^3, $p < 0.001$, paired t-test; n=7 animals), suggesting that the increase in $EGFP^+$ cells was the result of a lesion-induced proliferative response. As expected, the majority of $BrdU^+$ cells were in the subgranular zone at the hilar border. As shown in Figure 7A (right panel), BrdU-labeled cells were also observed in the denervated region, consistent with a glial response following lesion (Hailer et al., 1999, see also below). At 1 month, post-lesion, there was a corresponding increase in surviving $BrdU^+$ cells (Figure 7B, control: 4.2±0.8 X 10^3 cells/ mm^3; lesion: 7.5±1.2 X 10^3 cells/ mm^3, $p < 0.01$, paired t-test; n=7 animals). Despite the increase in proliferation, the percentage of surviving newborn granule cells was similar between hemispheres (Figure 7C, control: 39.6%; lesion: 34.7%, NS, Chi-squared test), suggesting that the survival rate was not altered by the lesion.

Dendritic outgrowth and synapse formation post-lesion

Adult-generated newborn granule cells extend dendrites into the inner molecular layer by 2 weeks post-mitosis, but have yet to receive excitatory inputs. By the 3rd week, the dendrites reach the outer 2/ 3rds of the molecular layer and are contacted by the perforant path (Overstreet, 2006). Unlike mature granule cells that are denervated by the perforant path lesion, we analyzed newborn cells that were dividing at the time of the injury. This approach allowed us to examine the effect of the perforant path lesion on dendritic outgrowth and synapse formation after perforant path fibers have already degenerated. Dendritic arbors at 14 days post-lesion were measured using POMC-EGFP mice. Dendrites and synaptic activity at 21 days post-lesion were measured in neurons that had been labeled with GFP using retroviral vectors at the time of lesion (pRubi, see

methods). As expected, the total length and branch number of dendrites increased between day 14 and 21 in the control (Figure 8A, left panels). However, the growth of dendrites and branches was significantly less post-lesion (Figure 8A, right panels and Figure 8B; *14 days* – control: 239.5±26.7μm; lesion: 202.0±26.4μm, $p < 0.05$, GLM, n=5 animals, 7-15 neurons per dentate gyrus; *21 days* – control: 1189.7±119.3μm, lesion: 807.2±109.8μm, $p < 0.0001$, GLM, n=5 animals, 5-10 neurons per dentate gyrus). Sholl analysis of all traces revealed that dendritic complexity was not affected in 14-day-old neurons, when the dendrites are confined to the inner molecular layer (Figure 8C, NS, Repeated Measures/ ANOVA), but there was a significant reduction in the distal dendritic complexity in 21 day-old neurons (Figure 8D, $p < 0.001$, Repeated Measures/ ANOVA), corresponding to the denervated zone.

In addition to the perforant path, dentate granule cells receive commissural/ associational excitatory inputs located in the inner molecular layer, which are not interrupted by the lesion and thus could provide synaptic input to adult-generated newborn neurons. To examine this possibility, we recorded miniature excitatory synaptic currents (mEPSCs) from 21-day-old granule cells that had been GFP-labeled with the pRubi retrovirus on the day of the lesion. mEPSCs were present at 21 days post-lesion, but the frequency was decreased in the denervated dentate gyrus compared to the contralateral control (Figure 9A, control: 0.13±0.01 Hz; lesion: 0.09±0.02 Hz, $p < 0.05$, paired t-test; n=11 and 12 neurons, respectively). The mEPSC amplitude was increased on the lesioned side (Figure 9B, right panel, control: 13.5±0.7 pA; lesion: 16.5±0.9 pA, $p < 0.05$, paired t-test; n=11 and 12 neurons, respectively). The distribution of a random sample of mEPSC amplitudes showed a rightward shift with fewer small events (5-15pA) and more

large events (15-50pA; Figure 9B, center panel, $p < 0.0001$, KS-test). The rise-time of mEPSCs was also faster (Figure 9C, right panel, control: 1.46±0.08 ms; lesion: 1.21±0.06 ms; $p < 0.01$, paired t-test; n=11 and 12 neurons, respectively). The distribution of rise-times showed a leftward shift with increase in fast-rising (0-1.5ms) and a decrease in slow-rising (1.5-3ms) events (Figure 9C, center panel, $p < 0.0001$, KS-test). The larger, more rapidly rising mEPSCs in the denervated dentate gyrus may indicate preferential input from synapses in the inner molecular layer that are closer to the somatic recording site. These results are consistent with the lack of vGlut1/ 2 staining in the denervated zone and thus the absence of sprouting across laminar boundaries (see Figure 1).

de novo dendritic spines in the denervated zone

The perforant path forms excitatory axons onto dendritic spines of mature granule cells. Following lesioning, dendritic spines are transiently reduced (Matthews et al., 1976a; Steward et al., 1983; Vuksic et al., 2011). We compared the impact of lesioning on preexisting dendritic spines on mature granule cells with its impact on *de novo* formation of dendritic spines on newborn neurons. Mature and newborn granule cells were GFP-labeled with retroviral (pRubi) and lentiviral (FUGW) vectors, respectively. At 21 days post-lesion, newborn neurons in the contralateral control had a large number of dendritic spines in the outer molecular layer (Figure 10A, top left). However there were fewer newly formed spines on the lesioned side (Figure 10A, top right, control: 1.53±0.17 spines/ µm; lesion: 1.22±0.12 spines/ µm, $p < 0.001$, GLM; n=7 animals). There was a similar reduction in the number of existing spines on mature granule cells following deafferentation (Figure 10B, top row, control: 2.36±0.18 spines/ µm; lesion: 1.61±0.13 spines/ µm, $p < 0.001$, GLM; n=5 animals). In contrast, there was a 45% increase in dendritic spines on newborn

neurons in the inner molecular layer (Figure 10A, lower row, control: 1.11±0.17 spines/ µm; lesion: 1.61±0.12 spines/ µm, $p < 0.001$, GLM; n=7 animals). Mature granule cells, however, did not show a change in spine density in the inner molecular layer (Figure 10B, lower panel; control: 2±0.16 spines/ µm; lesion: 2.02±0.23 spines/ µm, NS, GLM; n=5 animals). These results indicate that, following lesion, spine formation on newborn granule cells can occur throughout the molecular layer, but was most robust in areas that had intact glutamatergic axons.

We were surprised that newborn granule cells developed dendritic spines in the outer molecular layer in the absence of functional perforant path activity as measured by the field EPSPs. Likewise, mature granule cells show an initial decrease in spines following perforant path lesion, but then nearly completely recover (Steward et al., 1983; Vuksic et al., 2011). To evaluate whether these spines are associated with presynaptic terminals we examined the synaptic ultrastructure in the suprapyramidal blade of the dentate gyrus at 21 days post-lesion. In the dentate gyrus contralateral to the lesion, intact asymmetric (excitatory) synapses with presynaptic terminals and postsynaptic densities were easily apparent throughout the molecular layer (Figure 11A, left column) as well as the inner molecular layer in the lesioned hemisphere (Figure 11A, top right). However, synaptic structures were disrupted in the denervated zone. Degenerating nerve terminals were electron-dense and without clearly defined presynaptic vesicles, whereas post-synaptic densities were preserved (Figure 11A, bottom right). To quantify synaptic structures in each layer, 10 regions of interest from 3 non-adjacent sections in each dentate gyrus were imaged. A synapse was considered intact if there was a presynaptic terminal containing synaptic vesicles, a submembrane post-synaptic density (PSD), and close

apposition of pre- and post-synaptic membranes. As shown in Figure 11B, the number of postsynaptic densities was unaffected by the lesion (*PSDs* – control: 0.6/ μm^2; lesion: 0.51/ μm^2, NS, paired t-test; n=4 animals), but presynaptic terminals and intact/ normal synapses were markedly decreased in the outer molecular layer of the denervated dentate gyrus (*axon term. w/vesicles* – control: 0.85/ μm^2; lesion: 0.24/ μm^2, $p < 0.001$, paired t-test, n=4 animals; *synapses*: control: 0.28/ μm^2; lesion: 0.06/ μm^2, $p < 0.001$, paired t-test, n=4 animals). Reactive gliosis was also apparent in the denervated zone as previously described (Figure 11C, shaded region; also Hailer et al., 1999).

Because synapses on newborn neuron constitute only a small fraction of all synapses in the molecular layer, the analysis in Figure 11 largely, if not completely, represents synapses on mature granule cells. The relative retention of postsynaptic structures could simply represent slow turnover of pre-existing PSDs that are no longer innervated. However, the protocol we used for retroviral labeling of newborn neurons samples only new dendritic spines and synapses that formed after the lesion. To examine whether the dendritic spines on newborn neurons have intact synaptic ultrastructure, we performed immunoelectron microscopy on GFP-labeled newborn neurons using anti-GFP antibodies. Because of the relatively sparse labeling of newborn neurons with the retrovirus, sections of the molecular layer were chosen that contained several labeled dendritic trees (Figure 12A, black boxes). Occasional dendrites with punctate or electron labeling were seen in the inner and outer molecular layer in the control and deafferented dentate gyrus (Figure 12B). The low frequency of immunolabeled dendrites precluded a quantitative analysis of spines directly attached to labeled dendrites, thus we counted the number of postsynaptic densities (PSDs) contiguous with immunolabeled areas. Although

decreased in number, PSDs were found on newly formed dendritic spines in the denervated zone (Figure 12B, right panel, control: 0.71±0.1 PSDs/ μm^2; lesion: 0.38±0.06 PSDs/ μm^2, n=4 animals, 10 regions of interest from 4 non-adjacent sections per dentate gyrus), however they were not associated with normal presynaptic structures (control: 0.044±0.01 presynaptic terminals/ μm^2; lesion: 0 terminals/ μm^2; n=4 animals, 15 regions of interest from 5 non-adjacent sections per dentate gyrus) or with intact synapses (control: 0.03±0.01 synapses/ μm^2; lesion: 0 synapses/ μm^2; n=4 animals, 15 regions of interest from 5 non-adjacent sections per dentate gyrus). Given the semi-quantitative nature of this experiment, p-values could not be determined.

Discussion

We used a classic injury model – unilateral lesion of the perforant path – to demonstrate that selective deafferentation of the adult dentate gyrus alters the maturation and functional integration of newborn granule cells. We focused on newborn neurons dividing at the time of lesion and thus evaluated the initial neurogenic response as well as *de novo* dendritic outgrowth and synaptogenesis in the absence of excitatory input from the entorhinal cortex. This approach allowed us to compare mature granule cells that were denervated by the lesion, with newborn granule cells that were never innervated by the perforant path.

An initial neurogenic response to perforant path lesion

Adult-generated newborn neurons are highly sensitive to environmental and molecular stimuli (Gould and Tanapat, 1999; Vivar et al., 2012) as well as brain injury (Liu et al., 1998; Dash et al., 2001; Parent, 2003; Parent and Murphy, 2008). In our experiments, a

chronic denervating injury triggered proliferation of newborn granule cells, consistent with previous studies (Cameron et al., 1995; Gould and Tanapat, 1997). Although a substantial portion of newborn neurons normally undergo cell death (Kuhn et al., 2005; Sierra et al., 2010), in our experiments the same fraction of newborn cells survived at 30 days in the lesioned and non-lesioned hemisphere, indicating that the 'extra' new neurons had an equal chance of integrating into the circuit. The factors contributing to proliferation of new neurons are likely multifactorial and context-dependent. Seizures, trauma and ischemia acutely increase glutamate release and neural activity, whereas denervating injury might be expected to do the opposite. However, dentate granule cells show a transient increase in activity for 2-4 hours post-lesion as measured by c-fos immunoreactivity (Haas et al., 1999; and n=6 animals, not shown). Although the NMDA receptor antagonist MK-801 can block the post-lesion increase in activity (Nitsch and Frotscher, 1992), in our experiments it did not block the proliferation of newborn granule cells observed at 14 days post-lesion (1 mg/ kg IP, n=4 animals, Figure 13). Proliferation did correspond with time of microglial activation in the denervated zone (day 2-3, Figure 17; Gehrman et al., 1991; Hailer et al., 1999; Dissing-Olesen et al., 2007), and the subsequent appearance of reactive gliosis (day 7, Hailer et al., 1999). Reactive astrocytes produce growth inhibitors, such as cytokines, as well as trophic factors and growth substrates conducive to regeneration (Sofroniew, 2009; Sofroniew and Vinters, 2010). For example, astrocytes show increased expression of bFGF following injury (Gomez-Pinilla et al., 1992), thus potentially driving stem cell proliferation, differentiation, and survival (Gage et al., 1995).

Circuit reorganization following denervation

Although brain injury can stimulate neurogenesis, relatively little is known about the integration of newborn neurons into functional circuits post-injury. Perforant path lesions have traditionally been used to characterize mature granule cells and the reorganization of their inputs in the context of structural plasticity in the adult brain. For example, dendritic complexity and spine density of mature granule cells decrease in the outer molecular layer following removal of the perforant path (Parnavelas et al., 1974; Matthews et al., 1976a; Caceres and Steward, 1983; Diekmann et al., 1996; Schauwecker and McNeill, 1996; Vuksic et al., 2011), despite injury-induced sprouting of afferent axons from uninjured brain regions (Deller and Frotscher, 1997), such as the commissural/ associational axons (Gall and Lynch, 1981; Schauwecker and McNeill, 1995), septohippocampal cholinergic fibers (Stanfield and Cowan, 1982), and central noradrenergic fibers (Peterson, 1994). Thus, although dentate circuitry can reorganize post-lesion (Deller and Frotscher, 1997; Deller et al., 2007), sprouting of remaining axons is insufficient for complete morphological recovery (Diekmann et al., 1996).

Labeling newborn neurons that were dividing at the time of the lesion allowed us to examine their dendritic outgrowth and synapse formation in the absence of a major excitatory input. The dendrites of newborn neurons penetrated into the denervated zone but had simpler morphology, indicating that local presynaptic activity is important in the elaboration of dendrites on newborn neurons (e.g. Tashiro et al., 2006). The simpler morphology of newborn dendrites was comparable to the retraction of distal dendrites in mature granule cells, suggesting that presynaptic activity also plays a role in maintainance of preexisting dendrites (Diekmann et al., 1996). The increase in *de novo* dendritic spines in the inner molecular layer and the increase in the amplitude and rise time of EPSCs in

newborn neurons indicated that excitatory axons could form new synapses with newborn granule cells, however synaptogenesis appeared to be localized to the uninjured region. Whether sprouting axons cross laminar borders and form synapses on denervated mature granule cells has been controversial (Deller et al., 2001; del Turco et al., 2003; Phinney et al., 2004). However, in our experiments intact excitatory nerve terminals were absent from the outer molecular layer post-lesion, indicating that glutamatergic axons did not cross laminar barriers. Whether the laminar barriers reflect residual preexisting laminar cues or are produced post-lesion by microglia and reactive astrocytes is not yet clear (Bechmann and Nitsch, 2000; Collazos-Castro and Nieto-Sampedro, 2001; Deller et al., 2001; Deller et al., 2006).

Is a spine a marker of a functional excitatory synapse post-lesion?

The presence of dendritic spines is usually taken as a proxy for the presence of a functional glutamatergic excitatory synapse. Although decreased in number, dendritic spines on newborn neurons were present in the outer molecular layer in the absence of excitatory input. Importantly, unlike mature neurons, spines on newborn neurons formed >2 weeks after the lesion. Thus, one must conclude that in the setting of denervation or neural injury, dendritic spines can form on newborn neurons without intact perforant path axon terminals. In addition, a substantial number of dendritic spines on mature cells in the outer molecular layer were present three weeks after denervation in the absence of any functional or morphological excitatory synaptic input, which may represent either maintenance of existing spines or formation of new spines. Interestingly, postsynaptic specializations (junctional folds) at the frog neuromuscular junction are maintained following denervation (Birks et al., 1960), possibly because perisynaptic Schwann cells

come in direct contact with denervated junctional folds, release acetylcholine, and trigger small postsynaptic potentials (Katz and Miledi, 1959; Miledi and Slater, 1968). Spine densities on mature granule cells *in vivo* have been reported to recover to near-normal level by 30-180 days post-lesion (Parnavelas et al., 1974; Caceres & Steward, 1983; Vuksic et al., 2011), although it is not clear whether these spines are associated with presynaptic nerve terminals or whether regeneration requires presynaptic input. Similarly, dendritic spines form on deafferented cerebellar Purkinje cells of *weaver* transgenic mice, despite the lack of presynaptic parallel fibers (Hirano and Dembitzer, 1973; Sotelo, 1990). In organotypic entorhino-hippocampal cultures, *in vitro* denervation of mature granule cells did not affect new spine formation, but the authors observed changes in spine stability and synaptic activity at 3-4 days post-lesion (Vlachos et al., 2012a; 2012b). In our *in vivo* experiments, there was no evidence of intact presynaptic terminals in the denervated zone at 21 days post-lesion. Thus, mature granule cells can retain and regenerate spines without perforant path input post-lesion, whereas newborn neurons do not require perforant path input for spine formation in the outer molecular layer.

It is interesting to consider what signals might substitute for presynaptic terminals in the induction of *de novo* dendritic spines, or the maintenance of mature spines, following denervation. Because of the tissue reaction to denervation or neural injury, the environment for dendritic spine and synapse formation may differ markedly from normal development (Mori et al., 2005). For example, in addition to glutamatergic inputs, other transmitters - including GABAergic or cholinergic inputs - could serve as trophic signals following injury (Lauder, 1993; Ben-Ari, 2002; Overstreet-Wadiche et al., 2005). It is also possible that signals from reactive astrocytes or microglia that invade the denervated zone

could induce or maintain dendritic spines. For example, glia-derived signals might be neurotransmitters or trophic factors (Sofroniew and Vinters, 2010) as well as extracellular matrix proteins such as thrombospondins (Möller et al., 1996; Christopherson et al., 2005) or matrix metalloproteinases (Warren et al., 2012).

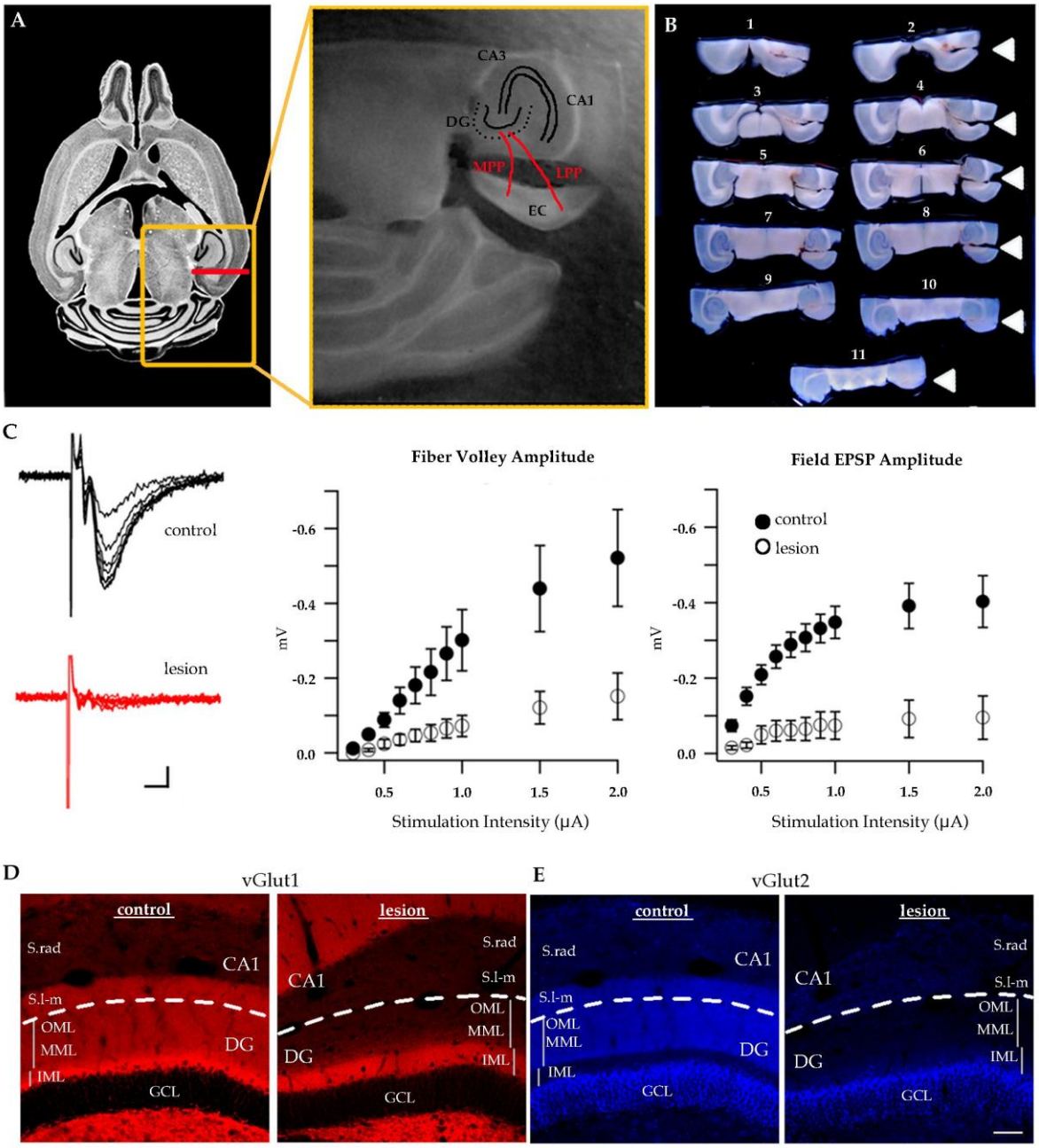

Figure 5 – Complete ablation of perforant path axons in the adult dentate gyrus.

(legend on next page)

Figure 5 – Complete ablation of perforant path axons in the adult dentate gyrus.

(A) A unilateral lesion of the entorhinal cortex (EC) transects the perforant path (red lines). *Left panel:* Horizontal section of a mouse brain from Allen Brain Atlas illustrating rostro-caudal position of the lesion (red line). Orange box outlines the position of the *middle panel*, which shows close-up of the lesioned perforant path (red lines, MPP and LPP) input to the dentate gyrus (DG). **(B)** Lesioned brains were cut in half along the top border of the orange box in (A), the cerebellum was removed, and the caudal half was horizontally sectioned dorsal to ventral (numbered in order of sectioning). Arrowheads indicate the location of the lesion, which is visible even in the ventral-most section (11). **(C)** *Left panel:* Example traces of field recordings from an acute brain slice at 14 days post-lesion. Whereas in the control dentate gyrus traces showed a robust fiber volley and an increase in the field EPSP with increasing stimulus intensity (black trace), the deafferented dentate gyrus showed no response regardless of stimulation intensity (red trace). Scale bar = 5ms/ 50μV. *Middle panel:* Measurements of fiber volley amplitude across a range of typical stimulation intensities. Fiber volley amplitudes in the deafferented dentate gyrus (white circles) were significantly reduced following lesion, as compared to the contralateral control (black circles, $p < 0.05$). The same was observed for field EPSPs (*right panel*), which were almost entirely absent from the lesioned tissue (white circles) compared to the contralateral control (black circles, $p < 0.001$). **(D)** . *Left panel:* vGlut1 immunostaining of glutamatergic nerve terminals typically labels the entire dentate molecular layer (IML, MML, OML), and CA1. *Right panel:* vGlut1 expression was drastically decreased at 21 days post-lesion in the denervated zone (MML, OML, CA1), but was unaffected in the intact inner molecular layer (IML, scale bar = 50μm). **(E)** *Left panel:* vGlut2 expression in the control dentate gyrus was localized to the supragranular zone of the granule cell layer (GCL), the middle/ outer molecular layers (MML, OML), and S.l-m of CA1. *Right panel:* At 21 days post-lesion, vGlut2 expression was decreased in the denervated region (MML, OML, and S.l-m of CA1), but was unchanged in the supragranular zone (bright band adjacent to the granule cell layer). Dashed lines separate dentate gyrus from CA1. Scale bar = 50μm. CA1 = cornu ammonis1, CA3 = cornu ammonis3, DG = dentate gyrus, EC = entorhinal cortex, GCL = granule cell layer, IML = inner molecular layer, LPP = lateral perforant path, MPP = medial perforant path, MML = middle molecular layer, OML = outer molecular layer, S.l-m = stratum lacunosum-moleculare, S.rad = stratum radiatum.

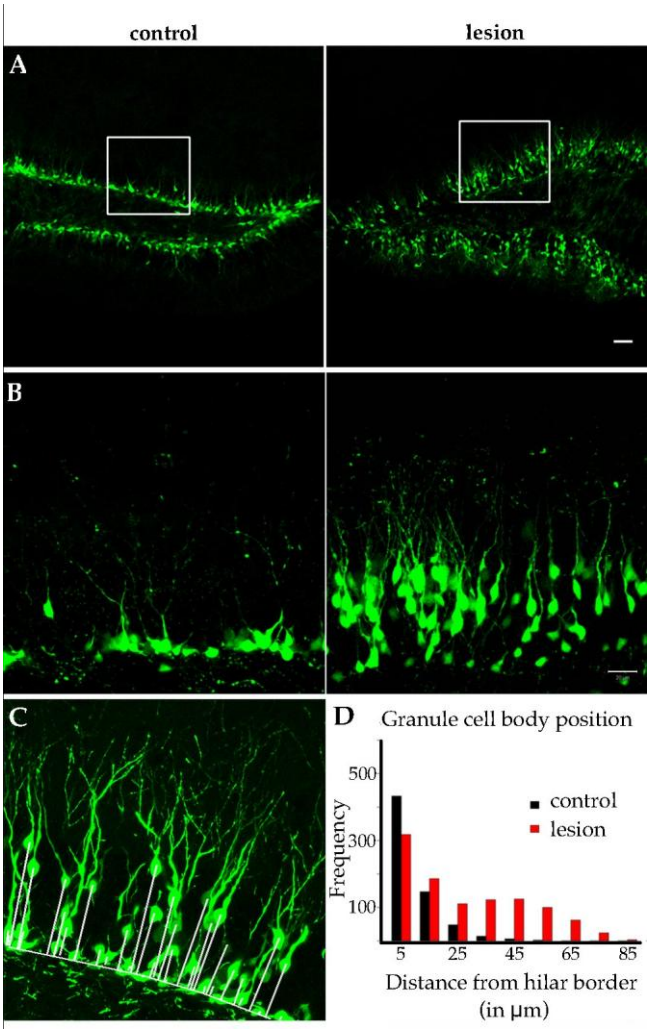

Figure 6 – Perforant path lesion triggered proliferation and outward migration of newborn granule cells.

(A) Dentate gyrus (10x magnification) from an adult POMC-EGFP transgenic mouse showed increased proliferation of newborn granule cells at 14 days post-lesion of the perforant path (*Right panel*) compared to the contralateral, non-lesioned control (*Left panel*). White squares represent area enlarged in (B). Scale bar = 50μm. (**B)** 40x magnification of suprapyramidal blade of the deafferented dentate gyrus (*right panel*) showed an increase in the number as well as in the outward migration of POMC-EGFP$^+$ cells post-lesion. Labeled cells in the contralateral control were restricted to the subgranular zone (*left panel*). Scale bar = 20μm. (**C)** Newborn granule cell body position within the granule cell layer was analyzed by measuring the distance between each POMC-EGFP$^+$ cell body and the hilar border (white lines). **(D)** Many newborn granule cells in the denervated dentate gyrus migrated away from the subgranular zone (red bars) compared to control (black bars), as revealed in the frequency distribution ($p < 0.0001$).

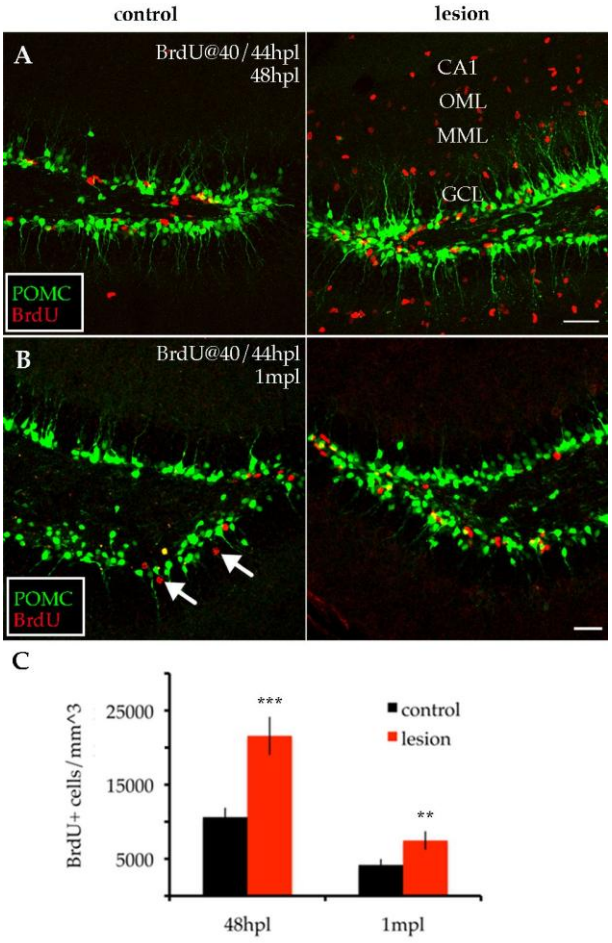

Figure 7 – Perforant path lesion caused proliferation of newborn granule cells in the ipsilateral dentate gyrus, but did not affect the fraction that survived.

Compressed 60 μm z-stacks from dentate gyrus of a POMC-EGFP transgenic mouse with newborn neurons labeled in green and immunolabeling for BrdU in red. **(A)** To examine granule cell proliferation, BrdU was injected at 40 and 44 hours post-lesion and tissue was evaluated at 48 hours post-lesion. In the control dentate gyrus (*left panel*), a few $BrdU^+$ cells were present near the hilar border. In the deafferented dentate gyrus (*right panel*), many $BrdU^+$ cells were present throughout the deafferented region (MML, OML, CA1), representing new granule cells as well as proliferating glia. To evaluate granule cell proliferation, $BrdU^+$ cells were counted only in the granule cell layer (GCL). Scale bar = 50μm. **(B)** To measure granule cell survival, BrdU was injected at 40 and 44 hours post-lesion, and tissue was evaluated at 1 month post-lesion. As at 48 hours, there were more $BrdU^+$ cells (red) in the granule cell layer on the lesioned side as well (*right panel*) compared to the control dentate gyrus (l*eft panel*). $BrdU^+$ cells were more widely dispersed within the granule cell layer (arrows), consistent with neuronal maturity, whereas $BrdU^+$ glia were no longer apparent in the molecular layer. Scale bar = 50 μm. **(C)** $BrdU^+$ cells within the granule cell layer were increased in the deafferented dentate gyrus (red bars) at 48 hours post-lesion ($p < 0.001$) and at 1 month post-lesion ($p < 0.01$). The percentage of surviving cells did not differ between the two hemispheres (34.7% lesioned vs. 39,6% non-

lesioned). ** = $p < 0.01$, *** = $p < 0.001$. Yellow cells are the result of z-stack compression and do not indicate co-localization.

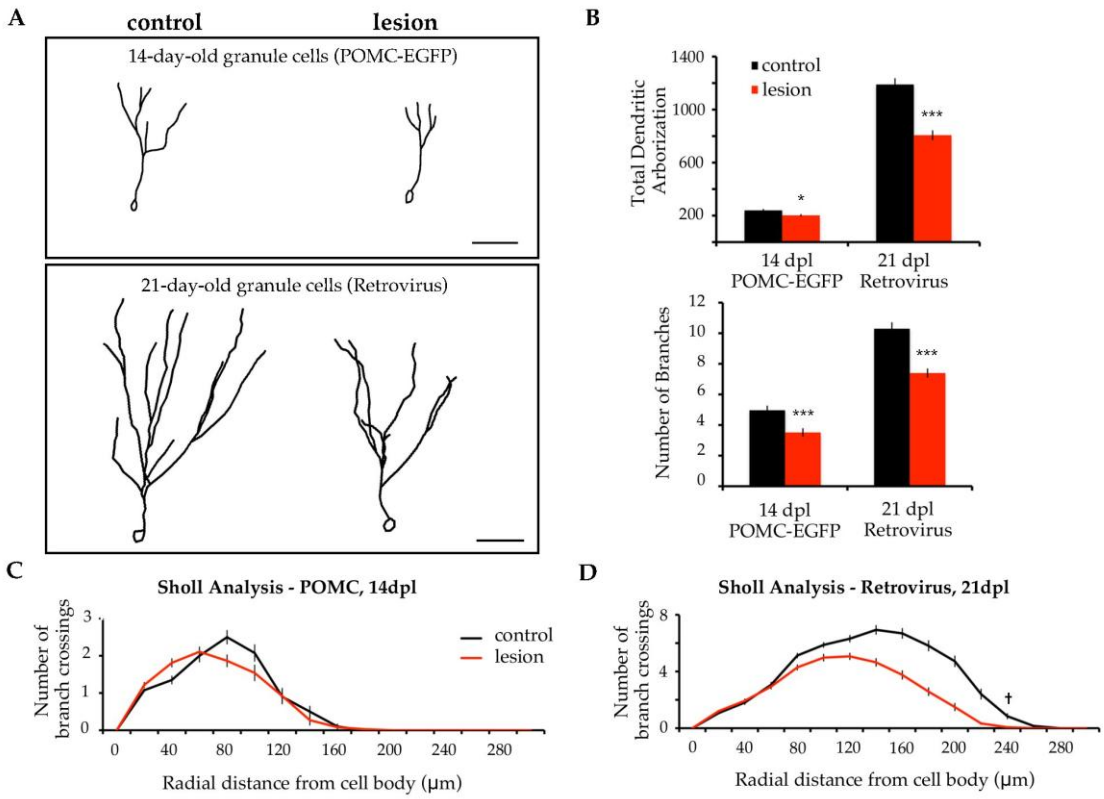

Figure 8 – Perforant path lesion reduced outgrowth and complexity of newborn granule cell dendrites.

(A) *Upper panel:* At 14 days post-lesion, dendritic arbors of 14-day-old POMC-EGFP$^+$ neurons were greatly reduced in total length and complexity on the lesioned side (*right*) compared with the contralateral control (*left*). *Lower panel:* Retrovirally infected 21-day-old granule cells at 21 days post-lesion also showed reduced dendritic outgrowth in the deafferented dentate gyrus (*right*). Scale bar = 50μm **(B)** *Top panel:* At both 14 and 21 days post-lesion, total dendritic length was significantly decreased ($p < 0.05$, $p < 0.001$). *Bottom panel:* The number of branches in 14- and 21-day-old granule cells (POMC-EGFP and Retrovirus, respectively) was decreased on the lesioned side ($p < 0.001$). **(C,D)** Sholl analysis of 14-day-old POMC-EGFP$^+$ granule cell dendrites at 14 days post-lesion (n=5 animals, 7-15 neurons per hemisphere), showed an apparent shift in dendritic complexity toward the granule cell/ inner molecular layer, where incoming fibers are intact (but these changes did not reach significance). However, Sholl analysis of retrovirally infected 21-day-old granule cell dendrites at 21 days post-lesion, showed a decrease in complexity of distal dendritic segments in the deafferented zone († = $p < 0.001$), relative to granule cells in the contralateral hemisphere, n=5 animals, 5-10 neurons per hemisphere). * = $p < 0.05$; *** = $p < 0.001$. Scale bars = 50μm.

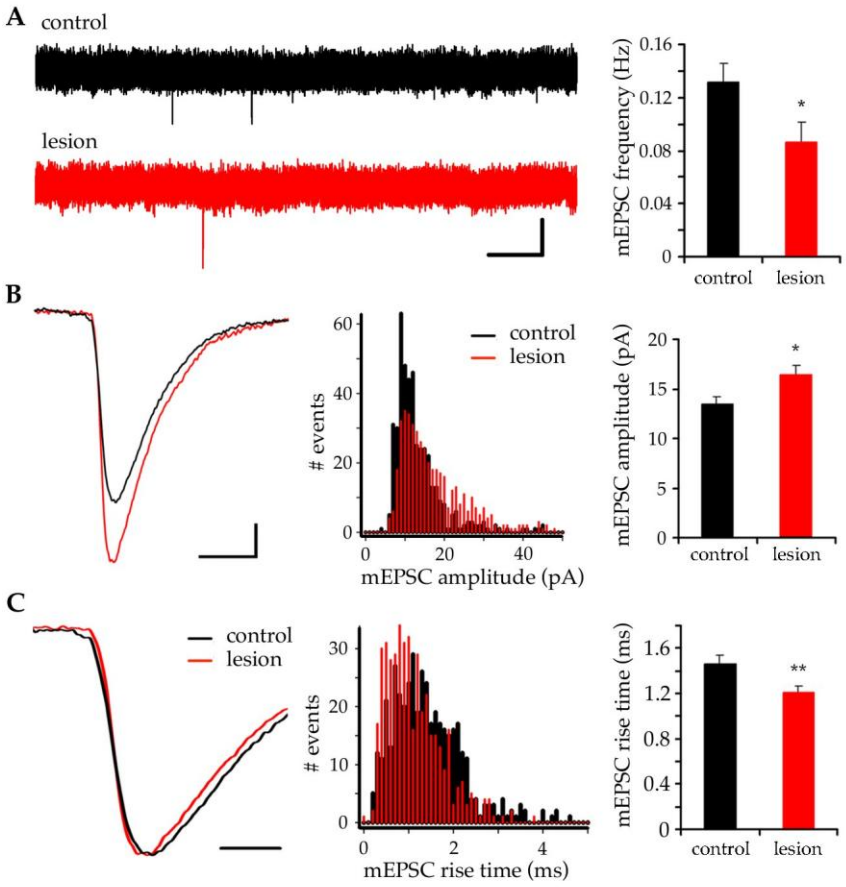

Figure 9 – Perforant path lesion decreased mEPSC frequency, but the amplitudes were increased and rise-times were faster in newborn granule cells.

(A) *Left panel:* Representative traces of spontaneous activity in 21-day-old granule cells at 21 days post-lesion (scale bar = 2s/ 20pA). Granule cells in the deafferented dentate gyrus (*bottom trace*) had fewer miniature EPSCs than the contralateral control (*top trace*). *Right panel:* mEPSC frequency on the lesioned hemisphere was significantly lower ($p < 0.05$). **(B)** *Left panel:* Exemplar traces of mEPSCs from lesioned and control hemispheres (scale bar = 5ms/ 2pA). Miniature events were larger in granule cells from the lesioned hemisphere (*red trace*) than from the control (*black trace*). *Middle panel:* The amplitude distribution of mEPSCs was shifted to the right in the lesioned hemisphere (*red bars*, $p < 0.0001$). *Right panel:* Mean mEPSC amplitude was significantly increased following lesion ($p < 0.05$). **(C)** *Left panel:* mEPSCs in 21-day-old granule cells from the deafferented (*red*) showed faster rise-times than control (*black*, scale bar = 2ms). *Middle panel:* Distribution of mEPSCs rise-times. Lesion shifted the distribution to the left (*red bars*) relative to the contralateral control (*black bars*, $p < 0.0001$). *Right panel:* mEPSC rise time were significantly faster following lesion ($p < 0.01$). * = $p < 0.05$, ** = $p < 0.01$.

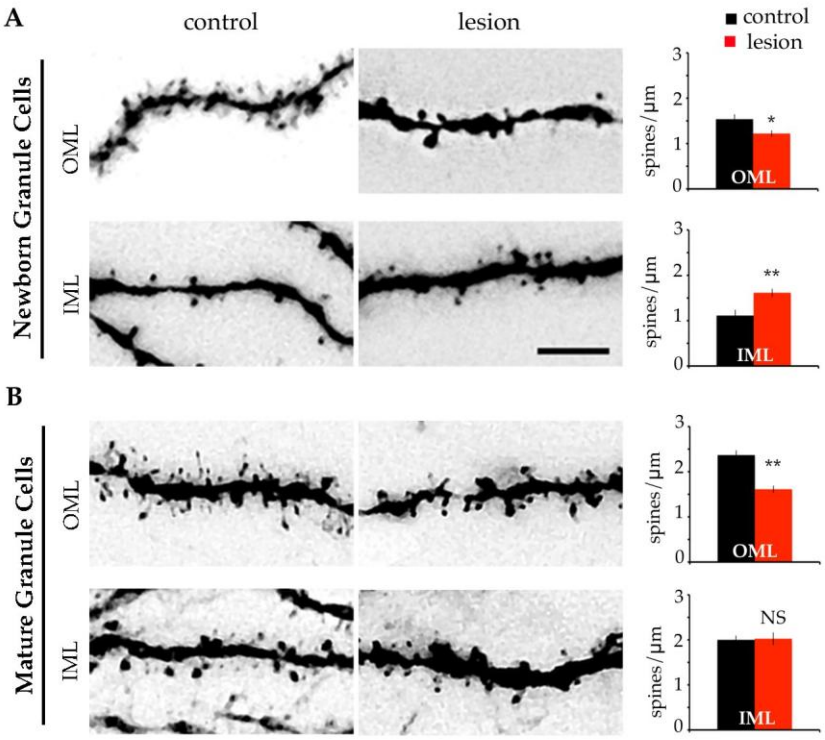

Figure 10 – Newborn granule cells showed layer-specific spine formation following lesion.

(A) Newborn granule cells at 21 days post-lesion. Newly formed dendritic spines on 21-day-old granule cells were present both in the outer molecular layer (OML, *top row*) and in the inner molecular layer (IML, *bottom row*). However, fewer dendritic spines formed in the denervated region (*top row, middle panel*) as compared to the contralateral control (*top row, left panel*). In contrast, newborn granule cells in the deafferented dentate gyrus developed more dendritic spines in the inner molecular layer (IML, *bottom row, middle panel*) compared to the contralateral side (*bottom row, left panel*). Spine density in the deafferented OML was significantly lower than control (*top row, right panel,* $p < 0.05$), but significantly higher than control in the IML (*bottom row, right panel,* $p < 0.01$). **(B)** Mature granule cells at 21 days post-lesion**.** Distal dendritic spines on mature granule cells were denervated by the lesion and were decreased in number (*top row, middle panel*) relative to the nonlesioned contralateral control (*top row, left panel*). However, unlike newborn granule cells, the number of dendritic spines on mature granule cells in the IML was not affected by the lesion (*bottom row*). Mature granule cells had lower dendritic spine density in the deafferented region (*top row, right panel,* $p < 0.01$) than those in the control hemisphere, but no change was observed in the inner molecular layer (*bottom row, right panel,* N.S.). OML = outer molecular layer, IML = inner molecular layer, * = $p < 0.05$, ** = $p < 0.01$. Scale bar = 5µm.

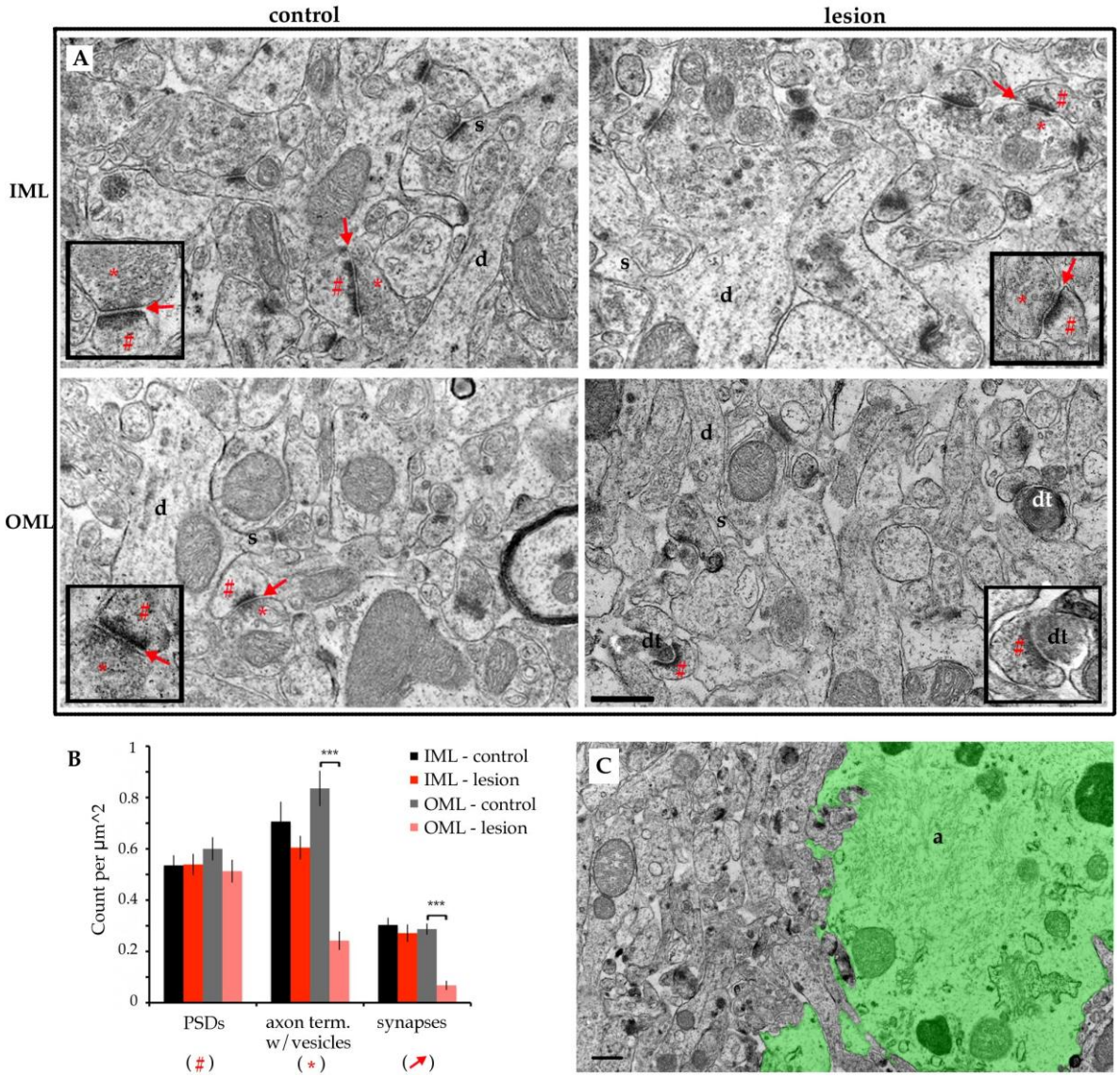

Figure 11 – Perforant path lesion decreased the number of presynaptic terminals and intact synapses in the denervated zone.

(legend on next page)

Figure 11 – Perforant path lesion decreased the number of presynaptic terminals and intact synapses in the denervated zone.

(A) *Top row:* Electron micrographs of the non-denervated inner molecular layer (IML) at 21 days post-lesion, showed normal tissue structure in the control (*left*) and lesioned (*right*) dentate gyrus. Both dentate gyri had synaptic vesicles/ axon terminals (*) at intact synapses (arrow) with postsynaptic densities (#). *Bottom row:* Electron micrographs of the denervated outer molecular layer (OML, *right panel)* as compared with the outer molecular layer on the contralateral control hemisphere (*left panel)*. In contrast to the control, the denervated region was devoid of presynaptic terminals (*) and instead showed electron-dense degenerating axons (dt) apposed to postsynaptic densities (#). *Insets* show higher magnification examples. **(B)** The synaptic composition in the inner and outer molecular layers was quantified by independently counting the number of postsynaptic densities (PSDs, [#]), the number of axon terminals (as indicated by presence of vesicles, [*]), and the number of intact synapses (arrows). At 21 days post-lesion, the number of postsynaptic densities was unchanged in either layer, however presynaptic terminals and intact synapses were substantially decreased in the denervated OML ($p < 0.001$), but unchanged in the non-denervated IML (N.S.). **(C)** Low-magnification micrograph (6800x) exemplifying reactive astrogliosis in the denervated outer molecular layer. Reactive astrocytes could occupy as much as 50% of the most severely affected regions (shaded green). **d** = dendrite, **s** = dendritic spine, **dt** = degenerating axon terminal, **a** = astrocyte. Scale bars = 500nm. *** = $p < 0.001$.

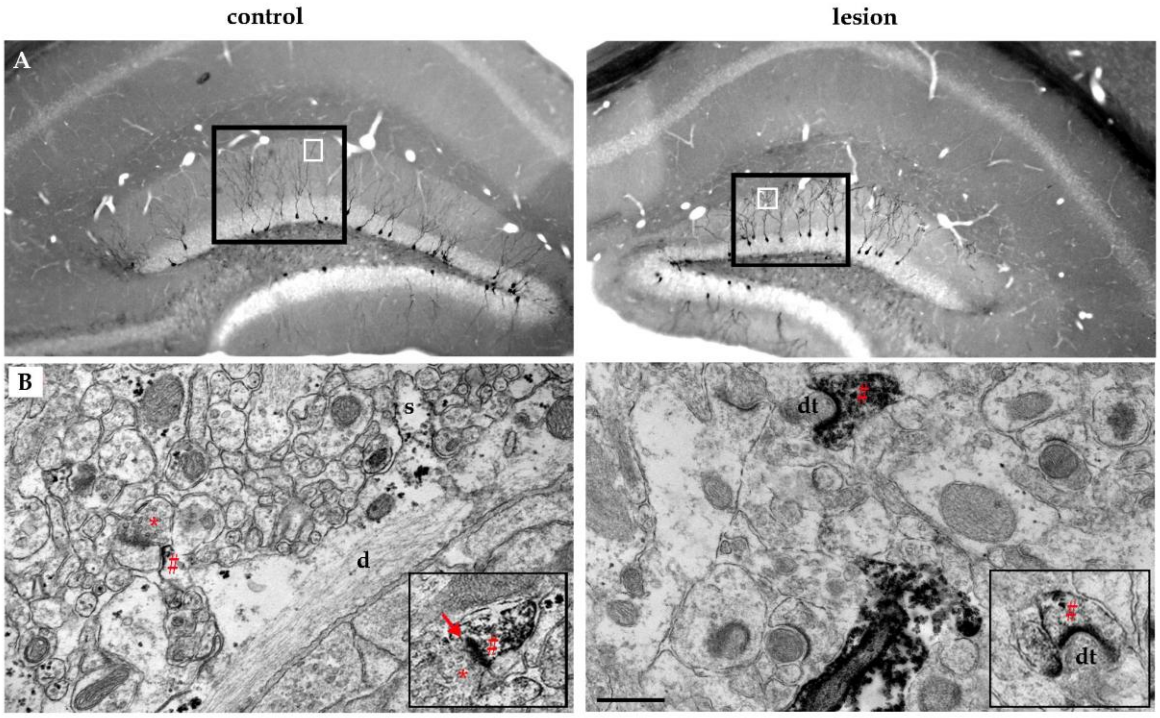

Figure 12 – Perforant path lesion did not preclude formation of post-synaptic specializations on newborn granule cell dendrites in the deafferented zone.

(A) Flat embeds of immunostained EM tissue at 21 days post-lesion, 40μm sections. Newborn neurons were labeled with retroviral injection on the day of the lesion, thus labeling granule cells that developed in the absence of perforant path input. Labeled newborn neurons were present in the control (*left panel*) and lesioned (*right panel*) dentate gyrus. Black squares outline densely immunolabeled regions of the suprapyramidal blades that were chosen for thin-sectioning and subsequent analysis. White squares indicate approximate regions pictured in B. **(B)** *Left panel:* Immuno-electron micrograph of the outer molecular layer in the control dentate gyrus, 75nm section. Labeled dendrite (d) of a 21-day-old control newborn granule cell had dendritic spines (s), a developing postsynaptic density (#), and initial features of a synapse forming with an axon terminal (*). *Left panel inset:* close-up of another newly formed synapse (arrow) between an axon terminal (*) and a labeled 21-day-old newborn granule cell with a postsynaptic density (#). *Right panel:* Immuno-electron micrograph of the denervated outer molecular layer in the lesioned hemisphere, 75nm section. A prominently labeled 21-day-old new granule cell had a postsynaptic density (#), which was apposed only by a degenerated axon terminal (dt). *Right panel inset:* another example of a labeled dendritic spine with a post-synaptic density (#) apposed by a degenerating terminal (dt). Post-synaptic densities in the denervated zone often were curvilinear, rather than the straight PSD characteristic of the control. Scale bar in B = 500nm.

CHAPTER 1 – ADDENDUM

MECHANISMS OF LESION-INDUCED PROLIFERATION AND DISPERSION OF NEWBORN GRANULE CELLS IN THE DENTATE GYRUS

Possible mechanisms of injury-induced proliferation and dispersion of newborn granule cells in the dentate gyrus

Lesion-induced proliferation of newborn granule cells.

In the adult dentate gyrus neurogenesis occurs throughout life, suggesting that the adult brain has at least a limited capacity to regenerate following injury. Proliferation of newborn neurons can be upregulated following injury and their functional integration and survival can impact the degree of recovery. Generally, neurogenesis is stimulated by increases in network activity, such as would occur during seizure (Overstreet-Wadiche et al., 2006; Parent, 2007). However, proliferation of newborn neurons is surprisingly also stimulated by lesion of the perforant path (Figures 6 and 7), which effectively decreases overall network activity (Figure 5). Consistent with such a decrease in excitatory activity, we saw deficits in dendritic arborization of newborn neurons following lesion. However, we hypothesized that the decline in glutamatergic innervation may be preceded by a burst of activity triggered by axon transection, which may trigger proliferation of newborn neurons. To address this possibility we used a marker of network activity, the immediate early gene c-fos. We measured c-fos immunoreactivity in the dentate gyrus at 2 and 6 hours after a unilateral perforant path lesion. As shown in Figure 13A, lesion of the perforant path triggered a dramatic increase in c-fos expression in the deafferented dentate gyrus at 2 hours post-lesion (right panel, red stain). This increase in activity was limited to mature granule cells, which make synaptic contacts with the perforant path. Newborn granule cells, labeled here with POMC-EGFP (green), do not yet receive perforant path

input and therefore do not show an increase in c-fos expression following lesion. The increase in c-fos expression appears to be transient, as it was back to baseline in the lesioned hemisphere at 6 hours post-lesion (data not shown). These results are consistent with a burst of activity triggered by mass glutamate release from cut perforant path axons and the subsequent absence of excitatory activity as these axons degenerate. Because excitatory transmission at these synapses is partially mediated by NMDA receptors, we were able to block the increase in c-fos immunoreactivity by pretreating the animal with the NMDA-receptor antagonist MK-801 20 minutes prior to the lesion procedure (injected intraperitoneally; Figure 13B, right panel). Because MK-801 eliminated the lesion-induced burst of activity, we reasoned that it may be able to prevent proliferation of newborn granule cells that was observed at 14 days post-lesion. However, despite pretreatment with MK-801, we saw no differences in proliferation or dispersion of newborn granule cells at 14 days post-lesion (Figure 13C, right panel; compare with Figure 6B). Thus, although aberrant excitatory activity may contribute to newborn granule cell proliferation, other injury-induced signaling cues, such as BDNF or inflammatory cytokines, are likely to be the primary trigger (Suh et al., 2009).

Lesion-induced dispersion of newborn granule cells.

In addition to increased granule cell proliferation following unilateral lesion of the perforant path, we observed increased dispersion of newborn neurons within the granule cell layer, as measured by the increase in the distance between cell bodies and the hilus border (Figure 6). Aberrant neuronal migration is a complex phenomenon observed in several developmental pathologies, such as lissencephaly, epilepsy, and autism (Fatemi, 2005). Thus, we hypothesized that some of the underlying causes of these pathologies,

including molecular cues such as reelin expression (Tissir and Goffinet, 2003), may also be altered in this lesion model. To test this hypothesis, we immunostained for reelin at different time points following perforant path lesion (Figure 14). At all time points tested, the unlesioned contralateral control showed slightly denser staining surrounding the hippocampal fissure (Figure 14A-D, left panels), the typical location of the GABAergic interneurons that secrete reelin in the adult hippocampus (Pesold et al., 1998). However, reelin expression following lesion of the perforant path increased in the outer molecular layer as early as 1 day post-lesion (Figure 14A) and remained elevated for at least 14 days (Figure 14E). The staining pattern in the deafferented dentate gyrus was also more diffuse than in the contralateral control, with signal detected in the deafferented zone (solid yellow lines).

Although the small number of animals precluded a quantitative analysis of this dataset, some speculation regarding the implications of these findings is in order. The increased staining in this region may depict lesion-induced ectopic migration of reelin-secreting interneurons into the deafferented zone or may simply represent the formation of a reelin gradient spanning the molecular layer (Figure 14E, inverted white triangle). These results are in conflict with an earlier study that found no changes in reelin mRNA expression following lesion of the perforant path (Haas et al., 2000), and are perhaps contradictory to the dogma that a *reduction* in reelin expression leads to aberrant neuronal migration (Katsuyama and Terashima, 2009; Haas and Frotscher, 2010). However, new roles for reelin signaling in the mature brain are emerging, suggesting that it may have both positive and negative effects on neuronal migration and laminar organization (Fatemi, 2005). In addition, the increase in reelin signaling we observed following lesion is

fairly minor and thus may have been missed in the earlier study, as no formal quantitation of reelin mRNA expression was done. Similarly, the differences may be attributable to the method of detection, i.e. the lesion may not have an effect on reelin mRNA expression, but may trigger increased translation of the protein. Although our results contradict earlier studies, the observed increase is theoretically possible, as lamina-specific increases in other matrix proteins, including tenascin-C and neurocan have been observed following perforant path lesion (Deller et al., 1997; Haas et al., 1999).

Although further experiments are necessary to verify the specificity of our antibody and the identity of the labeled cells in the deafferented zone, our results suggest a positive role for reelin in lesion-induced migration of neuronal precursors. For example, Hack et al. (2002) proposed that reelin is a detachment signal for migrating neuronal precursors in olfactory neurogenesis in the adult brain. In this slice culture experiment, addition of reelin triggered detachment of tangentially migrating neuronal precursors from their chains, thus stimulating their subsequent individual radial migration. However, if reelin was mutated, precursor cells remained in clusters and failed to radially migrate, suggesting that reelin is required for detachment from the migration chains. Although in the dentate gyrus radial glia aid granule cell migration, upregulation of reelin may stimulate detachment of new neurons from their neurogenic niche in the subgranular zone, thus increasing their outward migration into the granule cell layer. Interestingly, seizure studies, in which a reduction in reelin signaling is associated with granule cell dispersion (Heinrich et al., 2006), suggest that reelin is also important in the maintenance of a compact granule cell layer in the adult dentate gyrus. As such, aberrant granule cell migration following perforant path lesion may also be controlled by increased reelin

signaling, thus precluding ectopic localization of these cells. To address these questions, future experiments will need to conditionally manipulate reelin activity following lesion using either a tamoxifen-inducible reelin mutation or *in situ* viral knockdowns of this protein. Unfortunately, it is unlikely that *reeler* mice will be useful in such experiments because of their severe deficit in hippocampal cellular organization (Stanfield and Cowan, 1979). Such aberrant morphology would likely disrupt the lamination pattern and cell-cell interactions important for analysis of post-lesion circuit reorganization.

During development, newly generated granule cells migrate along radial glia to take their final positions within the granule cell layer (Rickmann et al., 1987). In the adult dentate gyrus, radial glia continue to provide a migratory scaffold for newly generated neurons (Förster et al., 2002; Weiss et al., 2003) and serve as a pool of granule cell precursors (Seri et al., 2001). Thus, if the radial glial population is affected following perforant path lesion, it may help to explain the increased proliferation and outward migration of newborn neurons observed following perforant path lesion. In our preliminary experiments, we saw an increase in the expression of the radial glial marker nestin at 14 days post-lesion (Figure 15), with many stained radial processes aligned within the granule cell layer (Figure 15A, arrowheads). Cell bodies of newborn neurons seemed to be in close proximity with the nestin-positive radial fibers (Figure 15B), however, further investigation is necessary to confirm these findings. Interestingly, the radial glial scaffold fails to form in the absence of reelin (Weiss et al., 2003), but is rescued if *reeler* brain slices are treated with recombinant reelin (Zhao et al., 2004). A particularly interesting finding from the latter study is that reelin must be in a specific topographical location relative to the glial scaffold in order to help establish its polarity. In the adult

hippocampus, reelin is synthesized in the outer molecular layer, with a gradient reaching across the molecular layer to interact with the radial glial population near the granule cell layer. Thus, perforant path lesion may trigger a complex sequence of increased reelin expression in the deafferented zone, subsequent enhancement of radial glial scaffolding, and aberrant granule cell migration, that in turn may be kept within the granule cell layer by increased reelin signaling.

Aberrant granule cell migration following lesion has several implications for post-injury circuit reorganization. For example, the strict lamination pattern in the dentate gyrus provides separation between dendrites and axons of the mature granule cells, thus segregating incoming and outgoing information. The importance of this segregation is evident following seizure, when lamination of granule cell bodies is perturbed. In this context, mossy fiber collaterals can aberrantly innervate granule cell dendrites, forming excitation loops that may trigger recurrent seizures (Wenzel et al., 2001). However, unlike in the seizure model, perforant path lesion does not trigger dispersion of newborn granule cells outside of the granule cell layer and newborn granule cells seem to properly establish their dendritic and axonal connections. Thus, proliferation of newborn neurons in this context may be an adaptive process, providing a highly plastic postsynaptic target for the sprouting axons in the inner molecular layer.

CHAPTER 1 – ADDENDUM: FIGURES

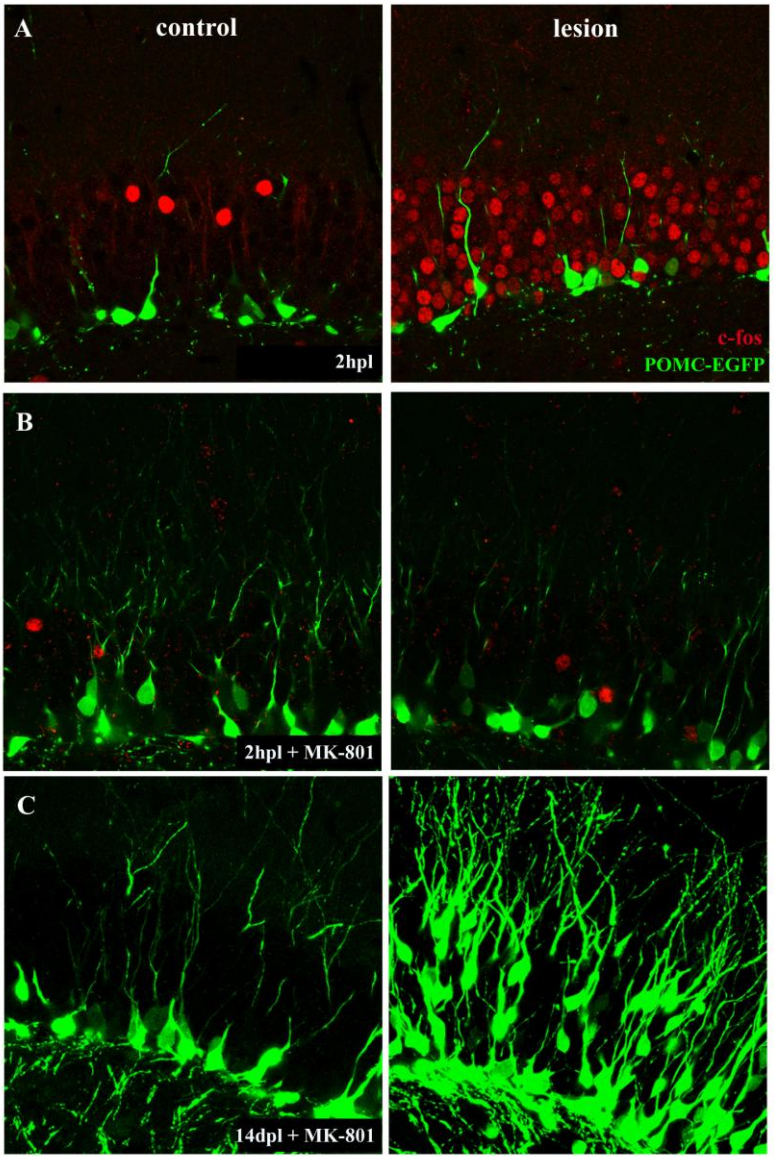

Figure 13 – Perforant path lesion stimulates a burst of activity, but cause for proliferation is more complex.

Single-layer snapshots. **(A)** Transection of perforant path axons triggers widespread expression of the immediate early gene c-fos (right panel, red) at 2 hours following injury, indicating an increase in network activity. Upregulation of c-fos expression is no longer detected at 6 hours post-lesion (not shown), suggesting that the activity burst is transient and associated with axon transection. Note the absence of c-fos immunoreactivity from 14 day-old neurons (POMC-EGFP) that do not yet receive perforant path input. **(B)** The postsynaptic response to the transient burst of activity can be dampened by injecting the animal with MK-801, a noncompetitive NMDA antagonist, 20 minutes prior to the lesion.

However, transiently blocking network activity does not prevent lesion-induced proliferation of newborn neurons (POMC-EGFP, right panel in **(C)**).

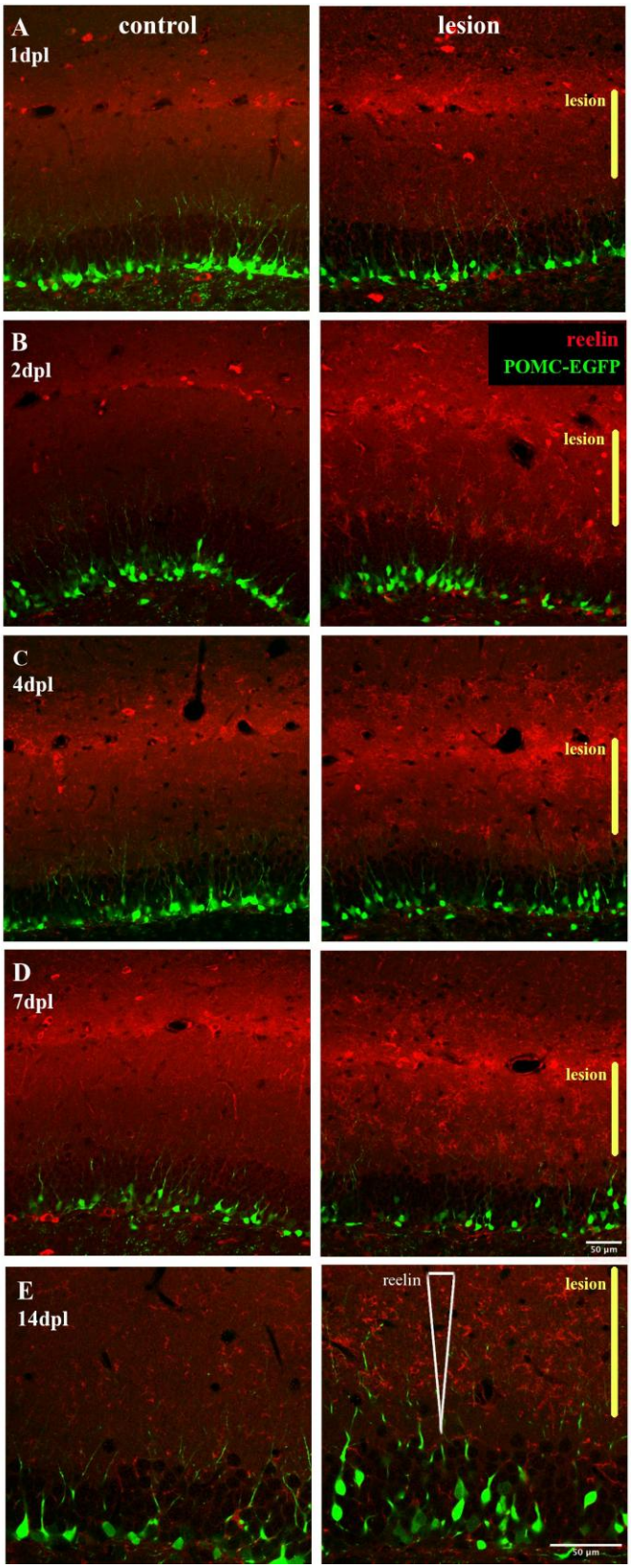

Figure 14 – Perforant path lesion may lead to an upregulation in reelin signaling in the deafferented zone. (legend on next page)

Figure 14 – Perforant path lesion may lead to an upregulation in reelin signaling in the deafferented zone.

During development, reelin is secreted from Cajal-Retzius cells residing in the outermost molecular layer in the dentate gyrus. However, in the adult brain reelin is secreted from GABAergic interneurons, but these cells reside in approximately the same region. **(A)** Snapshots of reelin immunostain in the lesioned (right panel) and contralateral control (left panel) dentate gyrus at 1 day post-lesion. In both hemispheres at this time point, the densest staining surrounds the source cells in the outer molecular layer. **(B)** At 2 days post-lesion, reelin expression is increased in the outer molecular layer (right panel) relative to the contralateral control (left panel) and labeled astrocyte-like cells can be seen throughout the molecular layer. The actual identity of these cells has not been determined and it is possible that labeling of these cells may be a consequence of non-specific staining or autofluorescence. **(C,D)** The increase in reelin expression in the outer molecular layer is sustained through 4- (C) and 7- (D) days post-lesion relative to the contralateral hemisphere, however a lamina-specific increase in labeling should be noted in the deafferented zone (solid yellow line, right panels). **(E)** Higher magnification image of the dorsal blade but at 14 days post-lesion. Increased lamina-specific reelin labeling can be observed throughout the denervated region (solid yellow line, right panel), but may form a decreasing gradient spanning the molecular layer (inverted white triangle, right panel) between reelin-secreting cells and the granule cell layer. Note the relatively stable population of newborn neurons (POMC-EGFP, green cells) throughout first week post-lesion.

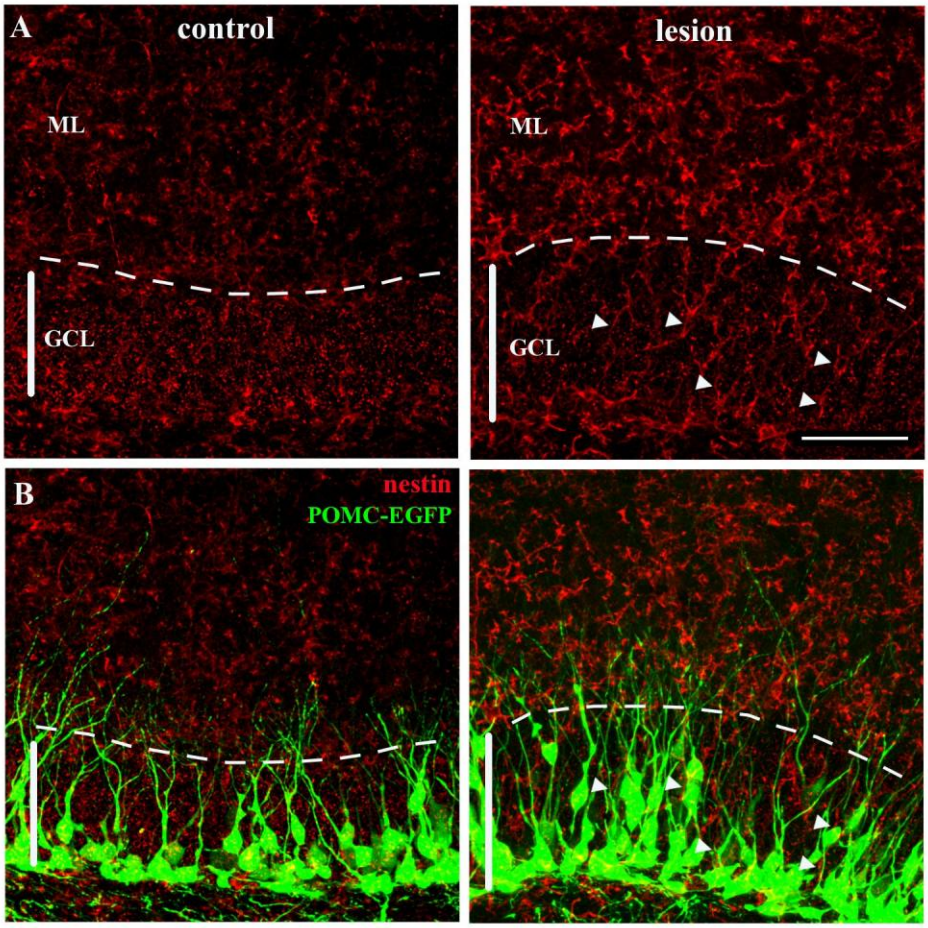

Figure 15 – Lesion triggers an increase in nestin-expressing radial glia.

(A) 14 days post-lesion: 50μm z-stack projection of the dorsal dentate gyrus stained for nestin, a marker for radial glial cells. Note the increase in radial fibers (arrowheads) throughout the granule cell layer (GCL) in the lesioned hemisphere (right panel) as well as an increase in reactive glia in the molecular layer (ML). **(B)** Green channel overlay of the same sections shown in A. Labeled cells are 14-day-old granule cells from POMC-EGFP transgenic mice. Note the typical increase in proliferation of newborn neurons observed at 14 days post-lesion (right panel). The granule cell layer (GCL) is delineated by the dashed white line, beyond which is the molecular layer (ML).

CHAPTER 2

ROLE OF EXTRACELLULAR ENVIRONMENT IN POST-LESION CIRCUIT REORGANIZATION

Laminar borders and axonal sprouting following lesion.

Although lesion of the perforant path triggers a variety of injury-induced responses, all circuit components – including reactive gliosis, axonal sprouting, and dendritic restructuring – undergo reorganization within their respective laminae. In the case of reactive gliosis, laminar segregation can be considered adaptive, as glia play an instrumental role in clearing axonal debris and maintaining the ion balance of the surrounding environment. However, in the case of neural circuit reorganization, laminar borders may prevent translaminar sprouting of intact axons, thus possibly diminishing the degree of post-lesion functional recovery. Interestingly, laminar specificity following lesion is reminiscent of the molecular profile during hippocampal development, suggesting that some developmental processes of laminar assembly and maintenance can be, at least partially, recapitulated following injury. Insights from the developing hippocampus may provide clues as to the mechanisms of post-lesion circuit reorganization and may thus aid in local experimental manipulation of the deafferented region.

Lamination in the developing dentate gyrus

Laminar borders in the dentate gyrus are defined early in development, with excitatory afferents segregating into their respective layers as early as embryogenesis (Frotscher et al., 2007). For example, perforant path axons from the entorhinal cortex reach

the dentate gyrus at embryonic day 19 (E19) and occupy predominantly the outer molecular layer. On the other hand, commissural/ associational axons first appear at post-natal day 2 (P2) and specifically populate the inner molecular layer (Super and Soriano, 1994; Förster et al., 2006). Interestingly, these afferents show the same laminar preference even if the order of innervation is experimentally reversed (Frotscher and Heimrich, 1993), thus implicating lamina-specific cues in axonal guidance during development. Such cues may arise in part from cell-cell interactions, with pioneer or established neurons providing a scaffold for innervation. For example, early in development, Cajal-Retzius cells populate the developing outer molecular layer and provide a temporary postsynaptic target for the incoming perforant path axons, prior to the availability of granule cell dendrites (Rihn and Claiborne, 1990; Ceranik et al., 2000). Thus, these "placeholder" cells attract perforant path fibers, resulting in laminar specificity (Supèr et al., 1998). Once perforant path axons are in place, most Cajal-Retzius cells degenerate, allowing synaptogenesis with the now sufficiently matured granule cell dendrites (Soriano and Del Rio, 2005). If the function of Cajal-Retzius cells is perturbed, perforant path fibers lack laminar specificity and terminate throughout the molecular layer (Del Rio et al., 1997). However, mutation of Cajal-Retzius cells does not affect the commissural/ associational axons. These axons arrive around P2, after granule cell dendrites have matured, suggesting that axon guidance cues can also be provided by the postsynaptic targets themselves. Indeed, commissural/ associational axons lose their laminar preference if migration of their targets, the newly generated granule cells, is perturbed (Gebhardt et al., 2002; Zhao et al., 2003). Furthermore, this effect is reversed if proper granule cell migration is experimentally restored (Förster et al., 2006).

Pre- and postsynaptic components of lesion-induced circuit reorganization

Many components of the developing dentate gyrus are retained in the adult brain, suggesting the theoretical possibility of lamina-specific reinnervation following lesion. Specifically, despite the absence of placeholder cells in the adult dentate gyrus, dendrites of mature granule cells as well as the nonlesioned fiber tracts may be able to synthesize guidance cues that direct sprouting axons toward the vacated dendritic spines. In our preliminary assessment of the interplay between pre- and postsynaptic components following lesion, we assessed the time course of axonal degeneration in parallel with the post-lesion response of dendritic spines. We used the vesicular glutamate transporter vGlut1 as a marker of excitatory axons and a postsynaptic density (PSD95) marker to label dendritic spines. Figure 16A shows the expression of these two proteins at baseline as well as in the contralateral dentate gyrus at all post-lesion time points tested. Diffuse vGlut1 staining (left panel, red) was visible throughout the dentate molecular layer, with a slight increase in intensity closer to the granule cell layer. Staining for PSD95 (right panel, blue) showed a similar expression pattern, but indicated a higher spine density in the inner molecular layer. vGlut1 expression began to decrease in the denervated region at 2 days post-lesion (Figure 16C, left panel) and was nearly gone by 7 days post-lesion (Figure 16E, left panel). In contrast, PSD95 staining was not affected by deafferentation (Figure 16B-E). This discrepancy between pre- and postsynaptic marker expression was sustained for at least 21 days post-lesion (Figure 16F), indicating that no excitatory reinnervation occurs in the deafferented zone. Thus, we conclude that postsynaptic targets alone are not sufficient to stimulate regenerative homotypic sprouting following lesion.

Extracellular matrix in development and following lesion

Role of the extracellular matrix in generation and maintenance of laminar borders.

Axon guidance and fasciculation during development can also be regulated by gradients of attractive or repulsive extracellular matrix molecules, including cell-adhesion molecules such as L1 and NCAM, soluble factors such as the semaphorins and netrins, ephrin receptors and their ligands, as well as ECM proteins, such as the chondroitin sulfate proteoglycans (CSPGs, Margolis and Margolis, 1997; Skutella and Nitsch, 2001). Extracellular matrix proteins, particularly CSPGs, are expressed throughout life, although their composition and spatiotemporal expression varies with age. These proteins assist in pattern cell migration and axonal outgrowth, regulate availability of growth factors and guidance molecules, and are involved in brain repair following injury (Carulli et al., 2005; Kwok et al., 2008). CSPGs are expressed during development and have been suggested to regulate laminar specificity of incoming perforant path axons (Pearlman and Sheppard, 1996; Raugh, 1997; Wilson and Snow, 2000; Kwok et al., 2012). For example, layer specificity of entorhinal afferents, but not of commissural/ associational afferents, is lost if the extracellular matrix molecule hyaluronan is perturbed (Förster et al., 2001; Zhao et al., 2003), suggesting that the extracellular matrix is required for proper lamination.

In addition to their role in development, extracellular matrix proteins play a major role in brain plasticity following injury. Proteoglycans, for example, are secreted by reactive astrocytes and can contribute to formation an impenetrable barrier to axonal growth (Matsui and Oohira, 2004). Interestingly, lamina-specific reactive astrogliosis is a prominent feature of the hippocampal response to lesion of the perforant path, suggesting that secretion of extracellular matrix proteins may be increased in the deafferented region. Therefore, reactive gliosis, alongside the subsequent increase in proteoglycan expression,

may prevent translaminar sprouting by reintroducing some of the developmental signals for laminar segregation. Figure 17 shows the time course of microglia (white) and astrocyte (red) activation following lesion. The molecular layer is outlined with dashed lines and the deafferented zone is indicated with a solid yellow line. At baseline, astrocytes had few branches and microglia were hardly detectable (Figure 17A). This section is representative of the contralateral control at all time points tested. At 1 day post-lesion, gliosis was minimal, as circuit reorganization is just beginning. At 2 days post-lesion, microglia in the deafferented zone began to increase in number and to acquire reactive morphology (Figure 17C, arrowheads), whereas astroglia remained at baseline. Within the next several days post-lesion, the microglial reaction peaked, with white clusters visible throughout the denervated region (Figure 17D-F). Reactive astrogliosis was delayed relative to the microglial response, with the first signs of astrocyte hypertrophy evident at 4 days post-lesion (Figure 17D) and the peak of reactivity around 7 days (Figure 17E). Although microglia returned to baseline shortly thereafter, astroglial hypertrophy was prolonged and was still evident at 1 month post-lesion (Figure 17F). However, note that reactive astrocytes remained within their domains and did not form an impenetrable glial scar, suggesting that astrogliosis in this context is an adaptive response to injury (Sofroniew, 2009). Although the small number of animals used for each time point precluded statistical analysis, these data reflect previously published work on the subject (Hailer et al., 1999).

The laminar specificity of the glial response to perforant path lesion reflects the location of degenerating axons, but also the stringency of laminar barriers in the adult brain. Reactive gliosis can contain the deafferented area, thus preserving incoming axons

in the inner molecular layer. However, reactive gliosis may also play a role in preventing translaminar sprouting during post-lesion circuit reorganization. For example, reactive astrocytes secrete extracellular matrix proteins (Fitch and Silver, 2008). As extracellular matrix proteins, such as proteoglycans, guide the lamination process of afferent fibers during development, their lesion-induced increase in the adult brain can reintroduce lamina-specific guidance cues for sprouting axons of uninjured afferents. Similarly, changes in the extracellular matrix composition may impact dendritic outgrowth of newborn granule cells that mature in the weeks following lesion. We began to test these hypotheses by looking at the time course of CSPG expression after unilateral transection of the perforant path. Under normal conditions and in the contralateral control, CSPG expression was largely diffuse, with slightly denser staining in some regions (Figure 18A). However, the density of CSPG staining was noticeably increased by 4 days post-lesion (Figure 18D) and this effect was sustained for at least two weeks thereafter (Figure 18F). As expected, the increase in CSPG expression corresponded with the lesion-induced activation of astrocytes and, like astrogliosis, was limited to the deafferented zone (Figure 18F, solid yellow line; note the sustained baseline expression of CSPG in the inner molecular layer). Although our data were not quantified because of the small number of animals used for these experiments, these results reflect the known responses of the extracellular matrix to lesion of the perforant path. For example, the proteoglycans brevican and neurocan, as well as tenascin-C, are upregulated in the denervated zone with a time-course consistent with their potential role in neurite outgrowth (Deller et al., 1997; Haas et al., 1999; Thon et al., 2000). Because these molecules are active during formation of the dentate gyrus, their re-expression following injury suggest that post-lesion circuit reorganization may be a recapitulation of development.

Manipulation of the post-lesion extracellular environment

Increased expression of chondroitin sulfate proteoglycans (CSPG) is well-documented in the context of spinal cord injury, where it is a major component of the impenetrable glial scar (Bartus et al., 2012). Various attempts have been made to aid regeneration past the glial scar by using enzymes that degrade the proteoglycans. For example, injection of chondroitinase ABC (chABC) near the site of the lesion reduces CSPG inhibition following spinal cord injury, thereby facilitating axonal regeneration and aiding compensatory plasticity of uninjured axons (Bradbury and Carter, 2011). In our preliminary experiments, we saw an increase in CSPG expression in the denervated zone following perforant path lesion, suggesting that the outer molecular layer may have an inhibitory effect on translaminar axonal sprouting as well as on dendritic outgrowth of newborn granule cells. Thus, blocking the CSPG response may reverse these deficits in the reorganizing circuit. To test this hypothesis, we stereotaxically injected chABC into the dorsal dentate gyrus in the lesioned hemisphere, with the contralateral dentate gyrus used as an unmanipulated control (no lesion, no chABC). Figure 19 (A-C) shows images of injection protocol optimization. As shown in Figure 19A, the dorsal hippocampus was unilaterally injected with 0.2μl of chABC (yellow needle, right side). Immunostaining for the digestion fragment C4S (red) shows the approximate spread of enzymatic activity (dashed yellow line). Although some C4S expression was detected in the uninjected contralateral dentate gyrus, it was limited to the medial corner of the granule cell layer and thus did not impact subsequent analysis of the dorsal blade. In future experiments, smaller volumes of the enzyme should be used to prevent contamination of neighboring areas. Figure 19(B,C) shows CSPG expression after treatment with chABC. Correctly

timing the chABC injection relative to the time of lesion was important in eliminating lesion-induced CSPG activity. If chABC was injected on the day of the lesion and tissue was examined at 14 days post-lesion, elevated CSPG expression was still detected in the deafferented dentate gyrus (Figure 19B, right panel). However, if the chABC injection coincided with the peak of CSPG expression (at 7 days post-lesion, see Figure 18E), lesion-induced activation of CSPG was blocked (Figure 19C, right panel). Thus, to evaluate post-lesion circuit reorganization and neurogenesis, chABC was injected at 7 days post-lesion. We also used an alternative approach to block CSPG expression following lesion – intraperitoneal (IP) injections of Xyloside, injected twice daily from 3 to 7 days post-lesion. Whereas chABC degrades already expressed CSPGs, Xyloside prevents CSPG synthesis. Treatment with Xyloside was delayed relative to the lesion because CSPGs were shown to have a beneficial effect within the first two days after an injury (Rolls et al., 2008). Unfortunately, Xyloside injections failed to block the increase in CSPG expression in the dentate gyrus when tissue was examined at 14 days post-lesion (Figure 19D, n=4); therefore, no further analysis was done. In the original study (Rolls et al., 2008), xyloside was used following spinal cord injury, which, unlike the perforant path lesion, is considered a maladaptive response to injury. Therefore, the parameters of effective xyloside injections may differ between the two models. Future experiments will need to address the timing of xyloside delivery as well as the concentrations necessary to achieve optimal block of CSPG synthesis in the dentate gyrus following lesion.

Dendritic outgrowth and spine density following digestion of CSPG.

Because of their role in inhibiting axonal regrowth following spinal cord injury, CSPGs have been studied predominantly with regard to axons, but evidence for the role of

CSPGs in dendritic outgrowth is scarce. However, a recent study looking at embryonic cortical neurons *in vitro* found that CSPGs counteract the increase in dendritic spines following treatment with BDNF, resulting in an overall decrease in spine density relative to the untreated control (Kurihara and Yamashita, 2012). Similarly, See et al. (2010) saw a significant decrease in neurite outgrowth of neural progenitors cultured in inhibitory concentrations of CSPG, although survival and differentiation of these cells was not affected. In our experiments, dendrites of newborn granule cells were shorter in the deafferented dentate gyrus and had decreased complexity in the denervated region (Figure 8). Interestingly, this region also contains increased expression of CSPGs, suggesting that changes in the composition of the extracellular matrix may impact the development of dendrites and dendritic spines. We tested this possibility *in vivo* by analyzing dendritic arbors and spine densities of newborn and mature granule cells after a combination of unilateral lesion + chABC. chABC was injected at 7 days post-lesion (Figure 19A,C) and tissue was examined either 7 or 14 days later (i.e. at 14 and 21 days post-lesion). As in our initial arborization and spine density experiments (Figures 8 and 10), the post-lesion time interval allowed examination of granule cells that were dividing at the time of the lesion. Dendritic spines were counted in the inner and outer molecular layers for mature- and 21-day-old granule cells at 21 days post-lesion. All sections used for analysis were stained for the CSPG digestion product C4S (Figure 19A) to ensure specific delivery of the enzyme only to the deafferented dentate gyrus. If the digestion product was detected in the contralateral hemisphere, control dendrite measurements were collected only from granule cells outside the C4S-stained zone. chABC treatment alone had no effect on dendritic arborization relative to the contralateral control. It is important to note that dendritic arbors of these cells were subject to the same post-lesion changes

described in Chapter 1. Thus, chABC treatment was employed to test whether CSPG upregulation following lesion underlies some of these changes.

Out of all granule cells examined, only the 14-day-old neurons in the deafferented dentate gyrus exhibited any improvements in their dendritic arbors following chABC treatment (data not shown). Although newborn neurons still had a lesion-induced decrease in the number of branches ($n=6$, $p < 0.001$, t-test), they no longer showed a deficit in their total dendritic length relative to the contralateral control ($n=6$, N. S., t-test). These results suggest that reducing post-lesion CSPG expression in the deafferented zone can create a more favorable environment for dendritic outgrowth, though excitatory innervation by the perforant path is still required for branching. However, chABC treatment did not ameliorate the lesion effects on dendritic spine density in 21-day-old and mature granule cells. Similar to our earlier dataset (Figure 10), we observed a decrease in spine densities on distal dendritic segments of mature and 21-day-old granule cells, as well as an increase in spine density on proximal dendritic segments in 21-day-old granule cells only, with these segments corresponding to the denervated and intact/ sprouting molecular layers, respectively. Two reasons may explain the lack of a phenotype in older granule cells. First, chABC activity is transient and thus requires optimization of delivery timing (Figure 19B). In our experiments, 14-day-old granule cells were analyzed at a shorter interval after chABC treatment than older cells (7 days vs. 14 days), raising the possibility that one chABC injection at 7 days post-lesion was insufficient to span the entire experimental period. Therefore, dendritic arborization and spine density of mature and 21-day-old granule cells should be re-tested at 21 days post-lesion after two injections of chABC at 7- and 14- days post-lesion. To avoid the necessity of repeated injections, in

may be preferable to use a chABC-expressing viral vector (Zhao et al., 2011). Second, CSPGs are only one of many types of extracellular matrix proteins that are impacted following lesion, suggesting that other inhibitors of dendritic outgrowth are present in the deafferented zone. Furthermore, CSPGs are only partially broken down by chABC, leaving behind intact core proteins that may themselves create an unfavorable environment for growth (Oohira et al., 1991; Bukhari et al., 2011). As such, future studies should explore the effects of other locally injected enzymes, such as hyaluronidase, that degrade either the entire CSPG complex or other matrix proteins elevated in this region. Effective delivery of these enzymes, as well as more stringent regulation of their spread in the tissue, may be instrumental in understanding the role of the extracellular matrix in laminar specificity, dendritic outgrowth, axonal sprouting, and functional recovery.

CHAPTER 2: FIGURES

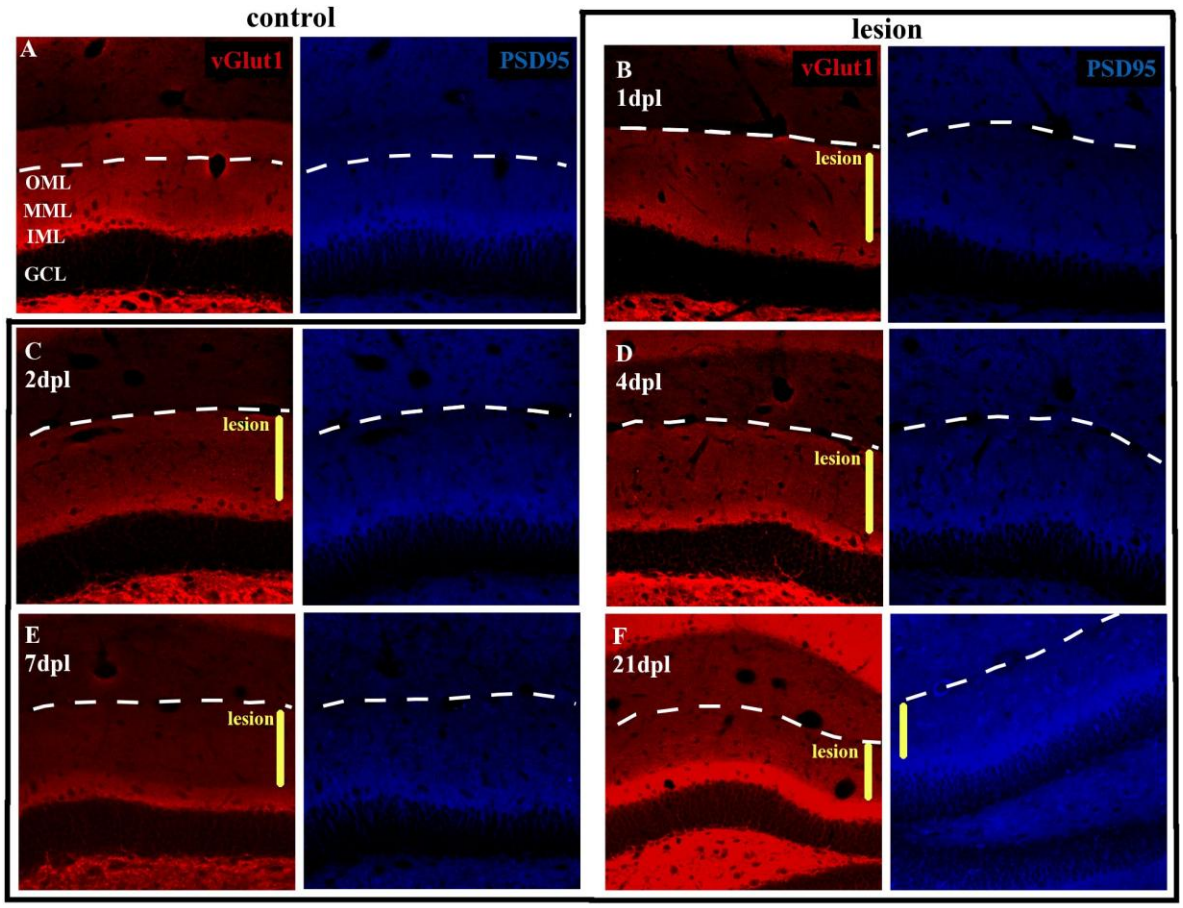

Figure 16 – Lesion alters vGlut1 expression in the deafferented zone, but not PSD95

Post-lesion time course of pre- and postsynaptic reorganization. vGlut1 (red) was used as a marker of excitatory axons and PSD95 (blue) was used as a marker of the postsynapse. Images in A-E are depictions of different channels from the same brain slice, separated for clarity. **(A)** Baseline expression of excitatory axons and postsynaptic densities in the control/ contralateral adult hippocampus. Both markers show diffuse staining throughout the molecular layer, but PSD expression is slightly elevated in the inner molecular layer (IML). **(B-E)** Deafferentation of the dentate gyrus by the perforant path lesion (solid yellow line) triggers a slow degeneration of excitatory axons in the middle and outer molecular layers, first detected at 2 days post-lesion (C, left panel) and almost entirely gone by 7 days post-lesion (E, left panel). Note also the increase in vGlut1 staining in the inner molecular layer starting at day 2 post-lesion, depicting sprouting of the uninjured afferents. Post-synaptic densities were not affected by the lesion (B-E, right panels). The lack of excitatory innervation persists at least through 21 days post-lesion (F, left panel). vGlut1 staining was also absent in 30 days post-lesion animals (not shown), suggesting no excitatory reinnervation occurred in the denervated zone.

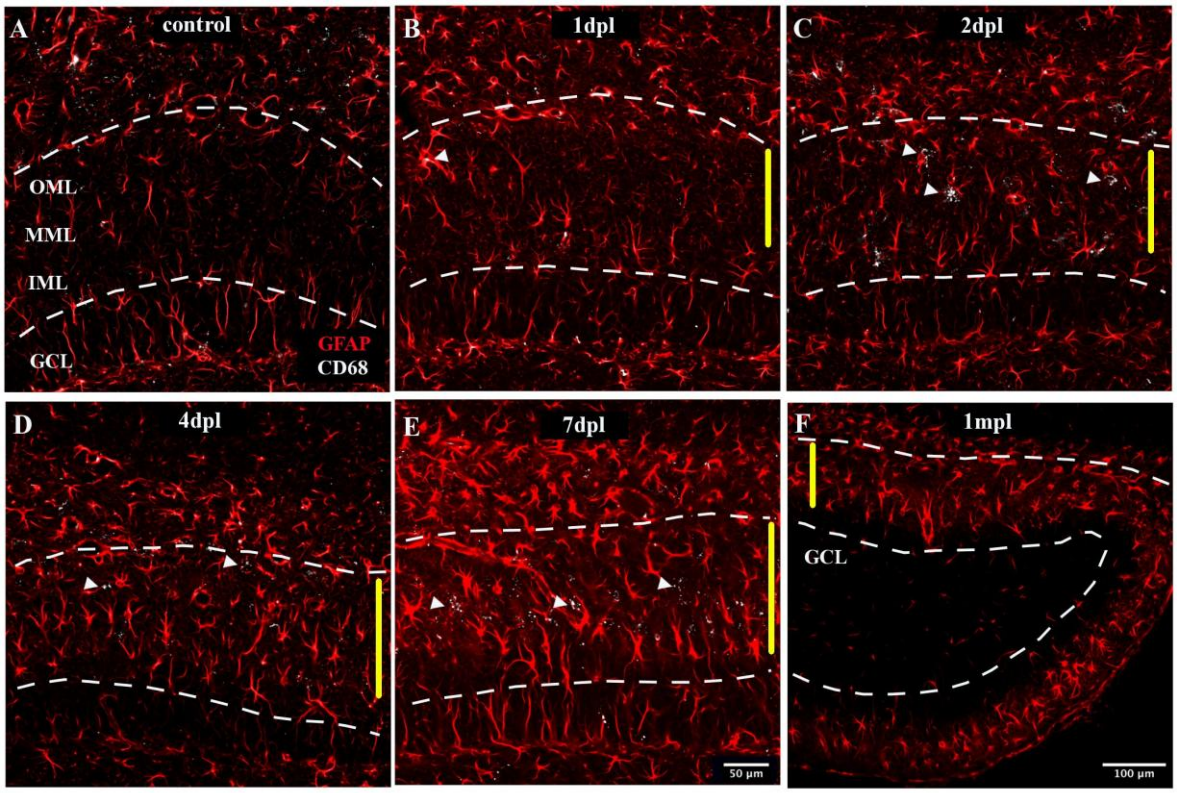

Figure 17 – Lamina-specific reactive gliosis in the denervated dentate gyrus.

Lesion of the perforant path triggers lamina-specific activation of microglia (CD68, white clusters) and astrocytes (GFAP, red). Dashed white lines outline the molecular layer, whereas the solid yellow line defines the deafferented region. **(A)** Representative section of the non-lesioned dentate gyrus for all time points post-lesion. Astrocytes have few branches and microglia are hardly noticeable. **(B)** Dentate gyrus at 1 day post-lesion. At this time point, circuit reorganization is just beginning to occur and changes in microglia (arrowhead) or astrocytes are not yet detectable. Deafferented region is marked by the solid white line on the right. **(C)** At 2 days post-lesion, microglia are in cluster formation, indicative of their activation (arrowheads). **(D)** By 4 days post-lesion, microglia are still active (arrowheads), but astrocytes in the deafferented zone (yellow bar) also begin to hypertrophy. This trend is also observed at 7 days post-lesion **(E)**. **(F)** By 1 month post-lesion, microglia have returned to their baseline expression level (not shown), however astrocytes remain active at least this long. Scale bar in E applies also to A-D.

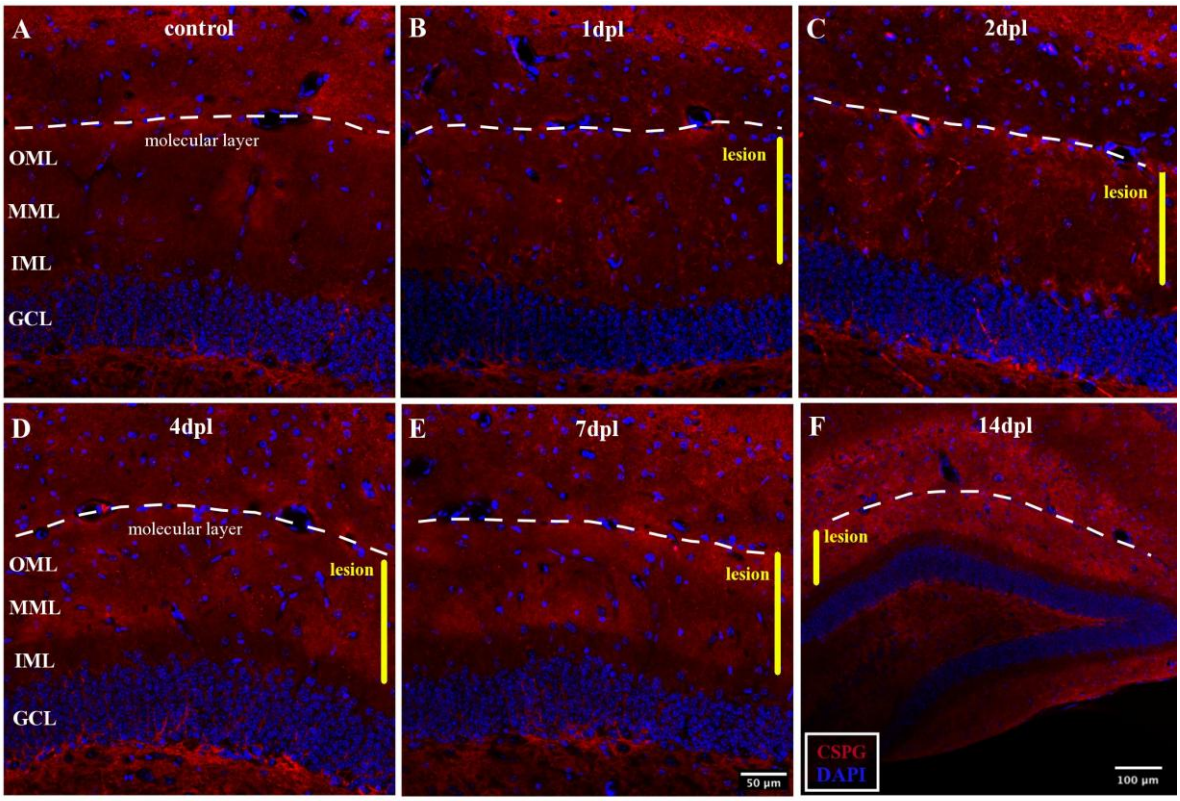

Figure 18 – Lamina-specific upregulation of CSPG following perforant path lesion.

Time course of CSPG expression following lesion. Dashed white line lies on the hippocampal fissure and depicts the border of the dentate molecular layer. The solid yellow line indicates approximate zone deafferented by the injury. **(A)** Representative example of baseline CSPG expression that can be observed in the contralateral control at all time points tested. The signal is largely diffuse, with some indication of more densely stained areas. **(B-F)** An increase in CSPG expression first becomes apparent at 4 days post-lesion (D) with dense clouds becoming more prominent. CSPG expression continues to increase, peaking at 7 days post-lesion (E) and persisting longer than two weeks (F). Attempts to eliminate injury-induced upregulation of CSPG must consider the timing of its expression as well as the half-life of enzymatic activity.

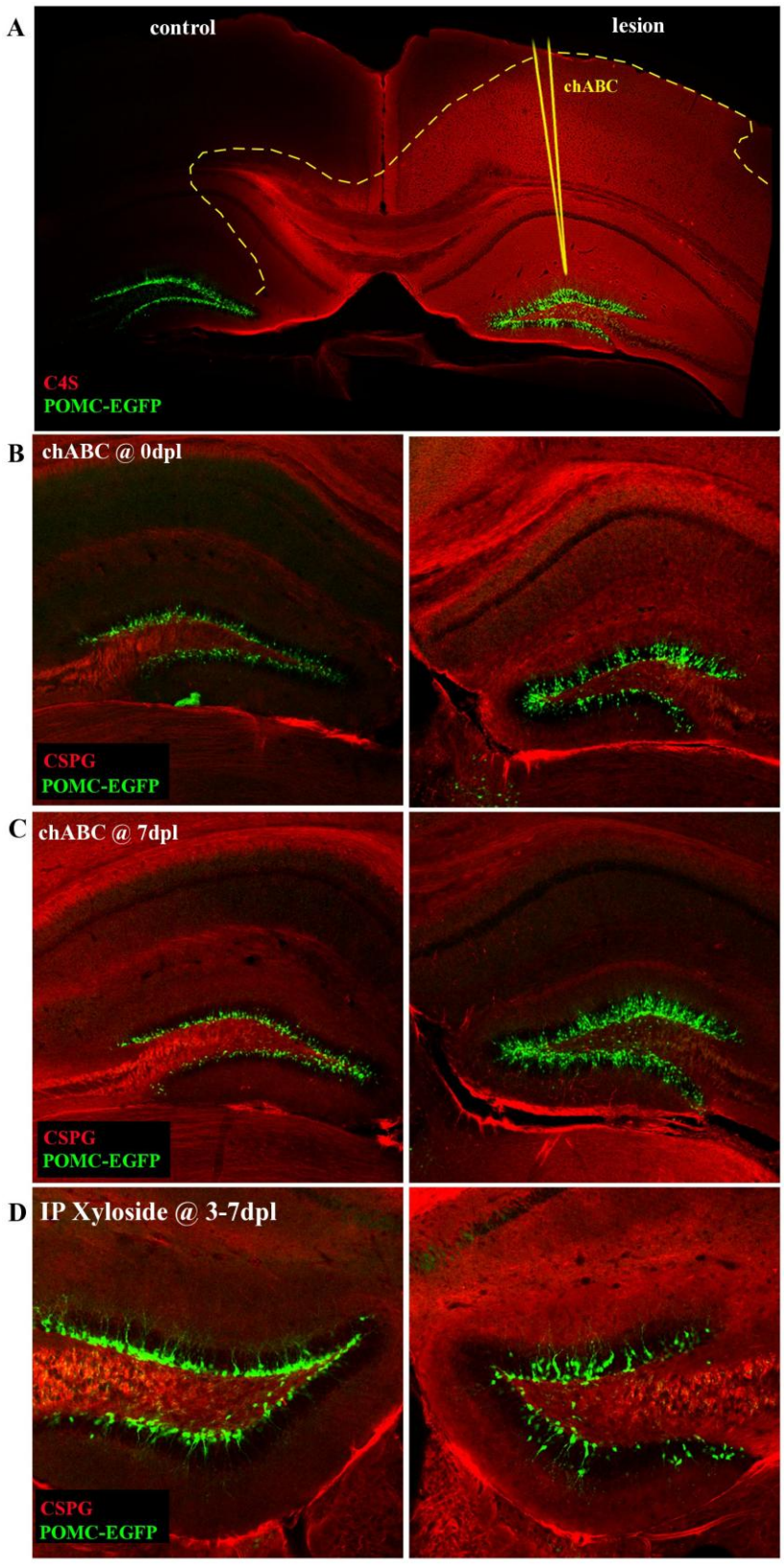
A
control
lesion
chABC
C4S
POMC-EGFP
B
chABC @ 0dpl
CSPG
POMC-EGFP
C
chABC @ 7dpl
CSPG
POMC-EGFP
D
IP Xyloside @ 3-7dpl
CSPG
POMC-EGFP

Figure 19

Figure 19 – CSPG upregulation following lesion can be knocked down by enzyme treatment, but timing is crucial.

(A) Chondroitinase ABC (chABC) was stereotaxically injected into the deafferented dentate gyrus. The approximate spread of enzymatic activity is outlined with a dashed yellow line. Although some crossover can be observed, the area of interest (the dorsal blade of the contralateral dentate gyrus) was typically not affected by the injection. Enzymatic activity was determined by staining for C4S (red), the product of CSPG digestion by chABC. **(B)** Immunostain of undigested CSPG (red) at 14 days post-lesion. chABC was injected on the day of the lesion (0dpl), prior to the peak of CSPG expression (see Fig. 5). CSPG expression was elevated in the lesioned hemisphere (right panel), despite injection of the enzyme, suggesting that CSPG expression outlasted enzymatic activity in the region. **(C)** Immunostain for undigested CSPG (red) at 14 days post-lesion. chABC was injected at 7 days post-lesion, during the peak of injury-induced CSPG expression (see Fig. 5). CSPG expression in the deafferented dentate gyrus was at baseline, suggesting that chABC prevented the increase in CSPG (right panel). Note the increased proliferation of newborn granule cells (POMC-EGFP) despite enzymatic acitivity. **(D)** At alternative approach to decreasing CSPG expression following injury. Xyloside was injected intraperitoneally (IP), twice daily, for 5 consecutive days, starting on the 3rd day post-lesion. Tissue shown here was stained for intact CSPG at 14 days post-lesion (7 days after the last Xyloside injection). A lamina-specific increase in CSPG expression is still observed in the deafferented dentate gyrus (right panel).

GENERAL DISCUSSION

LIMITS OF PLASTICITY

The perforant path model serves as an example of CNS plasticity that incorporates many features of the injury response. Neuroplasticity in the adult brain is a complex process that involves all aspects of the neural circuit – axonal sprouting and terminal bouton turnover, reorganization of dendrites and spines, activity-dependent modulation of synaptic strength, as well as adult neurogenesis. The dynamic nature of the adult brain gives hope for endogenous repair following injury, however, limits of neuroplasticity must be recognized in order to optimize potential medical treatments. Following perforant path lesion, newborn neurons show a greater degree of structural plasticity than mature granule cells by accommodating sprouting axons in the inner molecular layer. However, circuit-appropriate reinnervation of denervated targets is essential for functional recovery, and this aspect of recovery has yet to be fully explored. For example, following ischemic lesions, newborn neurons from the expanded ipsilateral SVZ can replenish cells lost in the striatum by migrating in chains toward the site of infarction, where they differentiate into medium spiny neurons (Arvidsson et al., 2002; Parent et al., 2002). Interestingly, migration of these cells can persist for at least one year after stroke (Kokaia et al., 2006), suggesting that repair mechanisms can remain active long after the insult. Some evidence shows that newly differentiated neurons in the striatum grow dendrites, form synapses, and have spontaneous post-synaptic activity, indicative of functional integration (Hou et al., 2008). However, whether these cells receive appropriate inputs is unknown (Burns et al., 2009). The importance of appropriate reinnervation is perhaps best exemplified by stem cell therapy following spinal cord injury. Although promising (Coutts and Keirstead, 2007; Bareyre, 2008), grafting of neural progenitor cells around the lesion site can trigger

aberrant axonal sprouting and subsequent pain hypersensitivity in the forepaw (Hofstetter et al., 2005). This issue potentially may be resolved by creating a more favorable environment for stem cell maturation and functional integration, including axon guidance molecules, growth factors, and, if necessary, immune suppressors (Liu et al., 2003; Williams and Lavik, 2009). The lamina-specific reorganization following perforant path lesion suggests that effective circuit regeneration and functional recovery will also require a rebalancing of the glial response and the extracellular environment that will allow appropriate synaptogenesis between new axons and dendrites.

SUMMARY AND CONCLUSIONS

It is well-established that adult-generated newborn neurons can navigate the adult environment and integrate into neural circuits, but the response of these neurons to *in vivo* denervation has not been documented. In our experiments, the net effect of the denervating injury on newborn neurons was to promote proliferation, consistent with the potentially positive influences of the injured environment on neural regeneration and repair. However, perforant path lesion also hindered dendritic development of newborn neurons, suggesting that excitatory activity is necessary for elaboration of outgrowing dendrites. Although this effect was perhaps expected in 21-day-old granule cells, it was surprising to see decreased dendritic outgrowth in 14-day-old granule cells, which do not yet make contacts with the perforant path. The reasons for the lesion effect on younger neurons are not yet clear, but likely involve changes in the extracellular environment or altered signaling of interneurons, which also may be affected by the injury.

Newly produced granule cells also showed enhanced structural plasticity. Specifically, newborn granule cells had an altered distribution of dendritic spines post-lesion, presumably to accommodate sprouting of intact commissural/ associational fibers in the inner molecular layer (Matthews et al., 1976b). The increase in spine density in the inner molecular layer may reflect the enhanced synaptic plasticity of newborn neurons relative to mature granule cells. For example, immature granule cells in the normal dentate gyrus exhibit decreased LTP induction thresholds at two-three weeks and increased LTP amplitudes at four-six weeks, which can be observed even with sparse glutamatergic innervation (Schmidt-Hieber et al., 2004; Ge et al., 2007; Lemaire et al., 2012). Thus, newborn neurons may out-recruit mature cells for sprouting collaterals and may

thus have an advantage in *de novo* synaptogenesis and circuit reorganization. Similarly, such post-lesion innervation of new dendrites by sprouting homotypic axons may provide a sufficient amount of excitatory input to ensure functional integration and survival of newborn granule cells, thus compensating for the degenerated perforant path.

Although lesion of the perforant path stimulates reorganization of the dentate gyrus, recovery is limited by laminar barriers. Laminar specificity is partially regulated by the injury-induced glial response that occurs in the denervated zone, as well as changes in the composition of the extracellular matrix, including upregulation of CSPGs and matrix metalloproteases. Such changes may impact axonal as well as dendritic reorganization following perforant path lesion and limit reinnervation of the deafferented dentate gyrus, especially with regard to homotypic sprouting and functional recovery. Thus, future experiments need to address the extracellular aspects of the post-lesion response by manipulating the local environment surrounding dendritic outgrowth and synaptogenesis.

REFERENCES

Abrous, D. N., Koehl, M., and Le Moal, M. (2005), Adult neurogenesis: from precursors to network and physiology. *Physiol. Rev*. 85(2), 523-69.

Akbik, F., Cafferty, W.B., and Strittmatter, S.M. (2012). Myelin associated inhibitors: a link between injury-induced and experience-dependent plasticity. *Exp. Neurol.* 235, 43-52.

Ambrogini, P., Lattanzi, D., Ciuffoli, S., Agostini, D., Bertini, L., Stocchi, V., Santi, S., Cuppini, R. (2004). Morpho-functional characterization of neuronal cells at different stages of maturation in granule cell layer of adult rat dentate gyrus. *Brain Res*. 1017(1-2), 21-31.

Arvidsson, A., Collin, T., Kirik, D., Kokaia, Z., Lindvall, O. (2002). Neuronal replacement from endogenous precursors in the adult brain after stroke. *Nat. Med*. 8(9), 963-70.

Balu, D. T., and Lucki, I. (2009). Adult hippocampal neurogenesis: regulation, functional implications, and contribution to disease pathology. *Cereb. Cortex* 19, 241-248.

Bareyre, F. M. (2008). Neuronal repair and replacement in spinal cord injury. *J. Neurol. Sci*. 265(1-2), 63-72.

Bartus, K., James, N. D., Bosch, K. D., Bradbury, E. J. (2012). Chondroitin sulphate proteoglycans: key modulators of spinal cord and brain plasticity. *Exp. Neurol*. 235(1), 5-17.

Bechmann, I., and Nitsch, R. (2000). Involvement of non-neuronal cells in entorhinal-hippocampal reorganization following lesions. *Ann. N. Y. Acad. Sci*. 911, 192-206.

Ben-Ari, Y. (2002), Excitatory actions of GABA during development: the nature of the nurture. *Nat. Rev. Neurosci.* 3(9), 728-39.

Ben-Ari, Y., and Gho, M. (1988). Long-lasting modification of the synaptic properties of rat CA3 hippocampal neurones induced by kainic acid. *J. Physiol*. 404, 365-84.

Birks, R., Katz, B., and Miledi, R. (1960). Physiological and structural changes at the amphibian myoneural junction, in the course of nerve degeneration. *J. Physiol.* 150, 145-68.

Bosse, F. (2012). Extrinsic cellular and molecular mediators of peripheral axonal regeneration. *Cell Tissue Res.* 349(1), 5-14.

Boulland, J. L., Jenstad, M., Boekel, A. J., Wouterlood, F. G., Edwards, R. H., Storm-Mathisen, J., Chaudhry, F. A. (2009). Vesicular glutamate and GABA transporters sort to distinct sets of vesicles in a population of presynaptic terminals. *Cereb. Cortex* 19, 241-248.

Bovolenta, P., and Fernaud-Espinosa, I. (2000). Nervous system proteoglycans as modulators of neurite outgrowth. *Prog. Neurobiol*. 61(2), 113–132

Bozdagi, O., Nagy, V., Kwei, K. T., Huntley, G. W. (2007). In vivo roles for matrix metalloproteinase-9 in mature hippocampal synaptic physiology and plasticity. *J. Neurophysiol*. 98, 334–344.

Bradbury, E. J., and Carter, L. M. (2011). Manipulating the glial scar: chondroitinase ABC as a therapy for spinal cord injury. *Brain Res. Bull*. 84(4-5), 306-16.

Brambilla, R., Bracchi-Ricard, V., Hu, W. H., Frydel, B., Bramwell, A., Karmally, S., Green, E. J., Bethea, J. R. (2005). Inhibition of astroglial nuclear factor kB reduces inflammation and improves functional recovery after spinal cord injury. *J. Exp. Med*. 202, 145–156.

Brown, C. E., Boyd, J. D., and Murphy, T. H. (2010). Longitudinal in vivo imaging reveals balanced and branch-specific remodeling of mature cortical pyramidal dendritic arbors after stroke. *J. Cereb. Blood Flow Metab*. 30(4), 783-91.

Brown, C. E., Wong, C., and Murphy, T. H. (2008) Rapid morphologic plasticity of peri-infarct dendritic spines after focal ischemic stroke. *Stroke* 39(4), 1286–1291.

Buckmaster, P. S., and Lew, F. H. (2011). Rapamycin suppresses mossy fiber sprouting but not seizure frequency in a mouse model of temporal lobe epilepsy. *J. Neurosci*. 31(6), 2337-47.

Bukhari, N., Torres, L., Robinson, J. K., Tsirka, S. E. (2011). Axonal regrowth after spinal cord injury via chondroitinase and the tissue plasminogen activator (tPA)/ plasmin system. *J. Neurosci*. 31(42), 14931-43.

Burns, T. C., Verfaillie, C. M., and Low, W. C. (2009). Stem cells for ischemic brain injury: a critical review. *J. Comp. Neurol*. 515(1), 125-44.

Caceres, A., and Steward, O. (1983). Dendritic reorganization in the denervated dentate gyrus of the rat following entorhinal cortical lesions: a Golgi and electron microscopic analysis. *J. Comp. Neurol*. 214, 387-403.

Cameron, H. A., McEwen, B. S., and Gould, E. (1995). Regulation of adult neurogenesis by excitatory input and NMDA receptor activation in the dentate gyrus. *J. Neurosci*. 15(6), 4687-92.

Cameron, H. A., and McKay, R. D. (2001). Adult neurogenesis produces a large pool of new granule cells in the dentate gyrus. *J. Comp. Neurol*. 435, 406–417.

Carulli, D., Laabs, T., Geller, H. M., Fawcett, J. W. (2005). Chondroitin sulfate proteoglycans in neural development and regeneration. *Curr. Opin. Neurobiol*. 15(1), 116-20.

Ceranik, K., Zhao, S., and Frotscher, M. (2000). Development of the entorhino-hippocampal projection: Guidance by Cajal-Retzius cell axons. *Ann. New York Acad. Sci*. 911, 43-54.

Chao, D. L., Ma, L., and Shen, K. (2009). Transient cell-cell interactions in neural circuit formation. *Nat. Rev. Neurosci.* 10(4), 262-71.

Chen, Z. L., Yu, W. M., and Strickland, S. (2007). Peripheral regeneration. *Annu. Rev. Neurosci.* 30, 209-33.

Christopherson, K. S., Ullian, E. M., Stokes, C. C., Mullowney, C. E., Hell, J. W., Agah, A., Lawler, J., Mosher, D. F., Bornstein, P., and Barres, B. A. (2005). Thrombospondins are astrocyte-secreted proteins that promote CNS synaptogenesis. *Cell* 120, 421–433.

Clusmann, H., Nitsch, R., and Heinemann, U. (1994). Long lasting functional alterations in the rat dentate gyrus following entorhinal cortex lesion: a current source density analysis. *Neuroscience* 61(4), 805-15.

Collazos-Castro, J. E., and Nieto-Sampedro, M. (2001). Developmental and reactive growth of dentate gyrus afferents: cellular and molecular interactions. *Restor. Neurol. Neurosci.* 19(3-4), 169-87.

Cotman, C., Gentry, C., and Steward, O. (1977). Synaptic replacement in the dentate gyrus after unilateral entorhinal lesion: electron microscopic analysis of the extent of replacement of synapses by the remaining entorhinal cortex. *J. Neurocytol.* 6(4), 455-64.

Coutts, M., and Keirstead, H. S. (2008). Stem cells for the treatment of spinal cord injury. *Exp. Neurol.* 209(2), 368-77.

Dash, P. K., Mach, S. A., and Moore, A. N. (2001). Enhanced neurogenesis in the rodent hippocampus following traumatic brain injury. *J. Neurosci. Res.* 63(4), 313-9.

Dayer, A. G., Ford, A. A., Cleaver, K. M., Yassaee, M., Cameron, H. A. (2003). Short-term and long-term survival of new neurons in the rat dentate gyrus. *J. Comp. Neurol.* 460(4), 563-72.

DeCarolis, N. A., and Eisch, A. J. (2010). Hippocampal neurogenesis as a target for the treatment of mental illness: a critical evaluation. *Neuropharmacology* 58(6), 884-93.

Del Río JA, Heimrich B, Borrell V, Förster E, Drakew A, Alcántara S, Nakajima K, Miyata T, Ogawa M, Mikoshiba K, Derer P, Frotscher M, Soriano E. (1997). A role for Cajal–Retzius cells and reelin in the development of hippocampal connections. *Nature* 385, 70–74.

Del Turco, D., Woods, A. G., Gebhardt, C., Phinney, A. L., Jucker, M., Frotscher, M., Deller, T. (2003). Comparison of commissural sprouting in the mouse and rat fascia dentata after entorhinal cortex lesion. *Hippocampus* 13(6), 685-99.

Deller, T., Del Turco, D., Rappert, A., Bechmann, I. (2007). Structural reorganization of the dentate gyrus following entorhinal denervation: species differences between rat and mouse. *Prog. Brain Res.* 163, 501-28.

Deller, T., Frotscher, M. (1997). Lesion-induced plasticity of central neurons: sprouting of single fibres in the rat hippocampus after unilateral entorhinal cortex lesion. *Prog. Neurobiol.* 53(6), 687-727.

Deller, T., Frotscher, M., and Nitsch, R. (1995). Morphological evidence for the sprouting of inhibitory commissural fibers in response to the lesion of the excitatory entorhinal input to the rat dentate gyrus. *J. Neurosci.* 15(10), 6868-78.

Deller, T., Frotscher, M., and Nitsch, R. (1996a). Sprouting of crossed entorhinodentate fibers after a unilateral entorhinal lesion: anterograde tracing of fiber reorganization with Phaseolus vulgaris-leucoagglutinin (PHAL). *J. Comp. Neurol.* 365(1), 42-55.

Deller, T., Haas, C. A., and Frotscher, M. (2001). Sprouting in the hippocampus after entorhinal cortex lesion is layer- specific but not translaminar: which molecules may be involved? *Restor. Neurol. Neurosci.* 19(3-4), 159-67.

Deller, T., Haas, C. A., Naumann, T., Joester, A., Faissner, A., Frotscer, M. (1997). Upregulation of astrocyte-derived tenascin-C correlates with neurite outgrowth in the rat dentate gyrus after unilateral entorhinal cortex lesion. *Neuroscience* 81, 829–846.

Deller, T., Nitsch, R., and Frotscher, M. (1996b). Layer-specific sprouting of commissural fibres to the rat fascia dentata after unilateral entorhinal cortex lesion: a Phaseolus vulgaris leucoagglutinin tracing study. *Neuroscience* 71(3), 651-60.

Diekmann, S., Ohm, T. G., and Nitsch, R. (1996). Long-lasting transneuronal changes in rat dentate granule cell dendrites after entorhinal cortex lesion. A combined intracellular injection and electron microscopy study. *Brain Pathol.* 6(3), 205-15.

Dissing-Olesen, L., Ladeby, R., Nielsen, H. H., Toft-Hansen, H., Dalmau, I., Finsen, B. (2007). Axonal lesion-induced microglial proliferation and microglial cluster formation in the mouse. *Neuroscience* 149(1), 112-22.

Dityatev, A., and Fellin, T. (2008). Extracellular matrix in plasticity and epileptogenesis. *Neuron Glia Biol.* 4, 235–247.

Dityatev, A., Frischknecht, R., and Seidenbecher, C. I. (2006). Extracellular matrix and synaptic functions. *Results Probl. Cell Differ.* 43, 69–97.

Dityatev, A., Schachner, M., and Sonderegger, P. (2010a). The dual role of the extracellular matrix in synaptic plasticity and homeostasis. *Nat. Rev. Neurosci.* 11, 735–746.

Dityatev, A., Seidenbecher, C. I., and Schachner, M. (2010b). Compartmentalization from the outside: The extracellular matrix and functional microdomains in the brain. *Trends Neurosci.* 33, 503–512.

Drakew, A., Müller, M., Gähwiler, B. H., Thompson, S. M., Frotscher, M. (1996). Spine loss in experimental epilepsy: quantitative light and electron microscopic analysis of

intracellularly stained CA3 pyramidal cells in hippocampal slice cultures. *Neuroscience* 70(1), 31-45.

Eroglu, C. (2009). The role of astrocyte-secreted matricellular proteins in central nervous system development and function. *J. Cell Comm. Sig.* 3, 167–176.

Falo, M. C., Fillmore, H. L., Reeves, T. M., Phillips, L. L. (2006). Matrix metalloproteinase-3 expression profile differentiates adaptive and maladaptive synaptic plasticity induced by traumatic brain injury. *J. Neurosci. Res.* 84(4), 768-81.

Fatemi, S. H. (2005). Reelin glycoprotein: structure, biology and roles in health and disease. *Mol. Psych.* 10, 251–257.

Fitch, M. T., and Silver, J. (2008). CNS injury, glial scars, and inflammation: Inhibitory extracellular matrices and regeneration failure. *Exp. Neurol.* 209(2), 294-301.

Frischknecht, R., and Gundelfinger, E. (2012). The brain's extracellular matrix and its role in synaptic plasticity. *Adv. Exp. Med. Biol.* 970, 153-71.

Förster, E., Tielsch, A., Saum, B., Weiss, K.H., Johanssen, C., Graus-Porta, D., Müller, U. & Frotscher, M. (2002) Reelin, Disabled 1, and beta 1 integrins are required for the formation of the radial glial scaffold in the hippocampus. *Proc. Natl Acad. Sci. USA*, 99, 13178–13183.

Förster, E., Zhao, S., and Frotscher, M. (2001). Hyaluronan-associated adhesive cues control fiber segregation in the hippocampus. *Development* 128, 3029-3039.

Förster, E., Zhao, S., and Frotscher, M. (2006). Laminating the hippocampus. *Nat. Rev. Neurosci.* 7, 259-268.

Frotscher, M., and Heimrich, B. (1993). Formation of layer-specific fiber projections to the hippocampus in vitro. *Proc. Natl Acad. Sci. USA* 90, 10400–10403.

Frotscher, M., Zhao, S., and Förster, E. (2007). Development of cell and fiber layers in the dentate gyrus. *Prog. Brain Res.* 163, 133-42.

Gage, F. H., Coates, P. W., Palmer, T. D., Kuhn, H. G., Fisher, L. J., Suhonen, J. O., Peterson, D. A., Suhr, S. T., Ray, J. (1995). Survival and differentiation of adult neuronal progenitor cells transplanted to the adult brain. *Proc. Natl. Acad. Sci. U S A* 92(25), 11879-83.

Gage, F. H., Olejniczak, P., and Armstrong, D. M. (1988). Astrocytes are important for sprouting in the septohippocampal circuit. *Exp. Neurol.* 102(1), 2-13.

Gall, C., and Lynch, G. (1981). Fiber architecture of the dentate gyrus following ablation of the entorhinal cortex in rats of different ages: evidence for two forms of axon sprouting in the immature brain. *Neuroscience* 6(5), 903-10.

Galtrey, C. M., and Fawcett, J. W. (2007). The role of chondroitin sulfate proteoglycans in regeneration and plasticity in the central nervous system. *Brain Res. Rev*. 54(1), 1-18.

Ge, S., Sailor, K. A., Ming, G. L., Song, H. (2008). Synaptic integration and plasticity of new neurons in the adult hippocampus. *J. Physiol*. 586(16), 3759-65.

Ge, S., Yang, C. H., Hsu, K. S., Ming, G. L., Song, H. (2007). A critical period for enhanced synaptic plasticity in newly generated neurons of the adult brain. *Neuron* 54(4), 559-66.

Gebhardt, C., Del Turco, D., Drakew, A., Tielsch, A., Herz, J., Frotscher, M., Deller T. (2002). Abnormal positioning of granule cells alters afferent fiber distribution in the mouse fascia dentata: morphologic evidence from reeler, apolipoprotein E receptor 2-, and very low density lipoprotein receptor knockout mice. *J. Comp. Neurol*. 445(3), 278-92.

Gehrmann, J., Schoen, S. W., and Kreutzberg, G. W. (1991). Lesion of the rat entorhinal cortex leads to a rapid microglial reaction in the dentate gyrus. *Acta Neuropathol*. 82, 442–455.

Giger, R. J., Hollis, E. R. II, and Tuszynski, M. H. (2010). Guidance molecules in axon regeneration. *Cold Spring Harb. Perspect. Biol*. 2(7), a001867.

Gómez-Pinilla, F., Lee, J. W., Cotman, C. W. (1992). Basic FGF in adult rat brain: cellular distribution and response to entorhinal lesion and fimbria-fornix transection. *J. Neurosci*. 12(1), 345-55.

Gottlieb, D. I., and Cowan, W. M. (1973). Autoradiographic studies of the commissural and ipsilateral association connection of the hippocampus and detentate gyrus of the rat. I. The commissural connections. *J. Comp. Neurol*. 149(4), 393-422.

Gould, E., and Tanapat, P. (1997). Lesion-induced proliferation of neuronal progenitors in the dentate gyrus of the adult rat. *Neuroscience* 80(2), 427-36.

Gould, E., Tanapat, P. (1999). Stress and hippocampal neurogenesis. *Biol. Psychiatry* 46(11), 1472-9.

Haas, C. A., Deller, T., Krsnik, Z., Tielsch, A., Woods, A., Frotscher, M. (2000). Entorhinal cortex lesion does not alter reelin messenger RNA expression in the dentate gyrus of young and adult rats. *Neuroscience* 97(1), 25-31.

Haas, C. A., and Frotscher, M. (2010). Reelin deficiency causes granule cell dispersion in epilepsy. *Exp. Brain Res*. 200(2), 141-9.

Haas, C. A., Frotscher, M., and Deller, T. (1999). Differential induction of c-Fos, c-Jun and Jun B in the rat central nervous system following unilateral entorhinal cortex lesion. *Neuroscience* 90(1), 41-51.

Haas, C. A., Rauch, U., Thon, N., Merten, T., Deller, T. (1999). Entorhinal cortex lesion in adult rats induces the expression of the neuronal chondroitin sulfate proteoglycan neurocan in reactive astrocytes. *J. Neurosci*. 19, 9953–9963.

Hack, I., Bancila, M., Loulier, K., Carroll, P., Cremer, H. (2002). Reelin is a detachment signal in tangential chain-migration during postnatal neurogenesis. *Nat. Neurosci*. 5(10), 939-45.

Hailer, N. P., Grampp, A., and Nitsch, R. (1999). Proliferation of microglia and astrocytes in the dentate gyrus following entorhinal cortex lesion: a quantitative bromodeoxyuridine-labelling study. *Eur. J. Neurosci*. 11(9), 3359-64.

Hamby, M. E., and Sofroniew, M. V. (2010). Reactive astrocytes as therapeutic targets for CNS disorders. *Neurotherapeutics* 7, 494–506.

Hegarty, D. M., Tonsfeldt, K., Hermes, S. M., Helfand, H., Aicher, S. A. (2010). Differential localization of vesicular glutamate transporters and peptides in corneal afferents to trigeminal nucleus caudalis. *J. Comp. Neurol*. 518(17), 3557-69.

Heinrich, C., Nitta, N., Flubacher, A., Müller, M., Fahrner, A., Kirsch, M., Freiman, T., Suzuki, F., Depaulis, A., Frotscher, M., Haas, C. A. (2006). Reelin deficiency and displacement of mature neurons, but not neurogenesis, underlie the formation of granule cell dispersion in the epileptic hippocampus. *J. Neurosci*. 26(17), 4701-13.

Hickmott, P. W., and Steen, P. A. (2005). Large-scale changes in dendritic structure during reorganization of adult somatosensory cortex. *Nat. Neurosci*. 8(2), 140-2.

Hirano, A., and Dembitzer, H. M. (1973). Cerebellar alterations in the weaver mouse. *J. Cell Biol*. 56, 478-486.

Hill, C. E., Beattie, M. S., and Bresnahan, J. C. (2001). Degeneration and sprouting of identified descending supraspinal axons after contusive spinal cord injury in the rat. *Exp. Neurol*. 171(1), 153-69.

Hjorth-Simonsen, A. (1972). Projection of the lateral part of the entorhinal area to the hippocampus and fascia dentata. *J. Comp. Neurol*. 146(2), 219-32.

Hjorth-Simonsen, A., and Jeune, B. (1972). Origin and termination of the hippocampal perforant path in the rat studied by silver impregnation. *J. Comp. Neurol*. 144(2), 215-32.

Hofer, S. B., Mrsic-Flogel, T. D., Bonhoeffer, T., Hübener, M. (2006). Lifelong learning: ocular dominance plasticity in mouse visual cortex. *Curr. Opin. Neurobiol*. 16(4), 451-9.

Hofstetter, C. P., Holmström, N. A., Lilja, J. A., Schweinhardt, P., Hao, J., Spenger, C., Wiesenfeld-Hallin, Z., Kurpad, S. N., Frisén, J., Olson, L. (2005). Allodynia limits the usefulness of intraspinal neural stem cell grafts; directed differentiation improves outcome. *Nat. Neurosci*. 8(3), 346-53.

Hosp, J. A., and Luft, A. R. (2011). Cortical plasticity during motor learning and recovery after ischemic stroke. *Neural Plast.* 2011, 871296.

Hou, S. W., Wang, Y. Q., Xu, M., Shen, D. H., Wang, J. J., Huang, F., Yu, Z., Sun, F. Y. (2008). Functional integration of newly generated neurons into striatum after cerebral ischemia in the adult rat brain. *Stroke* 39(10), 2837-44.

Huntley, G. W. (2012). Synaptic circuit remodelling by matrix metalloproteinases in health and disease. *Nat. Rev. Neurosci.* 13(11), 743-57.

Iliff, J. J., Wang, M., Liao, Y., Plogg, B. A., Peng, W., Gundersen, G. A., Benveniste, H., Vates, G. E., Deane, R., Goldman, S. A., Nagelhus, E. A., Nedergaard, M. (2012). A paravascular pathway facilitates CSF flow through the brain parenchyma and the clearance of interstitial solutes, including amyloid β. *Sci. Transl. Med.* 4(147), 147ra111.

Jansen, L. A., Uhlmann, E. J., Crino, P. B., Gutmann, D. H., Wong, M. (2005). Epileptogenesis and reduced inward rectifier potassium current in tuberous sclerosis complex-1-deficient astrocytes. *Epilepsia* 46, 1871–1880.

Jessberger, S., Römer, B., Babu, H., Kempermann, G. (2005). Seizures induce proliferation and dispersion of doublecortin-positive hippocampal progenitor cells. *Exp. Neurol.* 196(2), 342-51.

Katsuyama. Y., and Terashima, T. (2009). Developmental anatomy of reeler mutant mouse. *Dev. Growth Differ.* 51(3), 271-86.

Katz, B., and Miledi, R. (1959). Spontaneous subthreshold activity at denervated amphibian end-plates. *J. Physiol.* 146, 44-45P.

Kernie, S. G., and Parent, J. M. (2010). Forebrain neurogenesis after focal ischemic and traumatic brain injury. *Neurobiol. Dis.* 37(2), 267-74.

Kim, B. G., Dai, H. N., McAtee, M., Vicini, S., Bregman, B. S. (2006). Remodeling of synaptic structures in the motor cortex following spinal cord injury. *Exp. Neurol.* 198(2), 401-15.

Knowles, W. D. (1992). Normal anatomy and neurophysiology of the hippocampal formation. *J. Clin. Neurophysiol.* 9(2), 252-63.

Koistinaho, M., Lin, S., Wu, X., Esterman, M., Koger, D., Hanson, J., Higgs, R., Liu, F., Malkani, S., Bales, K. R., Paul, S. M. (2004). Apolipoprotein E promotes astrocyte colocalization and degradation of deposited amyloid-beta peptides. *Nat. Med.* 10, 719–726.

Kokaia, Z., Thored, P., Arvidsson, A., Lindvall, O. (2006). Regulation of stroke-induced neurogenesis in adult brain—recent scientific progress. *Cereb. Cortex* 16(suppl 1), i162–i167.

Kuhn, H. G., Biebl, M., Wilhelm, D., Li, M., Friedlander, R. M., Winkler, J. (2005). Increased generation of granule cells in adult Bcl-2-overexpressing mice: a role for cell death during continued hippocampal neurogenesis. *Eur. J. Neurosci.* 22(8), 1907-15.

Kurihara, D., and Yamashita, T. (2012). Chondroitin sulfate proteoglycans down-regulate spine formation in cortical neurons by targeting tropomyosin-related kinase B (TrkB) protein. *J. Biol. Chem*. 287(17), 13822-8.

Kwok, J. C., Afshari, F., García-Alías, G., Fawcett, J. W. (2008). Proteoglycans in the central nervous system: plasticity, regeneration and their stimulation with chondroitinase ABC. *Restor. Neurol. Neurosci*. 26(2-3), 131-45.

Kwok, J. C., Warren, P., and Fawcett, J. W. (2012). Chondroitin sulfate: a key molecule in the brain matrix. *Int. J. Biochem. Cell Biol*. 44(4), 582-6.

Lauder, J. M. (1993). Neurotransmitters as growth regulatory signals: role of receptors and second messengers. *Trends Neurosci.* 16(6), 233-40.

Lemaire, V., Tronel, S., Montaron, M. F., Fabre, A., Dugast, E., Abrous, D. N. (2012). Long-lasting plasticity of hippocampal adult-born neurons. *J. Neurosci.* 32(9), 3101-8.

Leranth, C., and Hajszan, T. (2007). Extrinsic afferent systems to the dentate gyrus. *Prog. Brain Res.* 163, 63-84.

Lewis, P. F., and Emerman, M. (1994). Passage through mitosis is required for oncoretroviruses but not for the human immunodeficiency virus. *J. Virol.* 68(1), 510-6.

Lichtenwalner, R. J., and Parent, J. M. (2006). Adult neurogenesis and the ischemic forebrain. *J. Cereb. Blood Flow Metab.* 26(1), 1-20.

Liu, C. Y., Apuzzo, M. L., and Tirrell, D. A. (2003). Engineering of the extracellular matrix: working toward neural stem cell programming and neurorestoration--concept and progress report. *Neurosurgery* 52(5), 1154-65.

Liu, J., Solway, K., Messing, R. O., Sharp, F. R. (1998). Increased neurogenesis in the dentate gyrus after transient global ischemia in gerbils. *J. Neurosci.* 18(19), 7768-78.

Lois, C., Hong, E. J., Pease, S., Brown, E. J., Baltimore, D. (2002). Germline transmission and tissue-specific expression of transgenes delivered by lentiviral vectors. *Science* 295, 868-872.

Liu, J., Solway, K., Messing, R. O., Sharp, F. R. (1998). Increased neurogenesis in the dentate gyrus after transient global ischemia in gerbils. *J. Neurosci.* 18, 7768-78.

Liu, K., Tedeschi, A., Park, K. K., He Z. (2011). Neuronal intrinsic mechanisms of axon regeneration. *Annu. Rev. Neurosci*. 34, 131-52.

Luikart, B. W., Schnell, E., Washburn, E. K., Bensen, A. L., Tovar, K. R., Westbrook, G. L. (2011a). Pten knockdown in vivo increases excitatory drive onto dentate granule cells. *J. Neurosci.* 31(11), 4345-54.

Luikart, B. W., Perederiy, J. V., Westbrook, G. L. (2011b). Dentate gyrus neurogenesis, integration and microRNAs. *Behav. Brain Res.* 227(2), 348-55.

Lynch, G., Matthews, D. A., Mosko, S., Parks, T., Cotman, C. (1972). Induced acetylcholinesterase-rich layer in rat dentate gyrus following entorhinal lesions. *Brain Res.* 42(2), 311-8.

Maier, I. C., and Schwab, M. E. (2006). Sprouting, regeneration and circuit formation in the injured spinal cord: factors and activity. *Philos. Trans. R. Soc. Lond. B. Biol. Sci.* 361(1473), 1611-34.

Margolis, R. U., and Margolis, R. K. (1997). Chondroitin sulfate proteoglycans as mediators of axon growth and pathfinding. *Cell Tissue Res.* 290(2), 343-8.

Marrone, D. F., LeBoutillier, J. C., and Petit, T. L. (2004b). Comparative analyses of synaptic densities during reactive synaptogenesis in the rat dentate gyrus. *Brain Res.* 996, 19-30.

Matsui, F., and Oohira, A. (2004). Proteoglycans and injury of the central nervous system. *Congenit. Anom.* (Kyoto) 44, 181-188.

Matthews, D. A., Cotman, C. and Lynch, G. (1976a). An electron microscopic study of lesion-induced synaptogenesis in the dentate gyrus of the adult rat. I. Magnitude and time course of degeneration. *Brain Res.* 115(1), 1-21.

Matthews, D. A., Cotman, C., and Lynch, G. (1976b). An electron microscopic study of lesion-induced synaptogenesis in the dentate gyrus of the adult rat. II. Reappearance of morphologically normal synaptic contacts. *Brain Res.*, 115, 23-41.

Mayer, J., Hamel, M. G., and Gottschall, P. E. (2005). Evidence for proteolytic cleavage of brevican by the ADAMTSs in the dentate gyrus after excitotoxic lesion of the mouse entorhinal cortex. *BMC Neurosci.* 6, 52.

Miledi, R., and Slater, C. R. (1968). Electrophysiology and electron-microscopy of rat neuromuscular junctions after nerve degeneration. *Proc. R. Soc. Lond. B. Biol. Sci.* 169(16), 289-306.

Milligan, E. D., and Watkins, L. R. (2009). Pathological and protective roles of glia in chronic pain. *Nat. Rev. Neurosci.* 10, 23-36.

Ming, G., and Song, H. (2011). Adult neurogenesis in the mammalian brain: significant answers and significant questions. *Neuron* 70(4), 687-702.

Mitchell, B. D., Emsley, J. G., Magavi, S. S., Arlotta, P., Macklis, J. D. (2004). Constitutive and induced neurogenesis in the adult mammalian brain: manipulation of endogenous precursors toward CNS repair. *Dev. Neurosci.* 26(2-4), 101-17.

Möller, J. C., Klein, M. A., Haas, S., Jones, L. L., Kreutzberg, G. W., Raivich, G. (1996). Regulation of thrombospondin in the regenerating mouse facial motor nucleus. *Glia* 17(2), 121-32.

Mostany, R., and Portera-Cailliau, C. (2011). Absence of large-scale dendritic plasticity of layer 5 pyramidal neurons in peri-infarct cortex. *J. Neurosci.* 31(5), 1734-8.

Mori, T., Buffo, A., and Götz, M. (2005). The novel roles of glial cells revisited: the contribution of radial glia and astrocytes to neurogenesis. *Curr. Top. Dev. Biol.* 69, 67-99.

Nadler, J. V., Cotman, C. W., and Lynch, G. S. (1977a). Histochemical evidence of altered development of cholinergic fibers in the rat dentate gyrus following lesions. I. Time course after complete unilateral entorhinal lesion at various ages. *J. Comp. Neurol.* 171(4), 561-87.

Nadler, J. V., Cotman, C. W., Paoletti, C., Lynch, G. S. (1977b). Histochemical evidence of altered development of cholinergic fibers in the rat dentate gyrus following lesions. II. Effects of partial entorhinal and simultaneous multiple lesions. *J. Comp. Neurol.* 171(4), 589-604.

Nagy, V., Bozdagi, O., Matynia, A., Balcerzyk, M., Okulski, P., Dzwonek, J., Costa, R. M., Silva, A. J., Kaczmarek, L., Huntley, G. W. (2006). Matrix metalloproteinase-9 is required for hippocampal late-phase long-term potentiation and memory. *J. Neurosci.* 26, 1923–1934.

Neumann, H., Kotter, M. R., and Franklin, R. J. (2009). Debris clearance by microglia: an essential link between degeneration and regeneration. *Brain* 132(2), 288-95.

Nitsch, R., and Frotscher, M. (1992). Reduction of posttraumatic transneuronal "early gene" activation and dendritic atrophy by the N-methyl-D-aspartate receptor antagonist MK-801. *Proc. Natl. Acad. Sci. USA* 89(11), 5197-200.

Oohira, A., Matsui, F., and Katoh-Semba, R. (1991). Inhibitory effects of brain chondroitin sulfate proteoglycans on neurite outgrowth from PC12D cells. *J. Neurosci.* 11(3), 822-7.

Overstreet, L. S., Hentges, S. T., Bumaschny, V. F., de Souza, F. S., Smart, J. L., Santangelo, A. M., Low, M. J., Westbrook, G. L., Rubinstein, M. (2004). A transgenic marker for newly born granule cells in dentate gyrus. *J. Neurosci.* 24(13), 3251-9.

Overstreet-Wadiche, L., Bromberg, D. A., Bensen, A. L., Westbrook, G. L. (2005). GABAergic signaling to newborn neurons in dentate gyrus. *J. Neurophysiol.* 94(6), 4528-32.

Overstreet-Wadiche, L. S., and Westbrook, G. L (2006). Functional maturation of adult-generated granule cells. *Hippocampus* 16(3), 208-15.

Parent, J. M. (2003). Injury-induced neurogenesis in the adult mammalian brain. *Neuroscientist* 9(4), 261-72.

Parent, J. M. (2007). Adult neurogenesis in the intact and epileptic dentate gyrus. *Prog. Brain Res.* 163, 529-40.

Parent, J. M., Elliott, R. C., Pleasure, S. J., Barbaro, N. M., Lowenstein, D. H. (2006). Aberrant seizure-induced neurogenesis in experimental temporal lobe epilepsy. *Ann. Neurol.* 59(1), 81-91.

Parent, J. M., and Murphy, G. G. (2008). Mechanisms and functional significance of aberrant seizure-induced hippocampal neurogenesis. *Epilepsia* 49 Suppl 5, 19-25.

Parent, J. M., Vexler, Z. S., Gong, C., Derugin, N., Ferriero, D. M. (2002). Rat forebrain neurogenesis and striatal neuron replacement after focal stroke. *Ann. Neurol.* 52(6), 802-13.

Parnavelas, J. G., Lynch, G., Brecha, N., Cotman, C. W., Globus, A. (1974). Spine loss and regrowth in hippocampus following deafferentation. *Nature* 248(443), 71-3.

Pearlman, A. L., and Sheppard, A.M. (1996). Extracellular matrix in early cortical development. *Prog. Brain Res.* 108, 117–134.

Perederiy, J. V., Luikart, B. W., Washburn, E. K., Schnell, E., Westbrook, G. L. (*in revision*). Neural injury triggers a biphasic response in adult-generated neurons in the dentate gyrus. *J. Neurosci.*

Pesold, C., Impagnatiello, F., Pisu, M.G., Uzunov, D.P., Costa, E., Guidotti, A., Caruncho, H.J., (1998). Reelin is preferentially expressed in neurons synthesizing gamma-aminobutyric acid in cortex and hippocampus of adult rats. *Proc. Natl. Acad. Sci. U. S. A.* 95, 3221-3226.

Peterson, G. M. (1994). Sprouting of central noradrenergic fibers in the dentate gyrus following combined lesions of its entorhinal and septal afferents. *Hippocampus* 4(6), 635-48.

Phinney, A. L., Calhoun, M. E., Woods, A. G., Deller, T., Jucker, M. (2004). Stereological analysis of the reorganization of the dentate gyrus following entorhinal cortex lesion in mice. *Eur. J. Neurosci.* 19(7), 1731-40.

Raineteau, O., and Schwab, M. E. (2001). Plasticity of motor systems after incomplete spinal cord injury. *Nat. Rev. Neurosci.* 2(4), 263-73.

Ramirez, J. J. (2001). The role of axonal sprouting in functional reorganization after CNS injury: lessons from the hippocampal formation. *Restor. Neurol. Neurosci.* 19(3-4), 237-62.

Rauch, U. (1997). Modeling an extracellular environment for axonal pathfinding and fasciculation in the central nervous system. *Cell Tissue Res.* 290, 349–356.

Reeves, T. M., and Steward O. (1988). Changes in the firing properties of neurons in the dentate gyrus with denervation and reinnervation: implications for behavioral recovery. *Exp. Neurol.* 102(1), 37-49.

Rickmann, M., Amaral, D. G., and Cowan, W. M. (1987). Organization of radial glial cells during the development of the rat dentate gyrus. *J. Comp. Neurol.* 264, 449479.

Rihn, L. L., and Claiborne, B. J. (1990). Dendritic growth and regression in rat dentate granule cells during late postnatal development. *Dev. Brain Res.* 54, 115-124.

Rolls, A., Shechter, R., London, A., Segev, Y., Jacob-Hirsch, J., Amariglio, N., Rechavi, G., Schwartz, M. (2008). Two faces of chondroitin sulfate proteoglycan in spinal cord repair: a role in microglia/ macrophage activation. *PLoS Med.* 5(8), e171.

Rothstein, J. D., Dykes-Hoberg, M., Pardo, C. A., Bristol, L. A., Jin, L., Kunci, R. W., Kanai, Y., Hediger, M. A., Wang, Y., Schielke, J. P., Welty, D. F. (1996). Knockout of glutamate transporters reveals a major role for astroglial transport in excitotoxicity and clearance of glutamate. *Neuron* 16, 675-686.

Scharfman, H. E., Goodman, J. H., and Sollas, A.L. (2000). Granule-like neurons at the hilar/ CA3 border after status epilepticus and their synchrony with area CA3 pyramidal cells: functional implications of seizure-induced neurogenesis. *J. Neurosci.* 20, 6144-58.

Schauwecker, P. E., and McNeill, T. H. (1995). Enhanced but delayed axonal sprouting of the commissural/ associational pathway following a combined entorhinal cortex/ fimbria fornix lesion. *J. Comp. Neurol.* 351(3), 453-64.

Schauwecker, P. E., and McNeill, T. H. (1996). Dendritic remodeling of dentate granule cells following a combined entorhinal cortex/ fimbria fornix lesion. *Exp. Neurol.* 141(1), 145-53.

Schmidt-Hieber, C., Jonas, P., and Bischofberger, J. (2004). Enhanced synaptic plasticity in newly generated granule cells of the adult hippocampus. *Nature* 429(6988), 184-7.

See J, Bonner J, Neuhuber B, Fischer I. (2010). Neurite outgrowth of neural progenitors in presence of inhibitory proteoglycans. *J. Neurotrauma.* 27(5), 951-7.

Seri, B., Garcia-Verdugo, J.M., McEwen, B.S., Alvarez-Buylla, A. (2001). Astrocytes give rise to new neurons in the adult mammalian hippocampus. *J. Neurosci.*, 21, 7153-7160.

Sierra, A., Encinas, J. M., Deudero, J. J., Chancey, J. H., Enikolopov, G., Overstreet-Wadiche, L. S., Tsirka, S. E., Maletic-Savatic, M. (2010). Microglia shape adult hippocampal neurogenesis through apoptosis-coupled phagocytosis. *Cell Stem Cell* 7(4), 483-95.

Silver, J., and Miller, J. H. (2004). Regeneration beyond the glial scar. *Nat. Rev. Neurosci.* 5, 146–156.

Simbürger, E., Plaschke, M., Fritschy, J. M., Nitsch, R. (2001). Localization of two major GABA(A) receptor subunits in the dentate gyrus of the rat and cell type-specific up-regulation following entorhinal cortex lesion. *Neuroscience* 102(4), 789-803.

Simbürger, E., Plaschke, M., Kirsch, J., Nitsch, R. (2000). Distribution of the receptor-anchoring protein gephyrin in the rat dentate gyrus and changes following entorhinal cortex lesion. *Cereb. Cortex* 10(4), 422-32.

Skutella, T., and Nitsch, R. (2001). New molecules for hippocampal development. *Trends Neurosci*. 24(2), 107-13.

Sofroniew, M. V. (2009). Molecular dissection of reactive astrogliosis and glial scar formation. *Trends Neurosci.* 32(12), 638-47.

Sofroniew, M. V., and Vinters, H. V. (2010). Astrocytes: biology and pathology. *Acta Neuropathol.* 119(1), 7-35.

Soriano, E. and Del Río, J. A. (2005). The cells of Cajal–Retzius: still a mystery one century after. *Neuron* 46, 389–394.

Soriano, E., and Frotscher, M. (1994). Mossy cells of the rat fascia dentata are glutamate-immunoreactive. *Hippocampus* 4(1), 65-9.

Sotelo, C. (1990). Cerebellar synaptogenesis: what we can learn from mutant mice. *J. Exp. Biol.* 153, 225–279.

Stanfield, B. B., and Cowan, W. M. (1979). The morphology of the hippocampus and dentate gyrus in normal and reeler mice. *J. Comp. Neurol*. 185, 393-422.

Stanfield, B. B., and Cowan, W. M. (1982). The sprouting of septal afferents to the dentate gyrus after lesions of the entorhinal cortex in adult rats. *Brain Res.* 232(1), 162-70.

Steward, O. (1976). Reinnervation of dentate gyrus by homologous afferents following entorhinal cortical lesions in adult rats. *Science* 194(4263), 426-8.

Steward, O. (1992). Signals that induce sprouting in the central nervous system: sprouting is delayed in a strain of mouse exhibiting delayed axonal degeneration. *Exp. Neurol.* 118(3), 340-51.

Steward, O., Cotman, C. W., and Lynch, G. S. (1973). Re-establishment of electrophysiologically functional entorhinal cortical input to the dentate gyrus deafferented by ipsilateral entorhinal lesions: innervation by the contralateral entorhinal cortex. *Exp. Brain Res.* 18(4), 396-414.

Steward, O., and J. A. Messenheimer (1978). Histochemical evidence for a postlesion reorganization of cholinergic afferents in the hippocampal formation of the mature cat. *J. Comp. Neurol*. 178, 697-710.

Steward, O., and Vinsant, S. L. (1983). The process of reinnervation in the dentate gyrus of the adult rat: A quantitative electron microscopic analysis of terminal proliferation and reactive synaptogenesis. *J. Comp. Neurol.* 214(4), 370-386.

Suh, H., Deng, W., and Gage, F. H. (2009). Signaling in adult neurogenesis. *Annu. Rev. Cell Dev. Biol.* 25, 253-75.

Supèr, H., Martínez, A., Del Río, J. A., and Soriano, E. (1998). Involvement of distinct pioneer neurons in the formation of layer-specific connections in the hippocampus. *J. Neurosci.* 18, 4616-4626.

Supèr, H., and Soriano, E. (1994). The organization of the embryonic and early postnatal murine hippocampus. II. Development of entorhinal, commissural, and septal connections studied with the lipophilic tracer DiI. *J. Comp. Neurol.* 344(1), 101-20.

Sutula, T. P., and Dudek, F. E. (2007). Unmasking recurrent excitation generated by mossy fiber sprouting in the epileptic dentate gyrus: an emergent property of a complex system. *Prog. Brain Res.* 163, 541-63.

Swanson, R. A., Ying, W., and Kauppinen, T. M. (2004). Astrocyte influences on ischemic neuronal death. *Curr. Mol. Med.* 4, 193-205.

Takano, T., Kang, J., Jaiswal, J. K., Simon, S. M., Lin, J. H., Yu, Y., Li, Y., Yang, J., Dienel, G., Zielke, H. R., Nedergaard, M. (2005). Receptor-mediated glutamate release from volume sensitive channels in astrocytes. *Proc. Natl. Acad. Sci. USA* 102, 16466-16471.

Tashiro, A., Makino, H., and Gage, F. H. (2007). Experience-specific functional modification of the dentate gyrus through adult neurogenesis: a critical period during an immature stage. *J. Neurosci.* 27(12), 3252-9.

Tashiro, A., Sandler, V. M., Toni, N., Zhao, C., Gage, F. H. (2006). NMDA-receptor-mediated, cell-specific integration of new neurons in adult dentate gyrus. *Nature* 442, 929-933.

Thon, N., Haas, C. A., Rauch, U., Merten, T., Fässler, R., Frotscher, M., Deller T. (2000). The chondroitin sulphate proteoglycan brevican is upregulated by astrocytes after entorhinal cortex lesions in adult rats. *Eur. J. Neurosci.* 12(7), 2547-58.

Tian, G. F., Azmi, H., Takano, T., Xu, Q., Peng, W., Lin, J., Oberheim, N., Lou, N., Wang, X., Zielke, H. R., Kang, J., Nedergaard, M. (2005). An astrocytic basis of epilepsy. *Nat. Med.* 11, 973–981.

Tissir, F., and Goffinet, A.M. (2003). Reelin and brain development. *Nat. Rev. Neurosci.* 4, 496–505.

Tuszynski, M.H., and Steward, O. (2012). Concepts and methods for the study of axonal regeneration in the CNS. *Neuron* 74, 777-791.

Ullian, E. M., Christopherson, K. S., and Barres, B. A. (2004). Role for glia in synaptogenesis. *Glia* 47(3), 209-16.

van Groen, T., Kadish, I., Wyss, J. M. (2002). Species differences in the projections from the entorhinal cortex to the hippocampus. *Brain Res. Bull.* 57(3-4), 553-6.

van Groen, T., Miettinen, P., and Kadish, I. (2003). The entorhinal cortex of the mouse: organization of the projection to the hippocampal formation. *Hippocampus* 13(1), 133-49.

van Praag, H., Kempermann, G., and Gage, F. H. (1999). Running increases cell proliferation and neurogenesis in the adult mouse dentate gyrus. *Nat. Neurosci.* 2(3), 266-70.

van Praag, H., Schinder, A. F., Christie, B. R., Toni, N., Palmer, T. D., Gage, F. H. (2002). Functional neurogenesis in the adult hippocampus. *Nature* 415(6875), 1030-4.

Vargas, M. E., and Barres, B. A. (2007). Why is Wallerian degeneration in the CNS so slow? *Annu. Rev. Neurosci*. 30, 153-79.

Vlachos, A., Bas Orth, C., Schneider, G., Deller, T. (2012a). Time-lapse imaging of granule cells in mouse entorhino-hippocampal slice cultures reveals changes in spine stability after entorhinal denervation. *J. Comp. Neurol*. 520(9), 1891-902.

Vuksic, M., Del Turco, D., Vlachos, A., Schuldt, G., Müller, C. M., Schneider, G., Deller, T. (2011). Unilateral entorhinal denervation leads to long-lasting dendritic alterations of mouse hippocampal granule cells. *Exp. Neurol*. 230(2), 176-85.

Warren, K. M., Reeves, T. M., and Phillips, L. L. (2012). MT5-MMP, ADAM-10, and N-cadherin act in concert to facilitate synapse reorganization after traumatic brain injury. *J. Neurotrauma.* 29(10), 1922-40.

Weiss, K. H., Johanssen, C., Tielsch, A., Herz, J., Deller, T., Frotscher, M., Förster, E. (2003). Malformation of the radial glial scaffold in the dentate gyrus of reeler mice, scrambler mice, and ApoER2/ VLDLR-deficient mice. *J. Comp. Neurol.*, 460, 56-65.

Wenzel, H. J., Robbins, C. A., Tsai, L. H. & Schwartzkroin, P. A. (2001). Abnormal morphological and functional organization of the hippocampus in a p35 mutant model of cortical displasia associated with spontaneous seizures. *J. Neurosci*. 21, 983-998.

Wilhelmsson, U., Bushong, E. A., Price, D. L., Smarr, B. L., Phung, V., Terada, M., Ellisman, M. H., Pekny, M. (2006). Redefining the concept of reactive astrocytes as cells that remain within their unique domains upon reaction to injury. *Proc. Natl. Acad. Sci. USA* 103, 17513-17518.

Williams, C. A., and Lavik, E. B. (2009). Engineering the CNS stem cell microenvironment. *Regen. Med.* 4(6), 865-77.

Wilson, M. T., and Snow, D. M. (2000). Chondroitin sulfate proteoglycan expression pattern in hippocampal development: potential regulation of axon tract formation. *J. Comp. Neurol*. 424(3), 532-46.

Xu, J., Xiao, N., and Xia, J. (2010). Thrombospondin 1 accelerates synaptogenesis in hippocampal neurons through neuroligin 1. *Nat. Neurosci.* 13, 22-24.

Zeng, L. H., Xu, L., Rensing, N. R., Sinatra, P. M., Rothman, S. M., Wong, M. (2007). Kainate seizures cause acute dendritic injury and actin depolymerization in vivo. *J. Neurosci*. 27(43), 11604-13.

Zhao, S., Chai, X., Förster, E., Frotscher, M. (2004). Reelin is a positional signal for the lamination of dentate granule cells. *Development*, 131, 5117-5125.

Zhao, S., Förster, E., Chai, X., Frotscher, M. (2003).Different signals control laminar specificity of commissural and entorhinal fibers to the dentate gyrus. *J. Neurosci*. 23, 7351-7357.

Zhao, R. R., Muir, E. M., Alves, J. N., Rickman, H., Allan, A. Y., Kwok, J. C., Roet, K. C., Verhaagen, J., Schneider, B. L., Bensadoun, J. C., Ahmed, S. G., Yáñez-Muñoz, R. J., Keynes, R. J., Fawcett, J. W., Rogers, J. H. (2011). Lentiviral vectors express chondroitinase ABC in cortical projections and promote sprouting of injured corticospinal axons. *J. Neurosci. Methods*. 201(1), 228-38.

Zimmer, J., Laurberg, S., and Sunde, N. (1986). Non-cholinergic afferents determine the distribution of the cholinergic septohippocampal projection: a study of the AChE staining pattern in the rat fascia dentata and hippocampus after lesions, X-irradiation, and intracerebral grafting. *Exp. Brain Res*. 64(1), 158-68.

Zuo, J., Hernandez, Y. J., and Muir, D. (1998). Chondroitin sulfate proteoglycan with neurite-inhibiting activity is up-regulated following peripheral nerve injury. *J. Neurobiol.* 34(1), 41-54.